

ANALYTICAL TOOLS FOR STRENGTH PREDICTION OF THERMALLY DETERIORATED HPC

Thesis

Submitted in partial fulfilment of the requirements for the
degree of
DOCTOR OF PHILOSOPHY

by

KULKARNI KISHOR SITARAM BHYGAYALAXMI



DEPARTMENT OF CIVIL ENGINEERING
NATIONAL INSTITUTE OF TECHNOLOGY KARNATAKA,
SURATHKAL, MANGALORE – 575 025
MARCH, 2014

DECLARATION

by the Ph.D. Research Scholar

I hereby declare that the Research Thesis entitled “**Analytical Tools for Strength Prediction of Thermally Deteriorated HPC**” which is being submitted to the **National Institute of Technology Karnataka, Surathkal** in partial fulfilment of the requirements for the award of the Degree of **Doctor of Philosophy in Civil Engineering** is *a bonafide report of the research work carried out by me.* The material contained in this Research Thesis has not been submitted to any University or Institution for the award of any degree.

KULKARNI KISHOR SITARAM BHYGAYALAXMI

Register No. - **082017CV08F02,**

Department of Civil Engineering

Place: NITK-Surathkal

Date: 24/03/2014

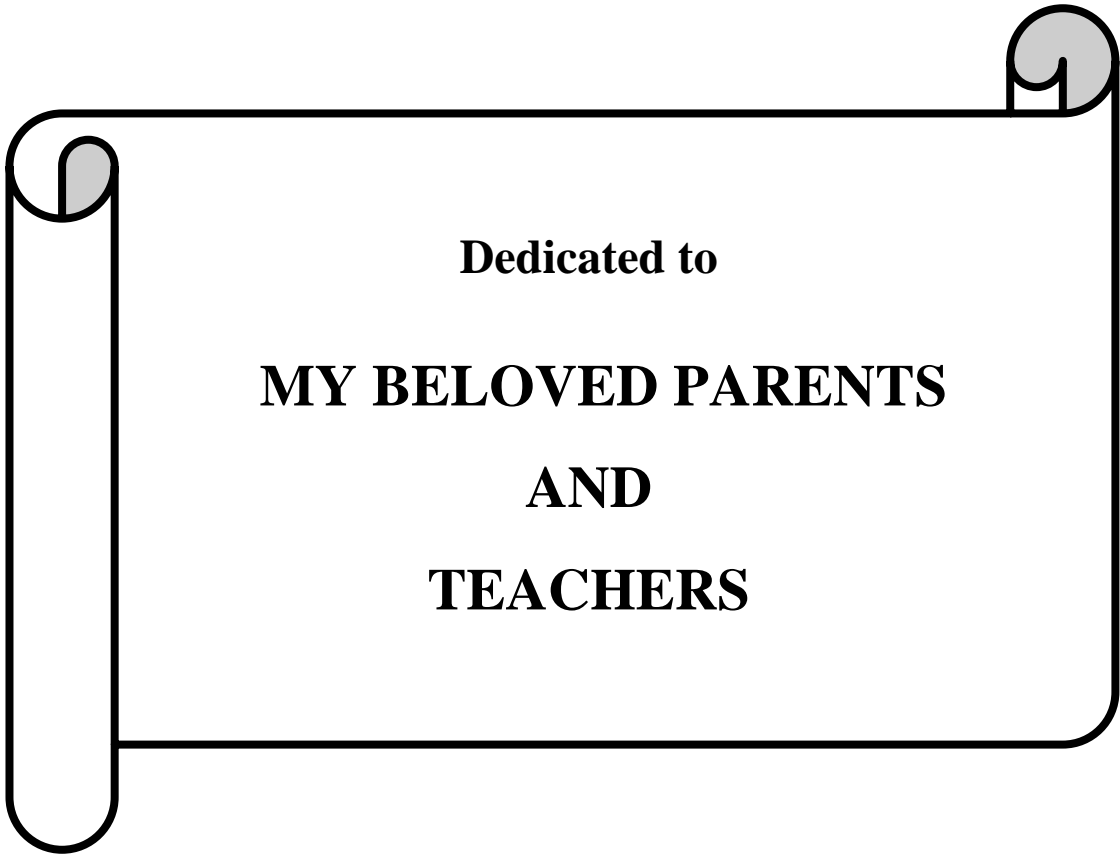
CERTIFICATE

This is to *certify* that the Research Thesis entitled “**Analytical Tools for Strength Prediction of Thermally Deteriorated HPC**” submitted by **Kulkarni Kishor Sitaram Bhygalaxmi** (Register Number: **082017CV08F02**) as the record of the research work carried out by him, is *accepted as the Research Thesis submission* in partial fulfilment of the requirements for the award of degree of **Doctor of Philosophy**.

Prof. Subhash C. Yaragal
Department of Civil Engineering,
(Research Supervisor)

Prof. K. S. Babu Narayan
Department of Civil Engineering,
(Research Supervisor)

Prof. Katta Venkataramana
Department of Civil Engineering
Chairman – DRPC



Dedicated to

MY BELOVED PARENTS

AND

TEACHERS

ACKNOWLEDGEMENT

First and foremost, I express my sincere heartfelt thanks and deepest gratitude to my research supervisors **Prof. K. S. Babu Narayan and Prof. Subhash C. Yaragal**, Department of Civil Engineering for their excellent guidance and kind cooperation throughout the research period, leading to successful completion of this research. Apart from the technical guidance, it was their constant affection, support and solace during the moments of despair that have been behind the successful completion of this report.

I am greatly indebted to RPAC members, Prof. Katta Venkataramana, Department of Civil Engineering and Prof. S. M. Kulkarni, Department of Mechanical Engineering, for their critical evaluation and very useful suggestions during the progress of the work.

I am thankful to, Prof. Katta Venkataramana, Head of Civil Engineering Department and Chairman DRPC, Prof. S. Shrihari, Secretary, DRPC and Prof. M. C. Narasimhan, and Prof. A. U. Ravishankar, former Heads of the Department of Civil Engineering, for their continuous support, encouragement and timely help during my entire research period.

I sincerely thank Prof. Harsha Vardhan, Prof. Mangalpadya Aruna and Mr. Chandrasahai Rai, Department of Mining Engineering, for providing me with laboratory facilities in the Department of Mining Engineering. I also thank Prof. S. M. Kulkarni, Faculty In charge, Research and Development Centre, NITK, Surathkal for permitting me to use muffle furnace. I would also wish to express my thanks to Prof. Vijay Desai, Department of Mechanical Engineering for his guidance during the experiments.

I gratefully acknowledge the financial support received from Board of Research in Nuclear Sciences (BRNS), Govt. of India, for research work. I am obliged to Council of Scientific and Industrial Research (CSIR), Govt. of India, for sanctioning me Foreign Travel Grant to visit Kumamoto University, Japan.

My warm regards are due to Prof. R. K. Dhir, Dr. M. R. Jones, Dr. Moray Newlands, Dr. Laszlo Csetenyi, Dr. Li Zheng, Mr. Steven Scott and Research Students of Concrete Technology Unit, University of Dundee, for sharing their knowledge during my UKIERI student research interaction.

I also like to extend my gratitude to all the teaching faculty and supporting staff of the Civil Engineering Department, for their encouragement, help and support provided during the research work.

I am very much thankful to all my friends and fellow research scholars of this institute for their continuous encouragement and suggestions during the course of my research work.

Invaluable cooperation and moral support was extended to me by my parents and sister, I lovingly acknowledge their help during this research period.

Finally, I am grateful to everyone who have helped and encouraged me during this research work.

Kishor S. Kulkarni

Place: NITK

Date: 24/03/2014

ABSTRACT

“Analytical tools for strength prediction of thermally deteriorated HPC” is an experimental study on development of analytical tools for strength prediction of High Performance Concrete (HPC) exposed to elevated temperatures. The prime objective is to study the behaviour of HPC at different exposure durations and temperatures. The work also focuses on the residual strength assessment of concrete exposed to elevated temperature by non-destructive testing.

Exhaustive review of literature has been done to understand the state of the art, to identify the points needing further research and then to design the experimental investigation. First phase of the study deals with properties of four types of HPC mixes that include unblended and blended mixes, with partial replacement of cement by Fly Ash (FA) and Ground Granulated Blast Furnace Slag (GGBFS), at exposure temperature range of 100°C-800°C and exposure duration of 1, 2 and 3 hours. Colour change and crack patterns have been observed. Porosity and density determination, Ultrasonic Pulse Velocity (UPV) measurements to assess the quality of concrete, have been made. Residual compressive and splitting tensile strengths have been determined by destructive testing.

Second phase explores the potential of drilling resistance test on thermally deteriorated concrete as an NDT tool. Drilling time for a designated depth of drilling and sound measurement while drilling have been recorded. Determination of residual compressive strength of plain and reinforced concrete, exposed to elevated temperature has been carried out in the third phase of experiments by core recovery tests to understand the behavioural differences.

From the above investigation very interesting conclusions have been drawn that highlight the superiority of blended concrete's fire endurance properties. The potential use of drilling time and sound levels as an NDT tool, nomographs that can be used as valid decision making tools in failure forensics and also elaborate the care and caution necessary in conducting and interpretation of core test results of fire damaged structural elements.

Key words: HPC, Blended, Elevated temperatures, Residual strength, Drilling resistance test, Core recovery test.

CONTENTS

CHAPTER 1	INTRODUCTION	1
1.1	High Performance Concrete	1
1.2	Performance of Concrete at Elevated Temperatures	2
1.3	Fire Resistance – Codal Recommendations	3
1.4	Strength Assessment of Concrete Subjected to Elevated Temperatures	6
1.5	Organization of the Thesis	6
CHAPTER 2	REVIEW OF LITERATURE	8
2.1	General	8
2.2	Characteristics of HPC at Elevated Temperatures	8
2.2.1	Surface Colour Change and Cracking	9
2.2.2	Spalling of Concrete	9
2.2.3	Concrete Porosity	11
2.2.4	Residual Strength of HPC at Elevated Temperature	11
2.3	Residual Concrete Strength Assessment Techniques	16
2.3.1	Visual Inspection	16
2.3.2	Colorimetry Test	17
2.3.2	Non Destructive Testing	18
2.3.4	Partially Destructive Testing	19
2.4	Literature Summery	21
2.5	Need For Extending and Refining the Understanding of HPC Behaviour at Elevated Temperature	22
2.6	Objectives of Present Investigation	23
CHAPTER 3	MATERIALS AND METHODS	25
3.1	General	25
3.2	Materials	25
3.2.1	Cement	25

3.2.2	Fine and Coarse Aggregate	27
3.2.3	Supplementary Cementitious Materials	28
3.2.4	Superplasticizer	29
3.2.5	Water	29
3.3	Methodology	30
3.3.1	Concrete Mix Design	30
3.3.2	Preparation of Specimen	32
3.3.3	Exposure to Elevated Temperatures	33
3.4	Tests on Exposed Concrete Specimens	35
3.4.1	Performance of HPC Blends at Elevated Temperatures	35
3.4.2	Assessment of Residual Strength of Concrete Exposed to Elevated Temperature by Drilling Resistance Test	40
3.4.3	Residual Compressive Strength of Concrete - Core Recovery Test	44
3.5	Summary	47

CHAPTER 4 STRENGTH PERFORMANCE OF HPC BLENDS AT ELEVATED TEMPERATURES 48

4.1	General	48
4.2	Physical Observations of Concrete Exposed to Elevated Temperature	48
4.2.1	Colour Change Pattern - Observations	48
4.2.2	Surface Cracking due to Elevated Temperatures	49
4.3	Loss in Weight of Concrete due to Elevated Temperature	52
4.4	Changes in Porosity of Concrete due to Elevated Temperature	54
4.5	Effect of Elevated Temperature on Concrete Density	56
4.6	UPV Recordings in Evaluation of Concrete Exposed to Elevated Temperature	58

4.7	Strength Retention Characteristics of Concrete Blends	61
4.8	Splitting Tensile Strength of Concrete	64
4.9	Statistical Analysis of Experimental Data	66
4.10	Prediction Equations for the Residual Strength Assessment of Concrete Exposed to Elevated Temperature	72
4.11	Strength Vs Time – Temperature	73
4.12	Summary	77
CHAPTER 5	DRILLING RESISTANCE –IN DAMAGE DIAGNOSIS	79
5.1	General	79
5.2	Drilling Resistance Test on Conventional Building Materials	79
5.3	Drilling Resistance Test on Concrete	80
5.4	Drilling Time Test on Concrete Exposed to Elevated Temperature	81
5.5	Sound Test on Concrete Exposed to Elevated Temperature	82
5.5.1	Recordings of Sound Levels Associated with Drilling Test	82
5.5.2	Impact Sound Test	84
5.6	Nomograph For Compressive Strength Ratio from Drilling Time Ratio and Temperature	85
5.7	Summary	86
CHAPTER 6	CORE RECOVERY- AS A MEANS OF NDT	87
6.1	General	87
6.2	Core Recovery Test on Plain Concrete Exposed to Elevated Temperature	87
6.2.1	Physical Observations	87
6.2.2	Compressive Strength	89
6.2.3	Equation for Standard Cube Compressive Strength Prediction, from Core Compressive Strength for	90

	Plain Concrete	
6.3	Core Recovery Test on Reinforced Concrete Exposed to Elevated Temperatures	90
6.3.1	Physical Observations	90
6.3.2	Porosity and Density	91
6.3.3	UPV Test on Core Sample	92
6.3.4	Compressive Strength	93
6.3.5	Equation for Standard Cube Compressive Strength Prediction, from Core Compressive Strength for Reinforced Concrete	94
6.4	Summary	95
CHAPTER 7	CONCLUSIONS	96
APPENDIX I		99
APPENDIX II		101
REFERENCES		141
LIST OF PUBLICATIONS		148
CURRICULUM VITAE		151

LIST OF FIGURES

Fig. No.	Title	Page No.
1.1	Minimum dimensions of reinforced concrete members for fire resistances	5
2.1	Photographs of different forms of spalling	10
2.2	Comparison of design curves for compressive strength ratio with temperature	15
2.3	Typical effect of heat upon the compressive strength of dense aggregate concrete after cooling	16
2.4	Probe penetration test setup	20
3.1	Grading curve for fine aggregate	28
3.2	Slump for different mixes	31
3.3	Details of reinforcement in beam	32
3.4	Muffle furnace and arrangement of specimen for exposure	34
3.5	Time temperature build up curve	34
3.6	Crack microscope	36
3.7	Submerged weight measurement set up	37
3.8	UPV test set up	38
3.9	Compression testing machine	39
3.10	Splitting tensile strength test	40
3.11	Rotary drilling machine	41
3.12	Dosimeter	42
3.13	Test setup for determination of drilling time	43
3.14	Steel ball and concrete specimen	44
3.15	Horizontal core cutter machine	45
3.16	Concrete core extracted from cube specimen	45
3.17	Vertical core cutting machine	46
3.18	Core extraction locations	47
4.1	Crack pattern for different mixes at 800°C	50

4.2	Crack pattern for HPC-O mix at 800°C	51
4.3	Variation in weight loss with temperatures for different retention period	54
4.4	Variation in porosity with temperatures for different retention periods	56
4.5	Variation in concrete density ratio with temperatures for different retention periods	58
4.6	Variation in UPV with temperatures for different retention periods	60
4.7	Variation in UPV ratio with temperature for different mixes	61
4.8	Variation in compressive strength ratio with temperatures for different retention periods	63
4.9	Variation in splitting tensile strength ratio with temperatures for different retention periods	66
4.10	S/N response graph for compressive strength	70
4.11	S/N response graph for splitting tensile strength	70
4.12	S/N response graph of experimental parameters for compressive strength	71
4.13	S/N response graph of experimental parameters for splitting tensile strength	72
4.14	Typical time temperature curve for 800°C temperature and 3 hours retention period	74
4.15	Plot between compressive strength ratio and time temperature factor	76
5.1	Penetration depth with drilling time for building materials	80
5.2	Penetration depth with drilling time for concretes with varying strengths	81
5.3	Penetration depth with drilling time for concrete exposed to temperature	82
5.4	Normalised A-weighted equivalent sound level with temperature	83
5.5	Impact sound level with temperature	84
5.6	Parallel scale nomograph for compressive strength ratio	85

6.1	Colour change in concrete cores	88
6.2	Variation in compressive strength ratio of standard cube and core with temperature	89
6.3	Variation in porosity with temperature	91
6.4	Variation in density with temperature	92
6.5	Variation in UPV with temperature	93
6.6	Compressive strength ratio of standard cube and core extracted from plain concrete and reinforced concrete beam with temperature	94

LIST OF TABLES

Table No.	Title	Page No.
1.1	Mineralogical and strength changes in concrete caused by heating	3
1.2	Minimum dimensions of reinforced concrete members for fire resistances	4
1.3	Nominal cover to meet specified period of fire resistance	5
2.1	Characteristics of the different forms of spalling	11
2.2	Simplified visual concrete fire damage classification	17
2.3	UPV criteria for concrete quality grading	19
3.1	Physical properties of cement	26
3.2	Chemical composition of cement	26
3.3	Sieve analysis of fine aggregate	27
3.4	Sieve analysis of coarse aggregate	28
3.5	Physical properties and chemical composition of SCM	29
3.6	Mix proportion per cubic meter of concrete	31
4.1	Colour change in concrete with temperature	49
4.2	Maximum width on surface and depth of surface crack for exposed concrete	52
4.3	Results of ANOVA for compressive strength of concrete	68
4.4	Results of ANOVA for splitting tensile strength of concrete	69
4.5	Residual compressive/splitting tensile strength prediction equations for different mixes based on exposure temperature and retention period	73
4.6	Area of the time temperature curve for different temperatures and retention period	75
4.7	Results of Compressive strength ratio and Time temperature factor	75
4.8	Summary of test results highlighting strength performance of HPC subjected to elevated temperature	77
6.1	Maximum width on surface and depth of surface crack	91

NOMENCLATURE

Abbreviations

HPC	: High Performance Concrete
SCM	: Supplementary Cementing Materials
NDT	: Non Destructive Techniques
UPV	: Ultrasonic Pulse Velocity
OPC	: Ordinary Portland Cement
PFA	: Pulverized Fly Ash
FA	: Fly Ash
GGBFS	: Ground Granulated Blast Furnace Slag
C-H [Ca(OH) ₂]	: Calcium Hydroxide, Portlandite
C-S-H	: Calcium Silicate Hydrate
ASTM	: American Society for Testing and Materials
IS	: Indian Standard
MRE	: Mean Relative Error
PCC	: Plain Cement Concrete
RCC	: Reinforced Cement Concrete

Notations

T	: Exposed Temperature in °C
RP	: Retention Period in hours
f_{cr}	: Compressive Strength Ratio
f_{c27}	: Compressive Strength at 27°C
f_{cT}	: Compressive Strength at T°C
f_{tr}	: Splitting Tensile Strength Ratio
f_{t27}	: Splitting Tensile Strength at 27°C
f_{tT}	: Splitting Tensile Strength at T°C
V_r	: Ultrasonic Pulse Velocity Ratio
V_{27}	: Ultrasonic Pulse Velocity at 27°C
V_T	: Ultrasonic Pulse Velocity at T°C
S/N	: Signal to Noise Ratio
TTF	: Time -Temperature Factor
DT_r	: Drilling Time Ratio
L_{eq}	: A-Weighted Equivalent Sound
f_{co}	: Core Compressive Strength
f_{cs}	: Standard Cube Compressive Strength

CHAPTER 1

INTRODUCTION

1.1 HIGH PERFORMANCE CONCRETE

High Performance Concrete (HPC) is the term used for concretes that possess higher strength, workability and durability vis-a-vis conventional concrete. Higher performance levels of HPC are accomplished by carefully selecting high quality ingredients and adopting judicious mix design. High performance concrete is being extensively used in a wide and varied range of structural applications to meet specific needs.

The term High Performance Concrete was first used by Mehta and Aitcin, (1990), for concrete mixtures possessing three characteristics, namely high strength, high workability, and high durability. Different definitions have been proposed for HPC. Neville, (2005) states that “the essential feature of HPC is that its ingredients and proportions are specially chosen so as to have particular appropriate properties for the expected use in a structure; these properties are usually high strength or impermeability”. High performance concrete is defined by the American Concrete Institute (ACI) as concrete that meets special combinations of performance and uniformity requirements that cannot always be achieved routinely using conventional constituents and under normal mixing, placing, and curing practices.

Attempts to attain high performance levels by increasing cement content, lead to excessive shrinkage and large evolution of heat of hydration problem, which in turn neglected the attainment of high performance characteristics (PCA report). Addition of supplementary cementitious materials suggested itself as an effective means of realising requirements of HPC by overcoming the adverse effects of high cement content mixes.

Supplementary Cementing Materials (SCM) also known as mineral admixtures are materials in finely divided form which help promoting and enhancing hydration of cement in formation of compounds of hydration. Their use makes microstructure of hardened cement matrix denser, stronger and less permeable.

Many of the supplementary cementitious materials have inherent characteristics that enhance workability of concrete. Super or ultraplasticizers are used to make HPC free flowing and self-compacting to make placement easier in demanding situations.

1.2 PERFORMANCE OF CONCRETE AT ELEVATED TEMPERATURES

Concrete being the most versatile and widely used construction material finds application in varied range of structures. Many of these like chimneys, furnaces and reactors have to sustain high temperatures and perhaps all structures have to perform at elevated temperatures in the event of fire accidents.

Concrete at elevated temperatures undergoes changes in its physical structure and chemical composition and loses its strength characteristics. The extent of changes and deterioration mainly depends on the temperature level, temperature build-up rate, exposure duration and to a great extent on the type of concrete itself. An elaborate account of mineralogical and strength changes of concrete caused by elevated temperature as has been presented by The Concrete Society, UK, Technical Report No. 68, 2008, is reported in Table 1.1.

Table 1.1: Mineralogical and strength changes in concrete caused by heating

Heating Temperature (°C)	Changes caused by heating	
	Mineralogical changes	Strength changes
70-80	Dissociation of ettringite	Minor loss of strength possible (<10%)
105	Loss of physically bound water in aggregate and cement matrix commences, increasing capillary porosity	
120-163	Decomposition of gypsum	
250-350	Oxidation of iron compounds causing pink/red discolouration of aggregate. Loss of bound water in cement matrix and associated degradation becomes more prominent	Significant loss commences at 300°C
450-500	Dehydroxylation of portlandite. Aggregate calcines and will eventually change colour to white/grey	
573	5% increase in volume of quartz (α to β quartz transition) causing radial cracking around the quartz grains in the aggregate	Concrete not structurally useful after heating in temperatures in excess of 550-600°C
600-800	Release of carbon dioxide from carbonates may cause a considerable contraction of the concrete (with severe micro-cracking of the cement matrix)	
800-1200	Dissociation and extreme thermal stress cause complete disintegration of calcareous constituents, resulting in whitish-grey concrete colour and severe micro-cracking	
1200	Concrete starts to melt	
1300-1400	Completely melted	

1.3 FIRE RESISTANCE – CODAL RECOMMENDATIONS

As per Indian code of practice, IS 456-2000, the following are the recommendations,

A structure or structural element required to have fire resistance should be designed to possess an appropriate degree of resistance to flame penetration; heat transmission and failure. The fire resistance of a structural element is expressed in terms of time in hours in accordance with IS 1641. Fire resistance of concrete elements depend upon

details of member size, cover to steel reinforcement detailing and type of aggregate used in concrete.

Minimum requirements of member dimensions and nominal cover for normal-weight aggregate concrete members so as to have the required fire resistance are depicted in Table 1.2, Figure 1.1, and Table 1.3.

Table 1.2: Minimum dimensions of reinforced concrete members for fire resistances

Fire resistance	Minimum Beam Width b	Rib Width of slabs b _w	Minimum Thickness of floors D	Column dimension (b or D)			Ribs		
				Fully Exposed	50% Exposed	One face Exposed	p < 0.4%	0.4% ≤ p ≤ 1%	p > 1%
hour	mm	mm	mm	mm	mm	mm	mm	mm	mm
0.5	200	125	75	150	125	100	150	100	100
1	200	125	95	200	160	120	150	120	100
1.5	200	125	110	250	200	140	175	140	100
2	200	125	125	300	200	160	-	160	100
3	240	150	150	400	300	200	-	200	150
4	280	175	170	450	350	240	-	240	180

p- percentage of steel reinforcement

The reinforcement detailing should reflect the changing pattern of the structural section and ensure that both individual elements and the structure as a whole contain adequate support, ties, bonds and anchorages for the required fire resistance.

Additional measures such as application of fire resistant finishes, provision of fire resistant false ceilings and sacrificial steel in tensile zone, should be adopted in case the nominal cover required exceeds 40 mm for beams and 35 mm for slabs, to give protection against spalling.

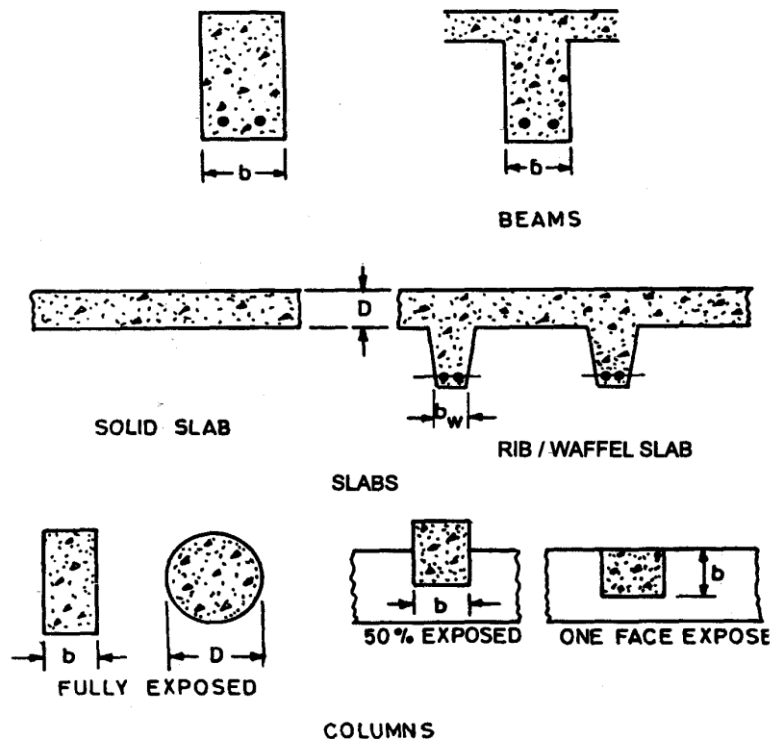


Fig. 1.1: Minimum dimensions of reinforced concrete members for fire resistances

Table 1.3: Nominal cover to meet specified period of fire resistance

Fire resistance (hour)	Beams		Slabs		Ribs		Columns
	Simply supported	Continuous	Simply supported	Continuous	Simply supported	Continuous	
0.5	20	20	20	20	20	20	40
1	20	20	20	20	20	20	40
1.5	20	20	25	20	35	20	40
2	40	30	35	25	45	35	40
3	60	40	45	35	55	45	40
4	70	50	55	45	65	55	40

1.4 STRENGTH ASSESSMENT OF CONCRETE SUBJECTED TO ELEVATED TEMPERATURES

Two methodologies which can be used separately or in combination are,

- Test the damage concrete directly to assess quality.
- Estimate levels of temperature exposure for ascertaining residual strength from available analytical tools.

As concrete structures are composite in nature, evaluation of the residual strength properties of concrete exposed to elevated temperature is very difficult task. Steps involved in assessment of concrete after it is exposed to elevated temperature include physical observation, and in-situ laboratory, non-destructive and partially destructive testing. For assessments, no single technique can be treated as superior to others. More than one technique may need to be employed and results have to be carefully interpreted at residual strength levels that are reliable.

Rebound hammer (Schmidt Hammer) and Ultrasonic Pulse Velocity (UPV) methods are the most commonly used Non Destructive Testing (NDT) methods for assessment of concrete characteristics. Ultrasonic pulse velocity method also helps in detection of internal cracks, voids and other defects.

1.5 ORGANIZATION OF THE THESIS

High performance concrete is being used extensively in recent times, since the demand for infrastructure is on the increase in the last two decades. The investment kick start economy and advancement in concrete technology, ease with which ready mix concrete can be made, transported, and placed, have all attracted the use. After the 9-11 attack on the World Trade Center, interest in the design of structures for fire resistance has greatly increased. Research interests on its performance at elevated temperature is attracting the attention of researchers now. Present work is an attempt in this direction.

High performance concrete with ground granulated blast furnace slag and fly ash as supplementary cementitious materials has been appraised at elevated temperatures. Potential application of drilling resistance as an NDT tool has been envisaged. For assessment of residual strength of HPC exposed to elevated temperature, core recovery tests have been proposed and validated for potential application.

Chapter 1 gives a brief account of HPC, performance of concrete at elevated temperatures and NDT, in strength assessment of concrete. A comprehensive review of literature has been presented in chapter 2 and in the light of literature review, the need and scope of the present investigation has been highlighted. To further our understanding of HPC, specific objectives were formulated for this research investigation.

Details of HPC employed, materials and methods adopted have been presented in chapter 3. Chapter 4 provides elaborate account of residual strength prediction equations obtained from analysis of experimental data obtained.

Drilling resistance test details along with the nomograph developed from the results are presented in chapter 5. Results of core compressive strength of HPC exposed to elevated temperature is given in chapter 6 and relation between core compressive strength and standard cube compressive strength obtained from results has also been presented.

Conclusions and contributions of present investigation have been summarised in chapter 7.

CHAPTER 2

REVIEW OF LITERATURE

2.1 GENERAL

High performance concrete, has become the part of spectrum of concrete, since the early 1990s, has found application in wide and varied range of structural elements and situations. In general, HPC is defined as a concrete that has a compressive strength of at least 60 MPa, with improved properties, when designed to fulfil certain specific requirements. The U.S. Federal Highway Administration (FHWA) states that “HPC is concrete that has been designed to be more durable and, if necessary, stronger than conventional concrete”. Forster (1994) defined HPC as "a concrete made with appropriate materials combined according to a selected mix design and properly mixed, transported, placed, consolidated, and cured so that the resulting concrete will give excellent performance in the structure in which it will be exposed, and with the loads to which it will be subjected for its design life.

The philosophy of HPC concrete design is ‘Strength’ through ‘Durability’ rather than ‘Durability’ through ‘Strength’. Though extended durability is a specific requirement of HPC its performance at elevated temperature has been and is being investigated.

A review of literature elaborating the state of the art knowhow about the behaviour of HPC subjected to elevated temperature is presented here.

2.2 CHARACTERISTICS OF HPC AT ELEVATED TEMPERATURES

Behaviour of concrete at elevated temperature is being investigated since 1940. The decades of 1960 and 1970, have seen an increase in fire resistance requirements of concrete, which in turn has promoted research in material and testing methods (Xiao, et al., 2006). The advent of HPC has renewed the research interest in concrete at

elevated temperatures and tremendous amount of analytical and experimental investigations are being carried out. An account of which is being presented in the following sections.

2.2.1 Surface Colour Change and Cracking

Elevated temperature exposure brings about change in colour of concrete. Upto 200°C, concrete colour does not change, while straw yellow, off-white, and red are colours of concrete at 400°C, 800°C and 1000°C, respectively as reported in the investigation by Short, et al. (2001) and Lin, et al. (2004). These colour changes correspond to a specific temperature range, which is an indicator of the maximum temperature to which the concrete surface is exposed to.

The hydration products (primarily C-S-H gel and CH) decompose quickly and result in serious cracks both within the hardened cement paste and around aggregate particles and these cracks definitely contribute to explosive spalling (Fu, and Li, 2011). Micro cracks are attributed to the development of difference in thermal expansion coefficients between components and by decomposition of Ca(OH)_2 and other ingredients (Noumowe, et al. 1996 and Li, et al., 2004). Poon, et al. (2001) has concluded in his findings that, due to pozzolanic reaction calcium hydroxide reduces in cement paste and leads to reduced cracking in the case of blended concretes.

2.2.2 Spalling of Concrete

Spalling is a type of damage, where concrete surface scales and falls off from the concrete along with explosion at high temperatures. High performance concrete appears to be more prone to spalling in fire than normal strength concrete as reported by Sanjayan and Stocks (1993). Sanjayan and Stocks (1993) have reported in their research findings that, spalling is mainly attributed to the dense, low permeability structure of the paste which does not readily allow moisture to escape from the heated concrete, thus resulting in high pore pressures and the development of micro cracks.

Spalling starts for HPC when temperature exceeds to 600°C as observed by Lau and Anson(2006) and Sideris, et al. (2009). This has two effects: a physical effect due to reduced ‘Van der Waals’ forces as water expands upon heating, and chemical effect whereby detrimental transformations can take place under hydrothermal conditions. Spalling can be grouped into four categories:

- (i) Aggregate spalling
- (ii) Explosive spalling
- (iii) Surface spalling
- (iv) Corner/sloughing-off spalling

The first three, occurs during the first 20–30 minutes of a fire and are influenced by the heating rate, while the fourth occurs after 30–60 minutes of fire and is influenced by the maximum temperature (Khoury, 2000). Figure 2.1 shows the photographs of different forms of spalling. Table 2.1 also presents the characteristics of different forms of spalling. Explosive spalling, is particularly dangerous type of failure and may affect the integrity and stability of a concrete structure. The internal vapour pressure may be the leading reason of concrete spalling as reported by Chan, et al. (2000), Peng, et al. (2008) and Dong, et al. (2008).



(a) Corner spalling (b) Surface spalling (c) Explosive spalling

Fig. 2.1: Photographs of different forms of spalling (Fu, and Li, 2011)

Table 2.1: Characteristics of the different forms of spalling (Khoury, 2000)

Spalling	Time of occurrence (minutes)	Nature	Sound	Influence	Main Influences
Aggregate	7-30	Splitting	Popping	Superficial	H, A, S, D, W
Corner	30-90	Non-violent	None	Can be serious	T, A, Ft, R
Surface	7-30	Violent	Cracking	Can be serious	H, W, P, Ft
Explosive	7-30	Violent	Loud bang	Serious	H, A, S, Fs, G, L, O, P, Q, R, S, W, Z

A- aggregate thermal expansion, D- aggregate thermal diffusivity, Fs-shear strength of concrete, Ft-tensile strength of concrete, G- age of concrete, H- heating rate, L- loading/restraint, O-heating profile, P- permeability, Q- section shape, R- reinforcement, S- aggregate size, T- maximum temperature, W- moisture content, Z- section size.

2.2.3 Concrete Porosity

Porosity is an important property of hardened concrete deemed to be responsible for severe strength deterioration. The total porosity of the concrete varies with saturation level and temperature of exposure. Luo, et al. (2000), Chan, et al. (2000), Lau and Anson, (2006), have presented correlation between the porosity and residual compressive strength of concrete. Studies have shown that the variation in porosity and pore size distribution as an indicator of the extent of degradation in compressive strength of HPC subjected to high temperature.

2.2.4 Residual Strength of HPC at Elevated Temperature

Important literature pertaining to residual strength of HPC at elevated temperatures is discussed.

Xu, et al. (2001) has investigated the impact of elevated temperature on Pulverized Fly Ash (PFA) concrete. Residual strength of concrete was tested on concretes made

with different water to binder ratios and PFA contents. This investigation has reported 8-9% gain in compressive strength for Ordinary Portland Cement (OPC) concrete, while concrete made with PFA gained about 10-15% strength when exposed to 250°C.

For 450°C high PFA concrete exhibits much better residual compressive strength than other mixes and 4% loss in compressive strength was observed when compared to the unexposed concrete. The strength losses for concretes made with low PFA content and OPC concrete differed between 18-14% for 450°C exposure temperature. For an exposure temperature of 650°C, residual compressive strength 65.8% and 51.1-56.2% of the unexposed concrete were retained for high PFA content, and other OPC and low PFA content respectively. The beneficial effect of PFA has been noticed on the residual strength of concrete when exposure temperatures were 450°C or 600°C. This has been attributed to the pozzolanic reaction consuming Ca(OH)_2 in the hydrates.

Poon, et al. (2001) carried out study on the compressive strength properties of high strength concrete containing Fly Ash (FA) and Ground Granulated Blast Furnace Slag (GGBFS) at elevated temperatures. Concrete mix containing 30% FA and 40% GGBFS replacement retained maximum residual compressive strength. For the concrete exposed to 200°C, 22% gain in strength was noted compared to ambient temperature strength. From 200°C to 400°C, blended concrete maintained their ambient temperature strength.

For the range of 400°C-600°C around 44% loss in compressive strength has been reported. For 800°C, severe deterioration in compressive strength was observed due to decomposition of C-S-H gel.

A drop in compressive and splitting tensile strength of FA based concrete when exposed to elevated temperatures has been reported by Li, et al. (2004). Compressive strength retained was to the extent of 82.3%, 63.2%, 58.1% and 21.3% at 200°C, 400°C, 600°C and 1000°C respectively when compared to the case of unexposed.

From the experimental results it was found that larger size specimen retains larger amount of strength after elevated temperature exposure.

Splitting tensile strength was retained to the extent of 85.7%, 81.8%, 51.9%, and 16.4% at 200°C, 400°C, 600°C and 1000°C respectively. Chen and Liu (2004) reported similar trend in splitting tensile strength loss and loss in compressive strength with increase in temperature up to 800°C.

Savva, et al. (2005) studied the influence of elevated temperatures on the compressive strength properties of blended cement concrete. The study has reported 5-39% increase in initial compressive strength for different FA based concrete mixes exposed upto 300°C. For OPC concrete, 5-6% increase in initial compressive strength was observed. As temperature increases from 300°C to 600°C, 68%-51% reduction in strength has been reported. Concrete with pozzolanic materials has shown better strength results than the pure OPC concretes, up to 300°C.

Xiao, et al., (2006) has studied the behaviour of HPC with GGBFS at elevated temperatures. Results show decrease in compressive strength of 13%, 38%, 49% and 84% at 200°C, 400°C, 600°C and 800°C exposure temperatures respectively. The relative residual cube compressive strength of HPC–GGBFS is close to the referenced normal strength concrete by Comite Euro-International du Beton (CEB).

Liu, and Huang, (2009) have investigated the effect of exposure durations on HPC subjected to 500°C. The result shows that, residual compressive strength of concrete decreases with increase in exposure duration. The residual compressive strength was observed to be 74%, 46.7%, 38.5% and 34.6% for exposure duration of 30, 60, 90 and 120 minutes respectively when compared to the case of specimen exposed but retention time being 0 minutes.

Teng, and Lo, (2009) carried out experimental investigation on image analysis and mechanical properties of high strength concrete with FA exposed to elevated temperature. From scanning electron microscope image analysis, it has been reported

that concrete with FA shows few and narrow microcracks at transition zone, compared to the control concretes. Fly ash concrete also shows better strength retention characteristics.

According to Hosam, et al., (2011), GGBFS concrete shows the best performance in term of residual compressive strength compared to other pozzolanic materials like FA and metakoline when used as cement replacement in concrete, under elevated temperature conditions.

Nadeem, et al. (2013) investigated the compressive strength properties of HPC made with 20% of FA by weight of cement at exposure temperature of 200°C to 800°C. The loss in compressive strength after exposure to 200°C, 400°C, 600°C and 800°C was upto 10%, 15%, 41% and 72% respectively. Changes taking place in the Interfacial Transition Zone (ITZ) has been analyzed and deterioration of ITZ has been analyzed found to be a major factor for strength loss at elevated temperatures. The physical condition of in HPC at three temperatures ranges namely; the low range temperatures (27–200°C), the medium range temperatures (200–400°C) and the high range temperatures (400–800°C) has been described.

Rahim et al. (2013) studied the influence of four factors on post fire residual compressive strength of HPC. The factors considered in the context of high performance concrete are cement content, FA content, super-plasticizer content and fine aggregate content. The cube specimen were cast and heated up to 200°C, 400°C, 600°C and 800°C target temperatures. It has been observed that, cement content is the major influencing factor for maximizing the residual strength for concrete subjected to temperatures up to 800°C, fine aggregate content is found to be the second most influencing parameter followed by FA content and superplasticizer dosage.

Comparisons of residual compressive strength prediction design curves by different standards are presented in Fig. 2.2. Residual concrete compressive strength curve proposed by American Society of Civil Engineers (ASCE) for normal strength concrete has not differentiated test type and different aggregate type. Eurocode and

Comite Euro-International du Beton (CEB) curves have considered the type of aggregates but not the test type. American Concrete Institute (ACI) 216.1 model has considered both, the effect of test type and nature of aggregates. All these models proposed by different standards, estimate unconservative results for mechanical properties of HSC at elevated temperatures. They do not specify the concrete compressive strength limit for their prescribed residual compressive strength v/s temperature curves. Finnish Code (RakMK B4) prescribes a residual compressive curve specifically for high strength.

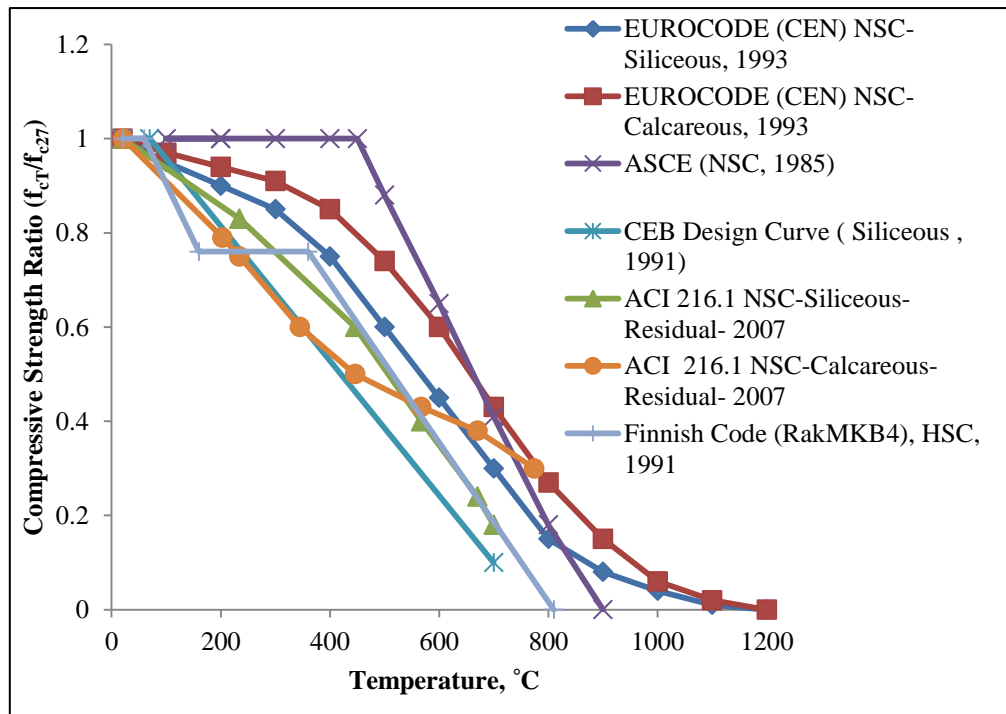


Fig. 2.2: Comparison of design curves for compressive strength ratio with temperature

Figure 2.3 shows the data from Bazant, and Kaplan, (1996), for residual compressive strength ratio of concrete samples exposed to the same temperatures, but for different retention periods. The results clearly indicate that a longer exposure duration to higher temperatures results in lower residual strength factor.

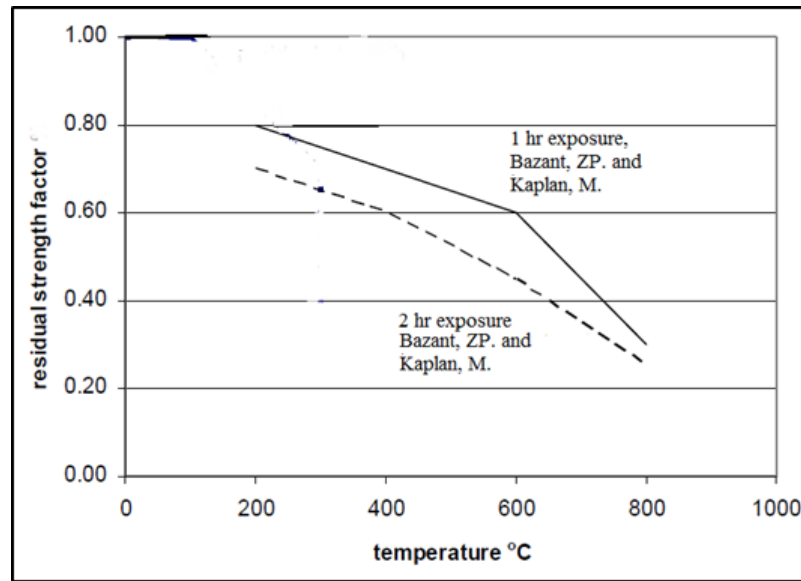


Fig. 2.3: Typical effect of heat upon the compressive strength of dense aggregate concrete after cooling (Technical Report No. 68, 2008)

2.3 RESIDUAL CONCRETE STRENGTH ASSESSMENT TECHNIQUES

The assessment of fire damaged concrete, starts with the collection of relevant information such as design of building, construction material, usage of building, cause of the fire and duration of fire spread, then followed by non-destructive testing. The following section presents a brief review of various techniques and steps involved for the assessment of residual strength of concrete exposed to elevated temperatures.

2.3.1 Visual Inspection

The visual inspection, aims to gather information about features such as, collapse, spalling, surface crazing, cracking, exposed reinforcement and excessively deflected members. A small hammer may be used to conduct a sound test, to detect delamination of concrete. Deformation of structural members and associated materials provide valuable information to develop a heat intensity map. Building materials for example, timber chars at 250°C, aluminium alloys melts at 650°C, sheet glass melts at 850°C, can give the indication of exposure temperature and duration.

Table 2.2 shows simplified visual concrete fire damage classification as provided in The Concrete Society, UK, Technical Report No. 68, 2008. The damage classification uses visual indications of damage, to assign each structural member a class of damage from 0 to 4. Each damage classification number has a corresponding category of repair, ranging from decoration to major repair.

Table 2.2: Simplified visual concrete fire damage classification

Class of Damage	Features Observed					
	Finishes	Colour	Crazing	Spalling	Reinforcement	Cracks/ Deflection
0 (Decoration required)	Un-affected	Normal	None	None	None exposed	None
1 (Superficial repair required)	Some peeling	Normal	Slight	Minor	None exposed	None
2 (General repair required)	Substantial loss	Pink/red ¹	Moderate	Localised	Up to 25% exposed	None
3 (Principal repair required)	Total loss	Pink/red ¹ Whitish grey ²	Extensive	Considerable	Up to 50% exposed	Minor/ None
4 (Major repair required)	Destroyed	Whitish grey ²	Surface lost	Almost total	Up to 50% exposed	Major/ Distorted
Note: ¹ Pink/red discolouration is due to oxidation of ferric salts in aggregates and is not always present and seldom in calcareous aggregate ² White grey discolouration due to calcination of calcareous components of cement matrix and (where present) calcareous or flint aggregate						

2.3.2 Colorimetry Test

Colorimetry test supports the other test and gives indirect indication of condition of concrete. The colour change is dependent on aggregate type and it is more pronounced for siliceous aggregate concrete. Colour test is carried out by taking images of concrete surfaces by digital camera. These images are analysed by using the software and can be described and quantified in terms of their components by use

of colour space. The colour space is divided into two groups either red, green, blue (RGB) or in terms of hue, saturation and intensity (HIS) (Short, et al., 2001).

Short, et al., (2001), used colour image analysis to quantify the colour of fire damaged concrete and reports that, it is a superior tool for subjective visual assessment. Lin, et al., (2004), developed a software called “Image colour intensity analyser” to investigate the relationship between surface colour changes of concrete and exposure temperatures.

2.3.3 Non Destructive Testing

Non Destructive Testing (NDT) does not impair the intended performance of the element or member under test. Primary objectives of NDT are to produce an immediate value of in-place concrete strength and to be used in structural capacity evaluation, or to locate internal defects in the concrete members which will assist in subsequent adequacy evaluation. Equipment used for investigation should be checked for the validity of its calibration, where possible against the reference provided by the manufacturer of equipment.

Ultrasonic Pulse Velocity Test

Widely employed non-destructive method for assessing the extent of damage to concrete structures after fire is by Ultrasonic Pulse Velocity (UPV). Table 2.3 shows the UPV criteria for concrete quality grading. Hoff, et al. (2000), reported that for high strength concrete after exposure to elevated temperatures, there was a gradual but significant decrease in pulse velocity with increasing exposure temperatures up to 900⁰C. Handoo et al., (2002), observed a reduction in UPV values on concrete specimens from 4.05 to 0.33 km/sec with the rise in temperature from 100⁰C to 700⁰C. For 800⁰C, the pulse could not be transmitted through the concrete which indicate, total deterioration in its physical state.

Table 2.3: UPV criteria for concrete quality grading (IS 13311-Part 1:1992)

UPV measurement, (km/sec)	> 4.5	3.5-4.5	3.0-3.5	< 3.0
Concrete Quality	Excellent	Good	Medium	Doubtful

Savva, et al. (2005) has reported reduction in UPV values to an extent of 25% and 77% at 300°C and 750°C temperature respectively. Arioz, (2009) observed 42% and 67% reduction in UPV values for concrete specimen exposed to 400°C and 1200°C. Yang et al., (2009) used UPV to quantitatively evaluate the residual compressive strength of concrete subjected to elevated temperatures. Based on experimental results, a relationship between the residual strength ratio and residual UPV ratio has been developed and general equations have been proposed for residual strength prediction.

2.3.4 Partially Destructive Testing

The assessment of fire damaged structures with only non-destructive techniques, is not possible, because of some limitations in the NDT such as, spalling of concrete, extensive cracking, sufficient calibration, nor can solely theoretical methods be relied upon, as their application implies knowing the effective temperature histories acting upon structural elements. Thus, the most advanced and promising testing methods are combination of experimental, non-destructive and partially destructive techniques.

Penetration Resistance Test (Windsor probe)

The rebound hammer measures hardness of the surface, whereas probe penetration tests, the resistance of the concrete below the surface. The principle of the probe penetration device involves driving a hardened steel rod or probe into the concrete. The driving force is delivered with a fixed charge placed in a gun with a consistent exit velocity. The correlation between penetration depth and concrete strength is established on plain concrete specimens, later this can be used on the concrete surface exposed to elevated temperature. This test gives an indication of the areas where

compressive strength is relatively lower compared to undamaged areas. Figure 2.4 shows the details of test setup (Bungey and Soutsos, 2001).

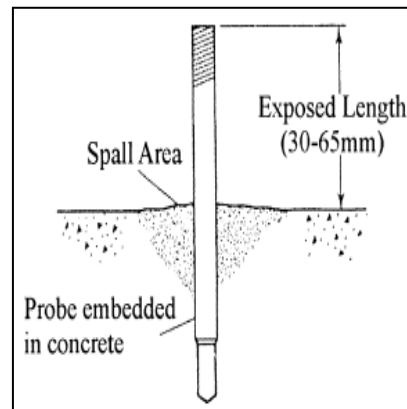


Fig. 2.4: Probe penetration test setup

Drilling Resistance Test on Rock

The drilling resistance test is used to identify the rock types or class and its mechanical properties. The process of drilling also produces sound as a by-product. One of possible ways to determine the actually drilled rock type (class) is to analyse the noise produced by drilling process. Zborovjan et al. (2003) and Miklusova et al. (2006) have studied the acoustic identification of rocks during drilling process. Vardhan, et al., (2009), have investigated the usefulness of sound level in determining rock and rock mass properties, using the jackhammer drill on a laboratory scale, by fabricating a jackhammer drill setup, wherein, the thrust applied can be varied while drilling the vertical holes.

Core Test

Core test enables visual inspections of the interior condition of the concrete. It also provides the specimens for laboratory compressive strength and other tests. The concrete core samples are taken using diamond tipped core bits on a power drill

machine. For compressive strength tests, at least three cores are needed for each location in the structure (Bungey, et al., 2006).

Strength of cores is generally lower than that of standard cylinders, caused by the effect of cutting, especially since cut aggregate particles are only partially embedded in the core and may not make a full contribution during testing (Neville, 2005, Bungey, et al., 2006). The moisture condition of the core also influences the measured strength and results about 10-15% lower strength than the dry specimen.

As the length to diameter ratio increases, measured strength decreases, this is due to effect of shape on stress distribution whilst under test. The direction of drilling also affects the strength of core, the measured strength of specimen drilled vertically relative to the direction of casting is likely to be greater than that for a horizontally drilled specimen (Bungey, et al. 2006). Thus core compressive strength values are converted to equivalent cube compressive strength by using corrective equations.

2.4 LITERATURE SUMMARY

From the review of literature, it has been found that concrete loses its strength when subjected to elevated temperatures in spite of its non-combustible nature and low thermal conductivity. High performance concrete has a dense microstructure by virtue of which, it possesses an extraordinary strength and durability properties. Few studies have indicated that the addition of silica fume highly densifies the pore structure of concrete, resulting in explosive spalling due to build-up of pore pressure by steam created as a result of elevated temperatures. Because of this, HPC experiences higher deterioration in strength when subjected to elevated temperature as compared to normal strength concrete. However few researchers have found HPC to perform better in some range of elevated temperatures. The performance of HPC depends on the constituent materials used to make HPC. Cement type and cement blend, high temperature conditions are few factors that have been found to influence the behaviour of concrete under elevated temperatures to a considerable extent.

Various researchers have reported increase in the strength properties of concrete, in the range of 100°C-300°C. This is due to the fact that formation of tobermorite (a product of lime and pozzolana at high pressure and temperature), which is reported to be two to three times stronger than the Calcium Silicate Hydrate (C-S-H) gel. Above 300°C, there is uniformity in opinions of various researches about the decrease in strength with increase in exposure temperature. Upto 600°C exposure temperature, FA and GGBFS based concrete mixes show, better performance due to the reduced amount of Ca(OH)₂. The pozzolanic materials such as GGBFS and FA are found to be beneficial in retaining higher residual compressive strength of HPC exposed to elevated temperature.

There are a few forensic engineering techniques that can be used by a structural or material engineer in order to assess residual properties of the fire damaged structures. The conventional UPV test qualitatively assesses the level of degradation of concrete, whereas the new techniques like drilling resistances can be used for assessing the thermally damaged concrete structure.

Many researchers have used various techniques; however the accuracy of each technique in assessing the residual strength after elevated temperature exposure is not clear from the literature. The correlation between the test results of various techniques and residual strength is not very clear. There is a need to develop some models that relate the indirect properties of concrete to its residual strength after elevated temperature exposure.

2.5 NEED FOR EXTENDING AND REFINING THE UNDERSTANDING OF HPC BEHAVIOUR AT ELEVATED TEMPERATURE

Based on the review of literature, following broad comments can be made on our understanding of HPC subjected to elevated temperatures. Various parameters such as exposure temperature, exposure duration and use of pozzolanic material, affects the physical and mechanical properties of HPC when subjected to elevated temperatures.

High performance concrete with pozzolanic materials has yielded encouraging results in terms of strength and durability characteristics. Nevertheless investigation of their performance at elevated temperatures is necessary. Very little work has been reported on heat resistant characteristics of concrete mixes with pozzolanic material blends at elevated temperatures. Available relationships for strength assessment of concrete exposed to elevated temperatures ignore the exposure duration and blend effects on residual strengths, hence, need refinement. In addition to understanding of strength and limitations of destructive and non-destructive testing in vogue, potential application of drilling resistance and sound test need to be investigated and exploited.

The need for better understanding the performance of blended HPC at elevated temperatures has been elaborated and the potential for including and exploiting drilling resistance and sound level tests for performance appraisal have been highlighted. Review of literature reveals that work in this direction is scarce and scattered and hence offers scope for further investigation as the one undertaken, which has been detailed in the following section.

2.6 OBJECTIVES OF PRESENT INVESTIGATION

In light of the need outlined and possible means, modes and methods discussed, the following objectives have been proposed for the research.

1. Detailed experimental investigation on effect of elevated temperatures on physical, compressive and splitting tensile strength properties of HPC (M70) with supplementary cementitious materials such as fly ash and ground granulated blast furnace slag and their performance appraisal vis a vis HPC without blends.
2. To perform drilling resistance test and recording of sound levels associated with drilling resistance test and impact echo on specimen, for data acquisition on strength and heat penetration resistance characteristics.

3. Core extraction from plain concrete and reinforced concrete specimen made of HPC exposed to elevated temperatures and determination of porosity and residual compressive strength.
4. Development of residual strength prediction equations and evaluation methods based on data acquired from experimental investigation.

CHAPTER 3

MATERIALS AND METHODS

3.1 GENERAL

The present investigation is undertaken to study the performance of HPC blends at elevated temperatures and for assessment of residual strength of concrete exposed to elevated temperature by various methods. This chapter describes the details regarding qualification of the constituent materials, concrete mix design, preparation and exposure of test specimens to elevated temperatures. The procedure followed to explore the effect of elevated temperatures and retention periods on blended HPC and also assessment of residual strength of concrete exposed to elevated temperatures by drilling resistance and core recovery tests are presented in this chapter.

3.2 MATERIALS

The basic ingredients of HPC should possess certain specific properties and requirements. The performance and quality of each ingredient has critical influence on the properties of HPC. Thus it becomes very essential to study the properties and characteristics of the ingredients before selecting them for proportioning of mix. The properties of materials used for different HPC mixes in the present investigation are explained in the following sections.

3.2.1 Cement

In this investigation commercially available 43 grade Ordinary Portland Cement (OPC) conforming to IS: 8112-1989 has been used. The cement was tested for its physical properties according to IS: 4031-1988 (part I to IV). The average compressive strength of three mortar cubes (area of face 50 cm^2) composed of one part of cement, three parts of standard sand (conforming to IS 650 : 1966) by mass

and $(P/4+3)$ percentage (of combined mass of cement and sand) water were prepared, stored and tested in the manner described in IS 4031. The test results are presented in Table 3.1. The cement was tested for the chemical composition according to IS: 4032:1985. The mean of three test results are presented in Table 3.2.

Table 3.1: Physical properties of cement

Sl. No.	Properties	Results	IS Specification
1	Specific gravity (Le-Chatelier's flask)	3.1	Not specified
2	Standard consistency (Vicat's apparatus) (P), %	30	Not specified
3	Fineness (Blaine's Air permeability), m^2/kg	327	225 (Min)
4	Initial setting time (Vicat's apparatus), minutes	60	30 (Min)
5	Final setting time, (Vicat's apparatus) minutes	245	600 (Max)
6	Soundness (Le-Chatelier's), mm	2	10 (Max)
7	Average compressive strength, MPa		
	3 days	31	23 (Min)
	7 days	39	33 (Min)
	28 days	56	43 (Min)

Table 3.2: Chemical composition of cement

Chemical composition	Results, %
Calcium oxide, CaO	63.5
Silica, SiO ₂	21.7
Alumina, Al ₂ O ₃	6.6
Ferric oxide, Fe ₂ O ₃	4.6
Magnesia, MgO	2.4
Alkali content, Na ₂ O	0.4
Sulfuric unhydrate, SO ₃	1.1
Insoluble residue	0.5
Loss on ignition	1.5

3.2.2 Fine and Coarse Aggregate

Fine aggregate (sand) was sourced from local river. The grading of fine aggregates conforms to Zone - III of IS 2386-1975. The particle size distribution as determined by sieve analysis is given in Table 3.3. The grading curve is indicated in Fig. 3.1. The specific gravity and fineness modulus of sand were found to be 2.65 and 2.33 respectively. The water absorption in dry state and compacted bulk density were found to be 1.5 % and 1600 kg/m³ respectively.

Table 3.3: Sieve analysis of fine aggregate

Sieve size (mm)	Weight retained (gm.)	Cumulative weight retained (gm.)	Cumulative % weight retained	Cumulative % finer	Range for Zone-III (IS 383-1970)
10	0	0	0	100	100-100
4.75	10	10	1.0	99.0	90-100
2.36	38	48	4.8	95.2	85-100
1.18	66	114	11.4	88.6	75-100
0.60	180	294	29.4	70.6	60-79
0.30	578	872	87.2	12.8	12-40
0.15	124	996	99.6	0.4	0-10
Pan	4	1000		-	-

The siliceous coarse aggregates of 20 mm and 12.5 mm size were obtained from local quarries and were taken in 1:1 proportion to make graded aggregate conforming to IS 383-1970 which is presented in Table 3.4. The specific gravity was found to be 2.67 and fineness modulus of coarse aggregate was 7.20. The water absorption in dry state was found to be 0.5%. Compacted bulk densities were found to be 1413 kg/m³ and 1459 kg/m³ for 20 mm and 12.5 mm size respectively.

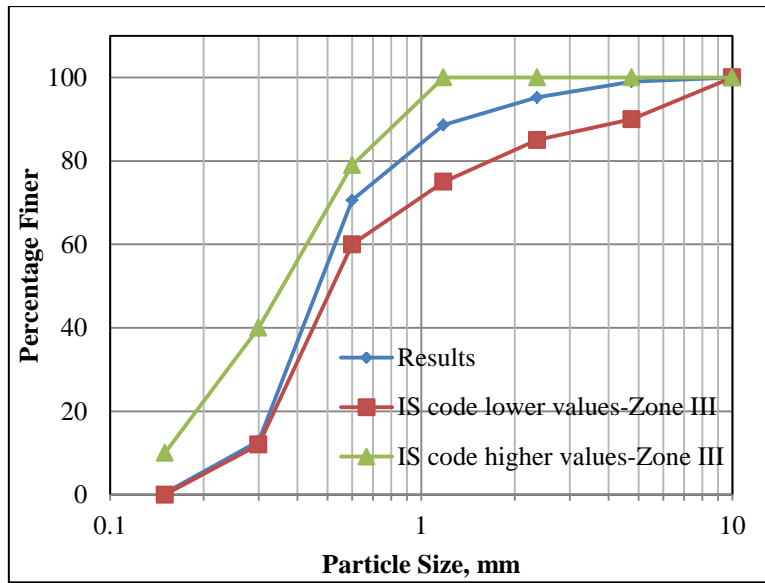


Fig. 3.1: Grading curve for fine aggregate

Table 3.4: Sieve analysis of coarse aggregate

I.S sieve size, (mm)	Percentage passing	I.S 383-1970 grading requirements		Remarks
		I % passing for single sized aggregate	II % passing for graded aggregate	
40	100.0	100	100	Satisfies graded size aggregate requirements
20	95.0	85-100	95-100	
10	40.0	0-20	25-55	
4.75	1.1	0-5	0-10	

3.2.3 Supplementary Cementitious Materials

In present investigation GGBFS and FA have been used as partial replacement to cement on mass by mass basis. Due to improved access to these materials, concrete producers can combine two or more of these materials to optimize concrete properties. Ground granulated blast furnace slag from M/s JSW Cement Ltd. was used which confirms to BS: 6699. Fly ash from M/s Raichur Thermal Power Station, Shakthinagar, Karnataka, has been used for the present investigation, which falls

under siliceous based fly ash as per IS 3812-2003. The physical properties and chemical composition of the above materials were presented in Table 3.5.

Table 3.5: Physical properties and chemical composition of SCM

Characteristics	GGBFS	FA
Physical Property		
Specific Gravity (Le-Chatelier's flask)	2.9	2.2
Fineness (Blaine's Air permeability), m ² /kg	410	290
Bulk Density, kg/m ³	1000-1100	1100-1200
Colour (Visual observation)	Cream white	Light grey
Chemical Composition (%)		
CaO	40.0	2.2
SiO ₂	35.0	56.7
Al ₂ O ₃	12.0	27.4
Fe ₂ O ₃	0.2	4.8
MgO	10.0	0.6

3.2.4 Superplasticizer

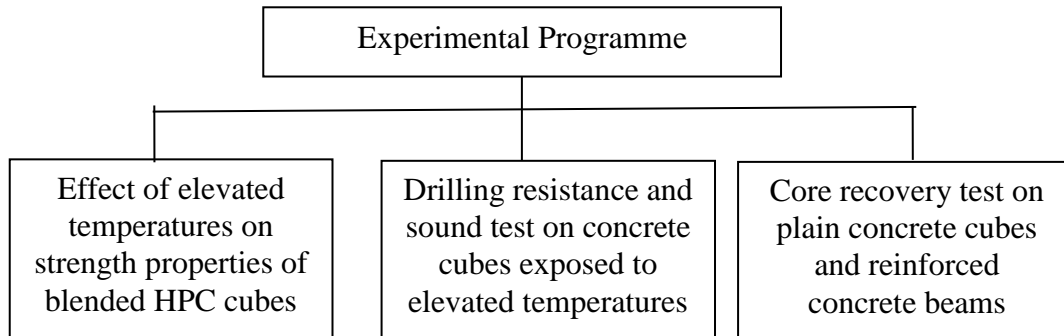
Sulphonated naphthalene polymer based High Range Water Reducing Admixture (HRWRA) was used. The specific gravity of HRWRA was 1.18. This HRWRA was a brown liquid and containing 41.34% solids.

3.2.5 Water

Water is an important ingredient of concrete as it actively participates in chemical hydration reaction of cement and pozzolanic reaction. In this investigation, potable water has been used for producing concrete and curing.

3.3 METHODOLOGY

Experimental programme was carried out in three phases as shown in flow chart.



The first phase of experimental programme was to study the effect of elevated temperatures on physical, compressive and splitting tensile strength properties of blended HPC. Second phase of experimental programme presents the results of drilling resistance test on concrete exposed to elevated temperatures. The determination of residual compressive strength of plain and reinforced concrete elements exposed to elevated temperatures by core recovery test have been detailed in third phase of experimental programme. The detailed experimental methodology has been presented in the following selection.

3.3.1 Concrete Mix Design

High performance concrete prepared with Ordinary Portland Cement (OPC), is referred to as HPC-O for ease of analysis and presentation. It was planned to design the HPC mix without silica fume because the fire behaviour of HPC with silica fume appeared to be worse than the concrete made with OPC as reported by researchers (Sarshar, and Khoury, 1993, Kodur and Sultan 2003). Thus, in the present investigation HPC is prepared with GGBFS and FA as a supplementary cementitious material. One mix prepared with partial replacement cement by 30% of GGBFS, is referred to as HPC-G. Second mix prepared with partial replacement cement by 30% of FA, is referred as HPC-F. The third mix prepared with partial replacement cement by equal combination of GGBFS and FA at 15% individually, is termed to as HPC-G-F.

High performance concrete has been designed for 28 days compressive strength of 70 MPa and slump of greater than 170 mm. These were prefixed designed levels. The test results are tabulated in Appendix I (A-1). The mix design involves the right selection of water/cement ratio. Then, quantity of water and cement were determined. The volume of entrapped air was assumed to be 2%. The coarse aggregate and fine aggregates were determined from the absolute volume basis. The proportions of GGBFS and FA are obtained by modifying the mix design calculations without altering the binder content. The final mix proportions were arrived at, after having several trials so as to obtain a slump more than 170 mm at a constant water–binder ratio (w/b) of 0.28. The slump was adjusted by adding different dosages of the superplasticizer. The mix proportions adopted are detailed in Table 3.6. Figure 3.2 shows obtained slumps for different mixes.

Table 3.6: Mix proportion per cubic meter of concrete

Mix Designation	OPC (kg)	GG-BFS (kg)	Fly ash (kg)	Fine aggregate (kg)	Coarse aggregate (kg)		Free water (kg)	Super-plasticizer (% by weight of binder)
					12.5 (mm)	20 (mm)		
HPC- O	500	--	--	630	589	589	140	2.0
HPC- G	350	150	--	626	590	590	140	1.6
HPC- F	350	--	150	611	572	572	140	1.6
HPC-G-F	350	75	75	619	579	579	140	1.6

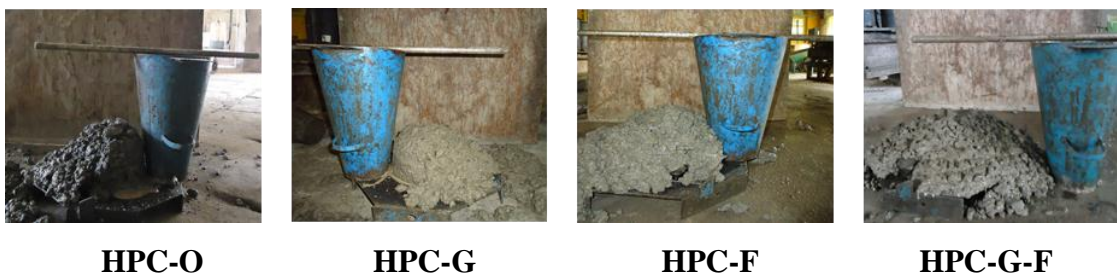
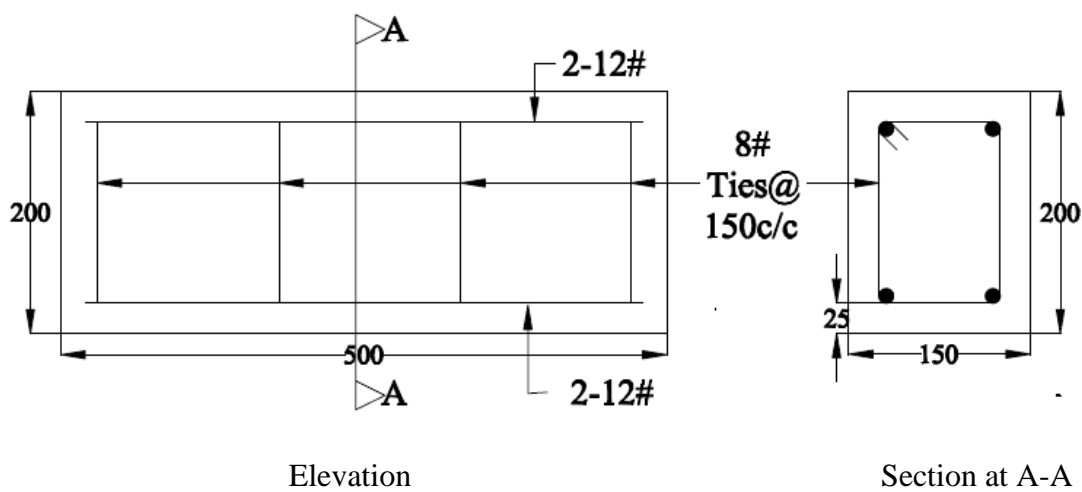


Fig. 3.2: Slump for different mixes

3.3.2 Preparation of Specimen

A horizontal shaft mixer was used for preparing the various concrete mixes. The concrete mixing was done as per the ASTM C 192- 90 a (1994). Compaction of concrete was done by using table vibrator. Then concrete cubes of size 100 mm× 100mm× 100 mm were cast and cured in water for 28 days. To study the effect of elevated temperatures and retention periods on HPC, 800 numbers (200 numbers for each of the above mix) of cubes were prepared. The details of test matrix are tabulated in Appendix I (A-2).

For assessment of residual strength of concrete exposed to elevated temperature by drilling resistance and core recovery test, 100 numbers of HPC-O mix concrete cubes were prepared. For evaluation by core recovery test, 8 numbers of reinforced concrete beam elements of size 150 mm × 200 mm × 500 mm were prepared. As the furnace chamber size is 600 mm × 300 mm × 300 mm, it was proposed to cast Reinforced Cement Concrete beams of size 500 mm × 150 mm × 200 mm. The thickness of the beam was fixed at 150 mm to facilitate extraction of cores 75 mm in diameter and 150 mm in height. Figure 3.3 shows the details of reinforcement. The details of test matrix are presented in Appendix I (A-3 and A-4).



Note: All dimensions are in mm and clear cover to main steel is 25 mm

Fig. 3.3: Details of reinforcement in beam

3.3.3 Exposure to Elevated Temperatures

Electric muffle furnace was used for the exposure of specimens to elevated temperature. After 28 days of curing 100 mm size cube specimens were taken out and air dried. Then specimens were exposed to elevated temperatures. For the first phase of experimental work exposed from 100°C to 800°C, at an interval of 100°C and retained for 1, 2 or 3 hours respectively in a muffle furnace. For the second phase of experimental work 100 mm size cube specimen were exposed from 100°C to 800°C, at an interval of 100°C and retained for only 2 hours of exposure duration.

For the third phase of experimentation, 100 mm size concrete cubes have been exposed to elevated temperatures from 100°C to 800°C, at an interval of 100°C, and retained for only 2 hours of exposure duration at designated temperatures. Reinforced concrete beam was exposed from 200°C to 800°C, at an interval of 100°C, and 2 hours of retention period. Figure 3.4 shows the muffle furnace and arrangement of specimen for exposure. Figure 3.5 shows the time temperature build up curve of muffle furnace.

Necessary precautionary measures were taken during placing of specimen and handling the specimen, such that all the sides of specimen were subjected to uniform temperature. For ensuring this, small pieces of ceramic tiles were placed below the specimen to allow heat from the bottom side also. After exposure to designated temperature the specimen were allowed to cool in the furnace to the room temperature. For cooling, the furnace was switched off and the specimen were left in the furnace until the interior of the furnace reached room temperature, with the furnace door being closed. The details of temperature build up and cooling time, for muffle furnace, for different temperature exposures are tabulated in Appendix I (A-5).



Fig. 3.4: Muffle furnace and arrangement of specimen for exposure

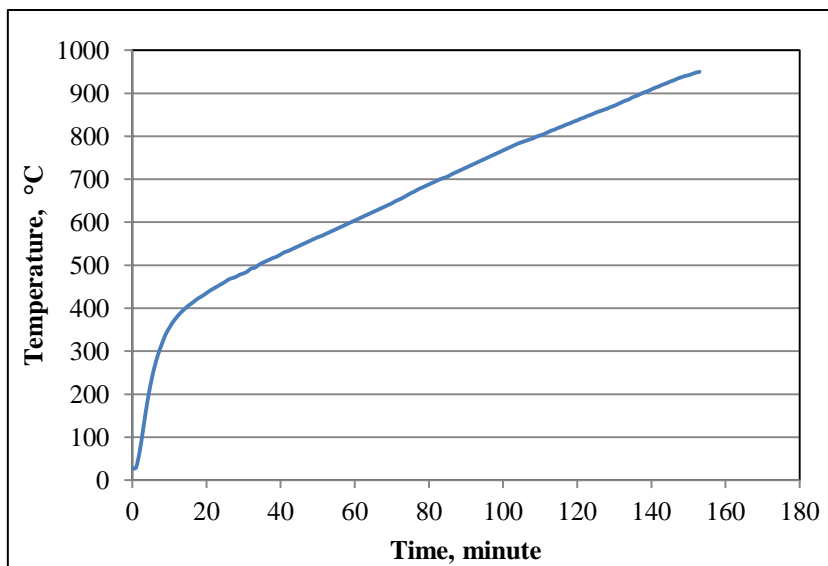


Fig. 3.5: Time temperature build up curve

3.4 TESTS ON EXPOSED CONCRETE SPECIMENS

The details of various testing methodology adopted for experimental study is presented in the following sections.

3.4.1 Performance of HPC Blends at Elevated Temperatures

This section presents the details of evaluation of the performance of HPC blends at elevated temperatures by physical observations, measurement of weight loss, determination of porosity and density, UPV and residual compressive and splitting tensile strength of concrete.

Physical observations

The surface colour image analyses were carried out by capturing the image by using an ordinary digital camera, SONY- 'DSC W-530'. By using the 'Jasc software - paint shop pro 7' the images were analyzed and Red (R), Green (G) and Blue (B) colour space values were measured. This RGB system is perceptually non-linear, non-intuitive and device dependent. However, calibration methods exist to transform the RGB space into a perceptually linear colour space by HIS colour space representing every colour with three components: Hue (H), Saturation (S), Intensity (I).

HIS is a linear transformation from RGB and thus inherits both RGB's device dependency and perceptual non-linearity. By using Gonzalez and Woods (1992) equations RGB values are converted in to HIS values. However after few attempts the resolution of the equipment that was being used could not support the quantification of colour change hence, attempts were given up and surface colour changes have been reported by visual observation.

Crack pattern, propagation and specimen shape deterioration (spalling of concrete) have been subjected to physical observation. Widest surface crack widths and depths

have been measured by crack microscope (Model: Elcometer 900, X50 magnification, shown in Fig. 3.6) having least count 0.02 mm.



Fig. 3.6: Crack microscope

Loss in weight of concrete after exposure

The weight of the specimen was measured before and after exposure to elevated temperature for weight loss evaluation. This allows quantifying the dehydration of concrete after each temperature exposure.

Change in porosity and density of concrete after exposure

Porosity and density of concrete were obtained by using water displacement method. Porosity of concrete was calculated based on the concept of weight gain due to water absorption and weight loss due to buoyancy. Equation 3.1 was used for the calculation of porosity of specimen and Equation 3.2 was used for the determination of density of concrete (Fares, et al. 2009).

$$P = \frac{M_{sat} - M_{dry}}{M_{sat} - M_{sat}^{imm}} \times 100 \quad (3.1)$$

Where,

P = Porosity,

M_{dry} = Mass of dried sample,

M_{sat} = Saturated mass of sample measured in air,

M_{sat}^{imm} = Saturated mass of sample measured in water,

and Density is

$$\rho = \frac{M_{dry}}{V} = \frac{M_{dry}}{M_{sat} - M_{sat}^{imm}} \quad (3.2)$$

After exposure to elevated temperature the specimens were cooled to room temperature and weighed for dry mass. Samples were immersed in water for 24 hours to make complete saturation. High humidity levels of greater than 90% that prevail in this region facilitate complete saturation in 24 hours. The saturated mass in water was determined. Figure 3.7 shows an arrangement made for measuring the submerged weight of specimen. Then the samples were wiped in order to remove the surface excess water, and saturated mass in air were determined. The concrete density ratio was reported as the ratio of density of concrete after exposure to $T^{\circ}\text{C}$ temperature, to the density of concrete at 27°C .



Fig. 3.7: Submerged weight measurement set up

Ultrasonic Pulse Velocity test

The Ultrasonic Pulse Velocity (UPV) test is a well-established popular non-destructive test method that determines the velocity of longitudinal waves through concrete. The Pulse velocity was measured according to IS 13311 (Part-1):1992 by using PUNDIT (Portable Ultrasonic Non Destructive Indicating Tester), UPV device is shown in Fig. 3.8. The transducers used were of 50 mm in diameter and maximum resonant frequency of 54 kHz. On the two sides of cubes the pulse velocity were measured (for one cube, two readings were taken), average of such 3 cubes is reported in this investigation. The UPV ratio (V_r) after heating was expressed as ratio V_T/V_{27} , where V_T is the UPV after exposure to $T^\circ\text{C}$ temperature and V_{27} is the initial UPV of concrete at 27°C .

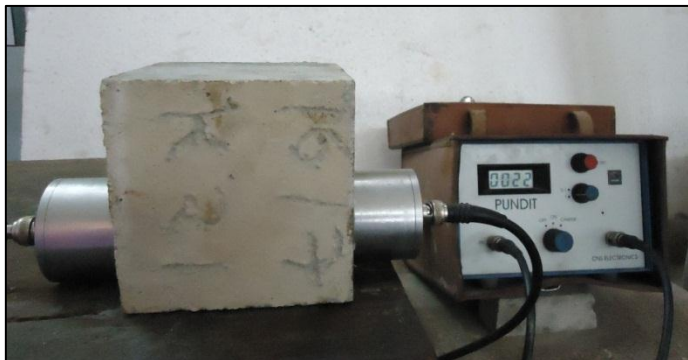


Fig. 3.8: UPV test set up

Compressive strength test

Compression testing machine of 3000 kN capacity was used for this purpose, which is shown in Fig. 3.9. The compressive strength test of concrete was carried as per IS 516 - 1959. The compressive strength ratio (f_{cr}) is expressed as ratio f_{cT}/f_{c27} , where f_{cT} is the compressive strength after exposure to $T^\circ\text{C}$ temperature and f_{c27} is the compressive strength of concrete at 27°C .



Fig 3.9: Compression testing machine

Splitting tensile strength test

Splitting tensile strength is an important property, because cracking in concrete is generally due to tensile stress and the failure in tension is often governed by micro cracking when concrete is exposed to elevated temperature. The splitting tensile strength test of concrete was carried as per IS 5816- 1999. Figure 3.10 shows the splitting tensile strength test setup. The splitting tensile strength ratio (f_{tr}) is expressed as ratio f_{tT}/f_{t27} , where f_{tT} is the splitting tensile strength after exposure to $T^{\circ}\text{C}$ temperature and f_{t27} is the splitting tensile strength of concrete at 27°C .



Fig 3.10: Splitting tensile strength test

3.4.2 Assessment of Residual Strength of Concrete Exposed to Elevated Temperature by Drilling Resistance Test

Drilling resistance test was carried out on a few building materials like wax, brick, wood, granite samples and cement mortar cubes and also on concrete exposed to elevated temperatures. This section presents the details of instruments used and methods adopted for the measurement of drilling time and sound produced during drilling.

Equipment / Instrumentation

Rotary Drilling Machine

Rotary Drill Machine was used for drilling the specimen using continuous thrust mechanism and rotation control. Figure 3.11 shows the rotary drilling machine. It consists of three major units:

1. The drilling unit
2. The water storage and supply unit
3. The hydraulic pump

The drilling unit consists of, a RPM controller and drilling mechanism. The hydraulic pump delivers water and feeds back to the supply unit, which is used by the drilling mechanism unit for applying thrust. The specific drilling work is more or less influenced by number of operational parameters such as bit type and size and shape, rotational speed and exerted thrust and it cannot be strictly regarded as a material constitutive property (Ersoy, and Waller, 1997).

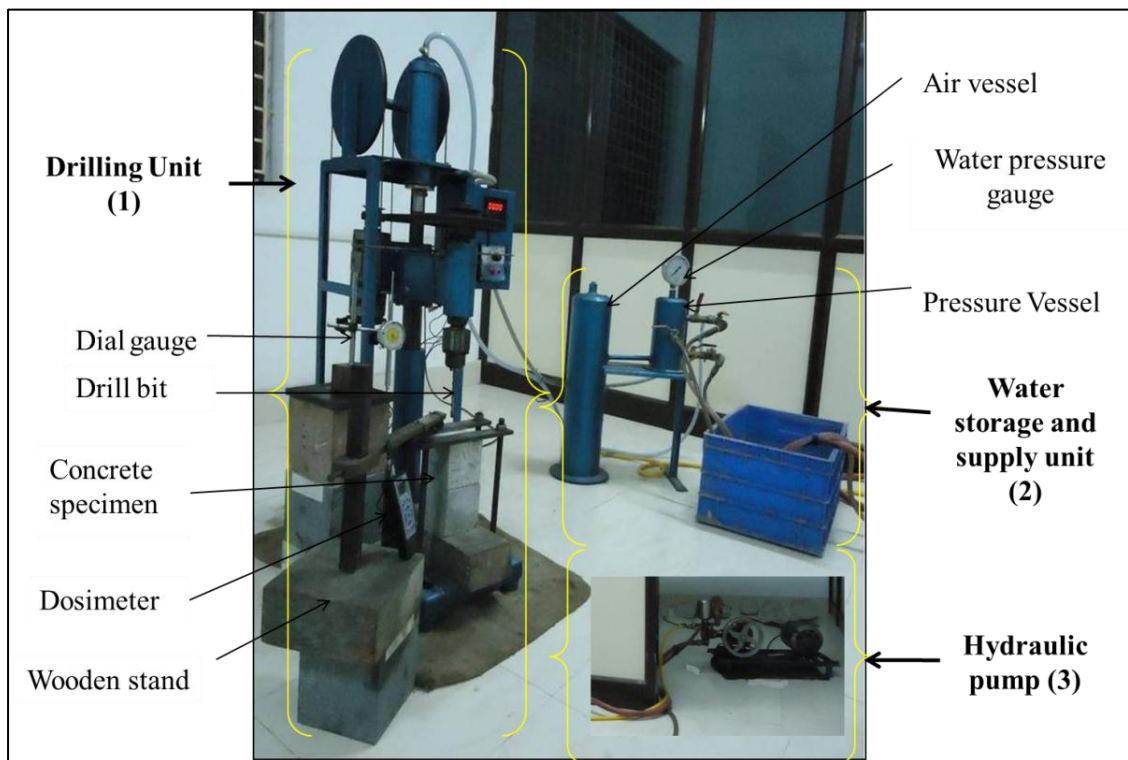


Fig. 3.11: Rotary drilling machine

(Source: Mining Engineering Department, NITK, Surathkal)

Since the drilling method affects drilling time and sound produced, an attempt was made to standardize the testing procedure. Throughout the drilling operation, relatively constant rotational speed and applied thrust was maintained, in order to obtain homogeneous data. Titanium Carbide drill bit of 8 mm diameter and 200 mm shank length was used for drilling operations.

Sound Level Meter

A Dosimeter, (Fig 3.12, Model: Spark 706 from Larson Davis, Inc., USA,) was used for sound measurements. Instrument is equipped with a detachable 10.6 mm microphone and 7.6 cm cylindrical mast type preamplifier. A Larson Davis CAL 200 precision acoustic calibrator was used for calibrating the sound level meter. Before taking sound measurement, the acoustical sensitivity of sound level meter was checked using calibrator.



Fig. 3.12: Dosimeter

(Source: Mining Engineering Department, NITK, Surathkal)

Determination of drilling time

For the determination of drilling time, concrete specimen was kept on drilling platform and clamped in order to avoid displacement while drilling. Figure 3.13 shows the test setup for the determination of drilling time. Drilling time measurements were carried out on specimen at a rotation speed of 300 RPM, and an applied thrust of 14 kg/cm² for building materials and 18 kg/cm² for concrete specimen.

The drilling time in seconds was noted at every 5 mm penetration depth of interval and penetration depth was monitored with the help of a dial gauge. The drilling time were measured on three faces of a cube which are mutually perpendicular to each other. The Drilling time ratio (DT_r) is expressed as ratio DT_T/DT_{27} , where DT_T is the drilling time after exposure to $T^\circ\text{C}$ temperature and DT_{27} is the drilling time of concrete at 27°C



Fig 3.13: Test setup for determination of drilling time
(Source: Mining Engineering Department, NITK, Surathkal)

Measurement of A-weighted equivalent sound level (L_{eq}) and Impact sound level

A-weighted equivalent sound level and impact sound test recording data during drilling resistance test were also carried out to enhance NDT capabilities. The instrument used (Model: Spark 706 from Larson Davis, Inc., USA) measures relative loudness of sound levels better than that perceived by human ear with the inbuilt data acquisition system that assigns weightage to background noise levels.

The A-weighted equivalent sound level, while drilling was recorded by a dosimeter continuously from beginning to 50 mm penetration depth. For this, microphone of dosimeter was placed 15 mm away from the periphery of the drill bit. A-weighted equivalent sound is the equivalent steady sound level of a noise energy averaged over a period. The sound level of 75 dB was recorded without any process of drilling which was mainly due to noise of the hydraulic pump and drilling unit.

Prior to drilling resistance test, impact sound test was carried out by dropping a steel ball of diameter 16 mm and weight 16.31 gram from a height of 1 m on the top of cube to be tested. Figure 3.14 shows steel ball and concrete specimen. With the help of dosimeter, impact sound was measured. The microphone of dosimeter was placed at the edge of the specimen. The background noise was measured to be 56 dB.

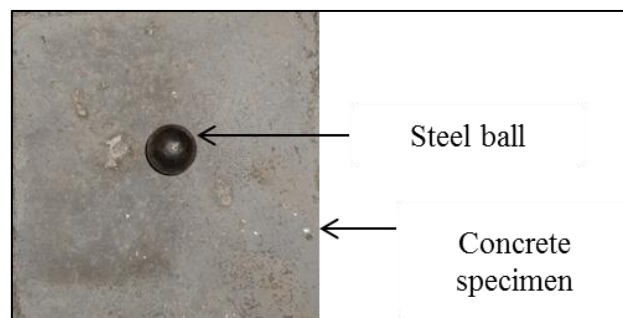


Fig. 3.14: Steel ball and concrete specimen

3.4.3 Residual Compressive Strength of Concrete - Core Recovery Test

Experimental approach carried out for the evaluation of residual compressive strength of plain and reinforced concrete elements exposed to elevated temperature by core recovery test are presented in the following section.

Core recovery test on plain concrete

Horizontal core cutting machine as shown in Fig. 3.15 was used to extract the cores from specimen after exposure to elevated temperature. A titanium carbide core bit was used for core extraction. The core of size 50 mm diameter and 100 mm height were extracted. Figure 3.16 shows extracted core from concrete specimen. Cores extracted from specimen were dried to room temperature and physical appearance was examined. Then cores were tested for compressive strength.

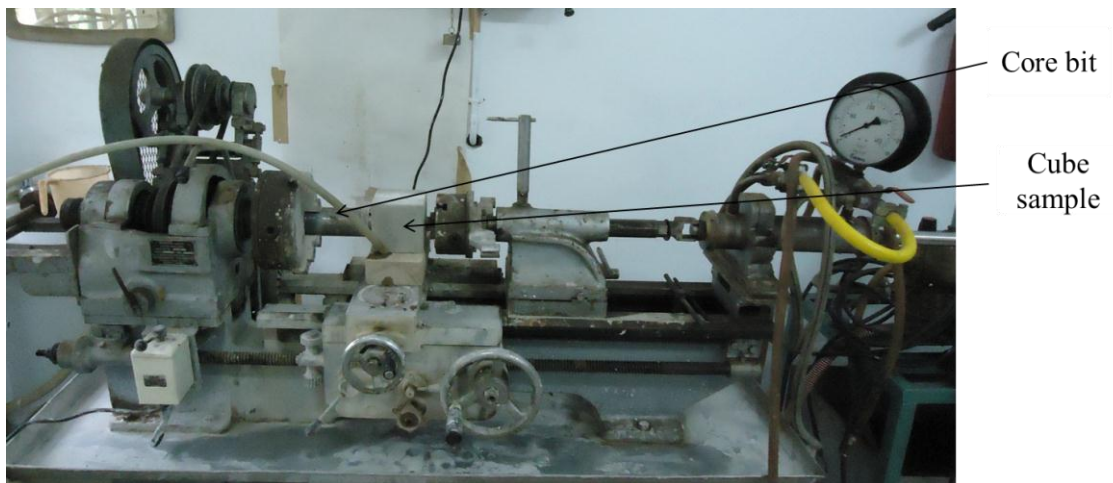


Fig. 3.15: Horizontal core cutter machine

(Source: Mining Engineering Department, NITK, Surathkal)



Fig. 3.16: Concrete core extracted from cube specimen

Core recovery test on reinforced concrete

Vertical core cutting machine was used to extract the cores from beam specimen after exposure to elevated temperature as shown in Fig 3.17. A diamond core bit of size 75 mm diameter \times 450 mm length was used for core extraction. The standard core size (1:2) of 70 mm diameter and 150 mm length were extracted. Then trimming was done with cutting machine and core length was made to 140 mm. Figure 3.18 shows the locations (perpendicular to casting face) where concrete cores were extracted. The porosity and density of core, were determined and UPV test was carried out on cores. Then cores were tested for the compressive strength without capping as core surface was smooth.



Fig. 3.17: Vertical core cutting machine

(Source: Civil Engineering Department, NITK, Surathkal)

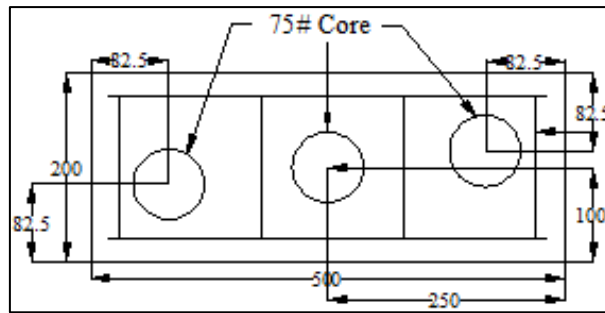


Fig. 3.18: Core extraction locations

3.5 SUMMARY

The basic ingredients of HPC satisfied the specific requirements. Different tests were performed to determine physical and mechanical properties of HPC before and after being subjected to elevated temperature as per standard methods. The assessment of concrete exposed to elevated temperature was carried out by non-destructive testing and partial destructive testing.

CHAPTER 4

STRENGTH PERFORMANCE OF HPC BLENDS AT ELEVATED TEMPERATURES

4.1 GENERAL

Results of experimental investigation on HPC blends at elevated temperatures are presented and discussed in the sections that follow. Statistical analysis of data obtained from tests has also been detailed and residual strength prediction equations have been proposed based on data analysis.

4.2 PHYSICAL OBSERVATIONS OF CONCRETE EXPOSED TO ELEVATED TEMPERATURE

The assessment of concrete exposed to elevated temperature always starts with physical observations such as concrete surface colour change, cracking and spalling patterns. This gives useful preliminary information on exposure levels. Physical observations on specimen exposed to elevated temperatures are presented in the following sections.

4.2.1 Colour Change Pattern - Observations

Surface colour corresponds with specific temperature range and is an important indicator of exposure temperature. Table 4.1 details colour change pattern from visual observation of concrete specimen exposed to elevated temperatures. The colour changes observed visually (i.e. Without aid of any sophisticated equipment or techniques) are similar to those reported by (Lau, 2006 and Arioz, 2009). Short, (2001) attributes colour changes from normal to pink or red to oxidation of compounds in fine and coarse aggregate at temperature level of 300°C and 600°C.

Table 4.1: Colour change in concrete with temperature

Temperature, (°C)	Type of mix			
	HPC-O	HPC-G	HPC-F	HPC-G-F
Up to 200°C	Normal	Normal	Normal	Normal
300°C	Pink	Pink	Pink	Pink
400°C	Brown	Brown	Blackish brown	Blackish brown
600°C	Red	Red	Red	Red
Above 700°C	Buff	Buff	Buff	Buff

4.2.2 Surface Cracking due to Elevated Temperatures

Visible surface cracks and spalling of concrete were not observed on cube specimen, for retention periods of 1 and 2 hours, for temperatures range 100°C-500°C. At 600°C-800°C range, cracks and spalling have been observed. Whereas for retention period of 3 hours, cracking and spalling have been observed at a lower temperature level of 500°C. At 600°C-800°C range, cracking and spalling are more pronounced, indicating that retention period and temperature levels both have important bearing on heat penetration.

Figure 4.1 shows the crack pattern observed at 800°C for different mixes. It can be observed that blended concrete shows less crack density over unblended concrete. Poon, et al. (2001), Xu, (2001) and Li, et al. (2004) in their research findings, have reported that cracks occur on the surface of concrete due to difference in the rates of expansion of aggregates and cement paste. The rehydration of dissociated Ca(OH)_2 is yet another deteriorating reaction in the cement paste at elevated temperatures that contribute to cracking. For blended concrete, unhydrated pozzolana particles react with calcium hydroxide and produce C-S-H like gels. Hence it is inferred that such expansions and dissociation are less in the case of blended concretes in the light of present investigation.

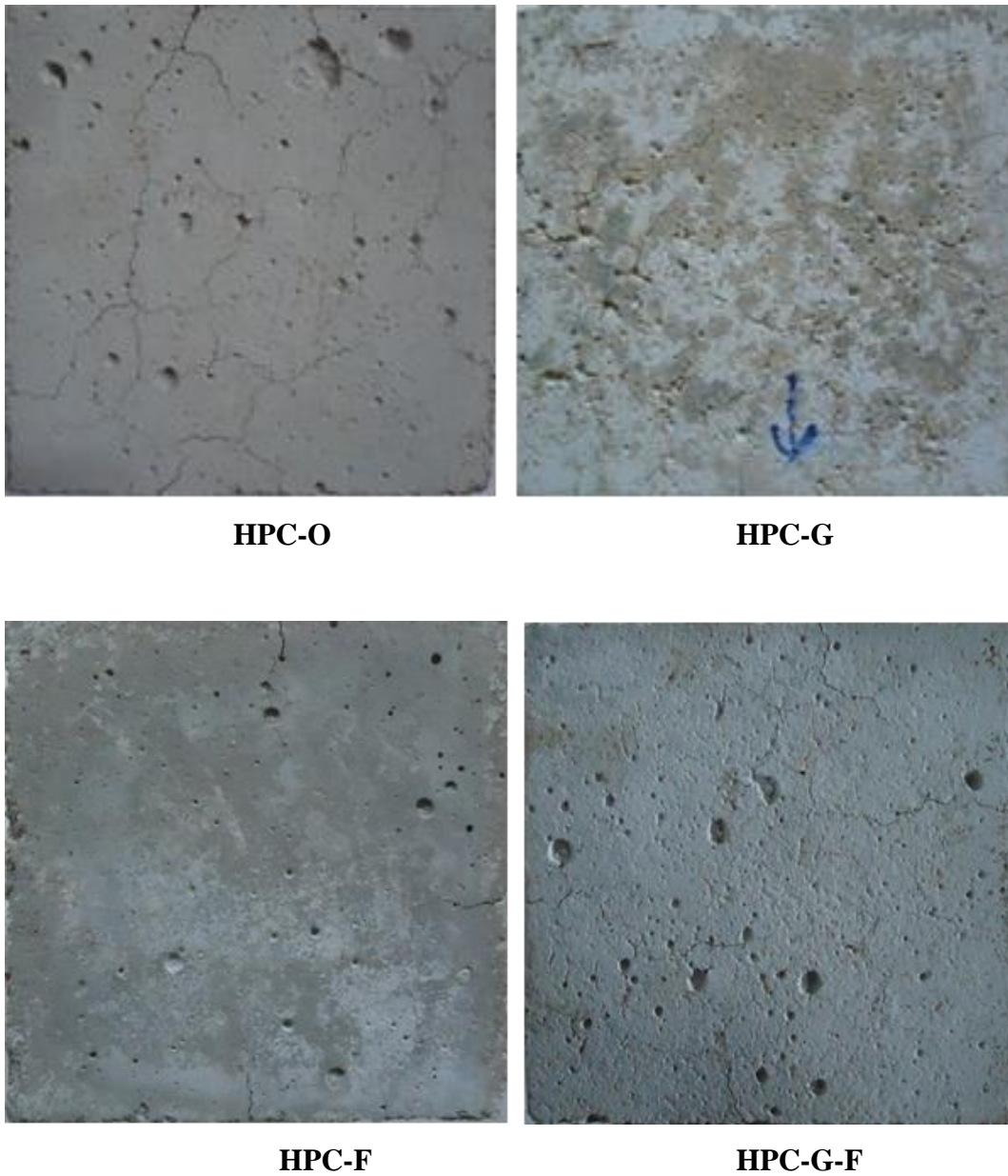


Fig. 4.1: Crack pattern for different mixes at 800°C

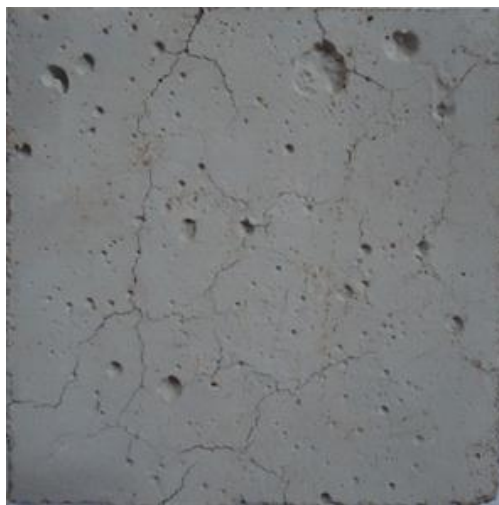
Crack pattern observed for HPC-O mix at 800°C is shown in Fig. 4.2, for different retention periods. It is seen that retention period increases crack density. Table 4.2 presents maximum crack widths measured. Intensity of crack width is more for unblended concrete at all levels of exposure temperatures and retention periods in comparison to blended concretes.



1hour



2 hours



3hours

Fig. 4.2: Crack pattern for HPC-O mix at 800°C

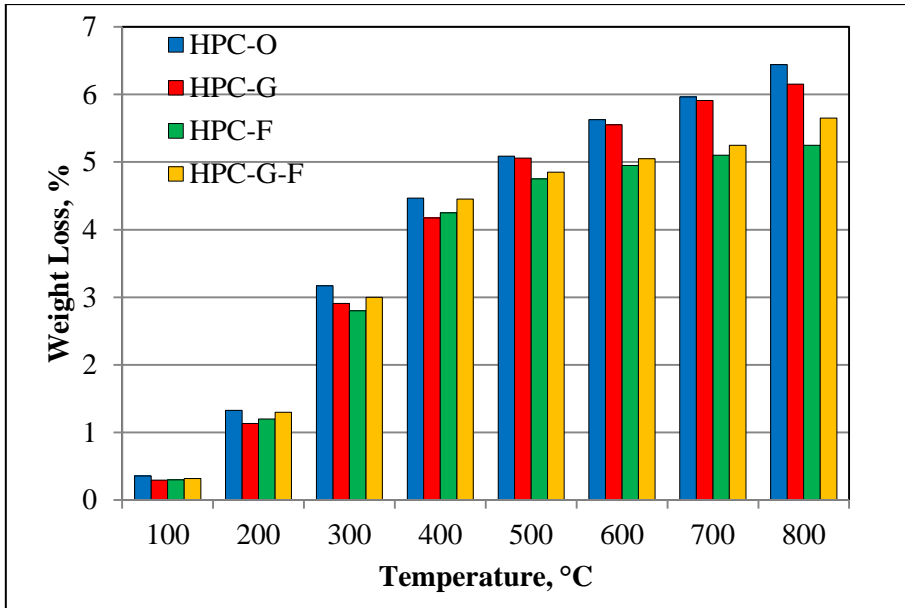
Table 4.2: Maximum width on surface and depth of surface crack for exposed concrete

Temperature, (°C)	Retention Period, (hours)	Crack width and depth, (mm)			
		HPC-O	HPC-G	HPC-F	HPC-G-F
700	1	0.3, 20	0.2, 20	No cracks	0.2, 15
800		0.34, 20	0.2, 20	0.2, 15	0.2, 10
600	2	0.1, 5	0.08, 5	No cracks	No cracks
700		0.3, 30	0.2, 20	0.14, 20	0.16, 20
800		0.4, 30	0.3, 20	0.2, 10	0.3, 20
500	3	0.2, 5	Minor cracks	No cracks	No cracks
600		0.3, 30	0.3, 10	0.2, 15	0.2, 10
700		0.4, 20	0.3, 15	0.2, 15	0.2, 20
800		0.4, 30	0.3, 25	0.2, 20	0.3, 20

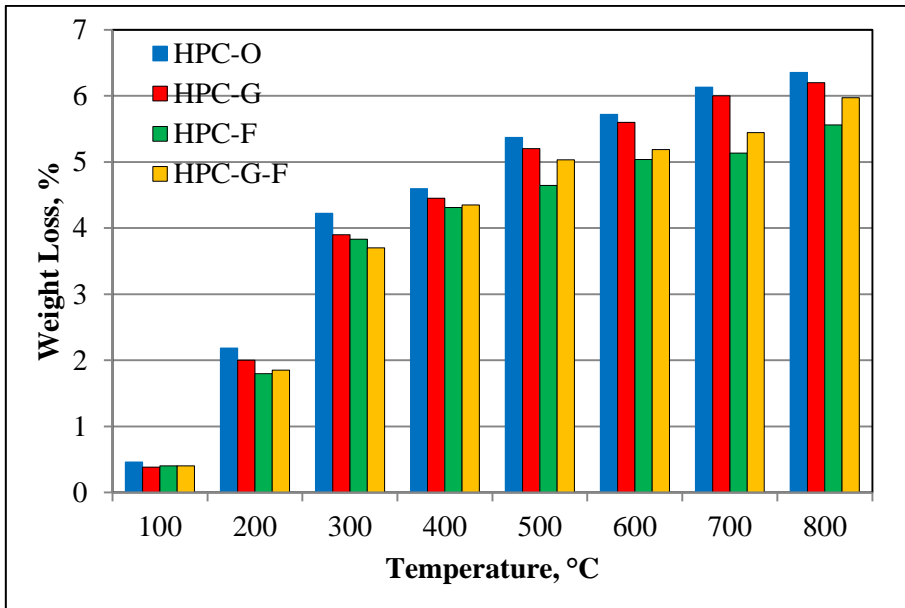
4.3 LOSS IN WEIGHT OF CONCRETE DUE TO ELEVATED TEMPERATURE

The weight loss in concrete due to elevated temperatures can be related to changes in physical properties. The variation of weight with elevated temperatures for different retention periods is presented in Fig 4.3. The test results are tabulated in Appendix II, B-1 to B-6. For all concrete types tested, there is an increase in weight loss with temperature. For 300°C, for retention periods of 1 hour, 2 hours and 3 hours, about 3.5%, 4% and 4.5% loss in weight respectively have been obtained. 5%, 5.35% and 5.5% loss in weight respectively have been reported for 600°C. At 800°C, exposure levels the corresponding weight losses are 5.9%, 6% and 6.3%.

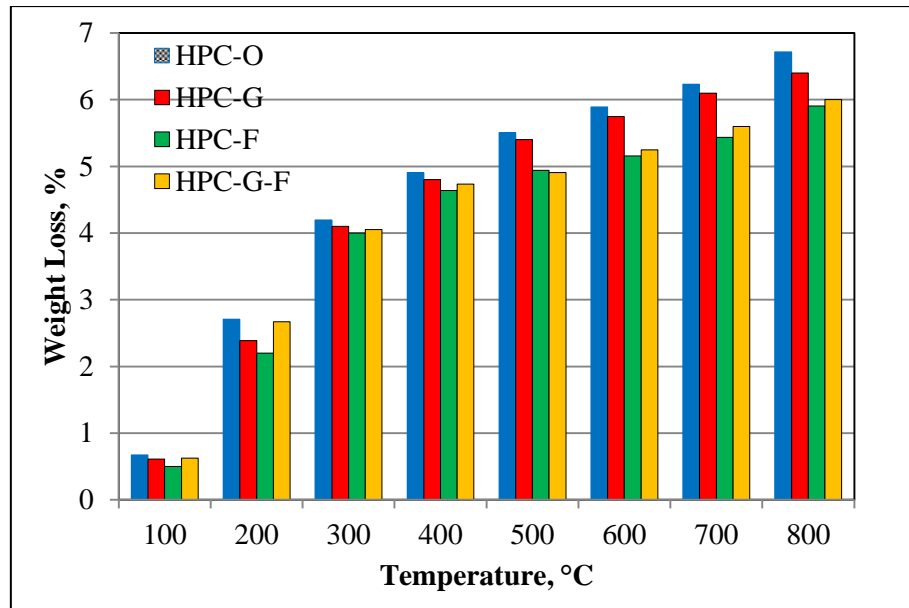
However, in the present work no detailed study was undertaken to attribute the weight loss to any specific case. Losses have been attributed to release of free water contained in the capillary pores and due to change in composition of C-S-H gel and spalling (Noumowe et al., 1996, Arioz, 2007 and Uysal, et al. 2012, Ling et al., 2012).



(a) 1 hour



(b) 2 hours



(c) 3 hours

Fig. 4.3 (a)-(c): Variation in weight loss with temperatures for different retention periods

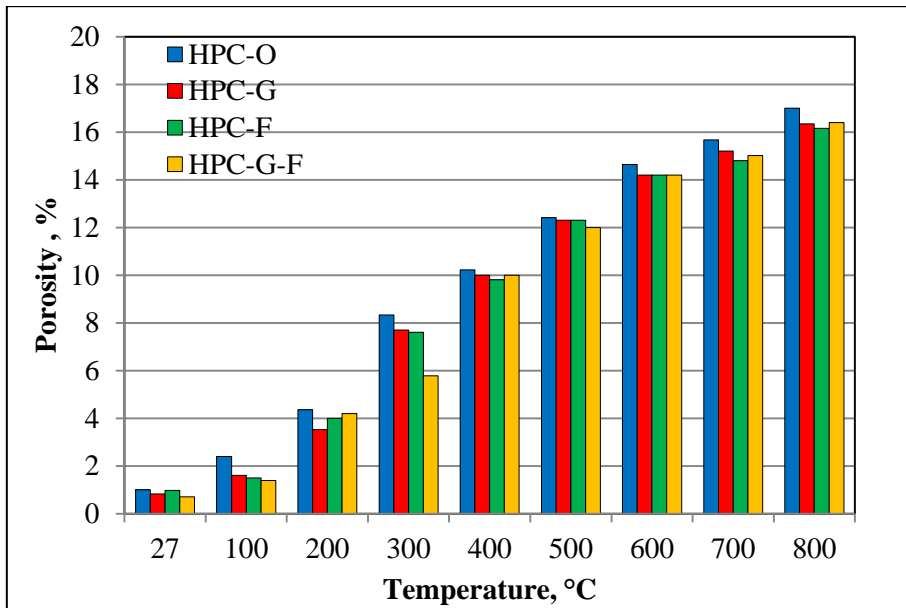
4.4 CHANGES IN POROSITY OF CONCRETE DUE TO ELEVATED TEMPERATURE

Porosity gives indirect information regarding the strength of concrete. Variation in porosity at elevated temperatures for different retention periods has been depicted in Fig. 4.4 (a) – (c). The test results of change in porosity are tabulated in Appendix II, B-7 to B-12. As the temperature increases porosity of concrete increases. For 1 hour retention period the increase in porosity is around 7.3%, 14.3% and 16.4% for 300°C, 600°C and 800°C temperature levels respectively over porosity at ambient temperature level.

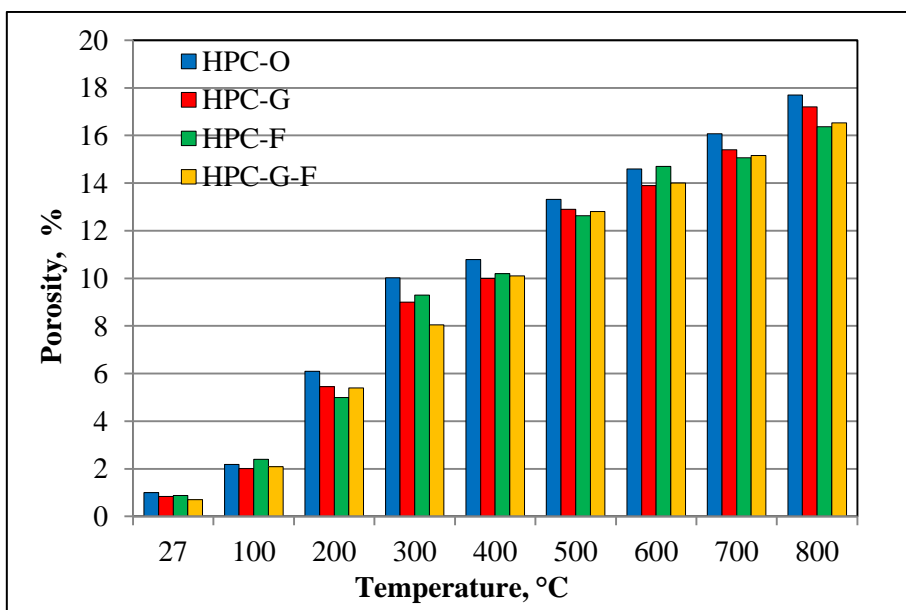
For 2 hours retention period corresponding values are 9.1%, 14.4% and 16.9%. Whereas, 11.2%, 17.6% and 20.6% are porosities for 3 hours retention period.

The porosity increases with temperature observed herein, are consistent with previous works where such losses have been attributed to departure of bound water, micro

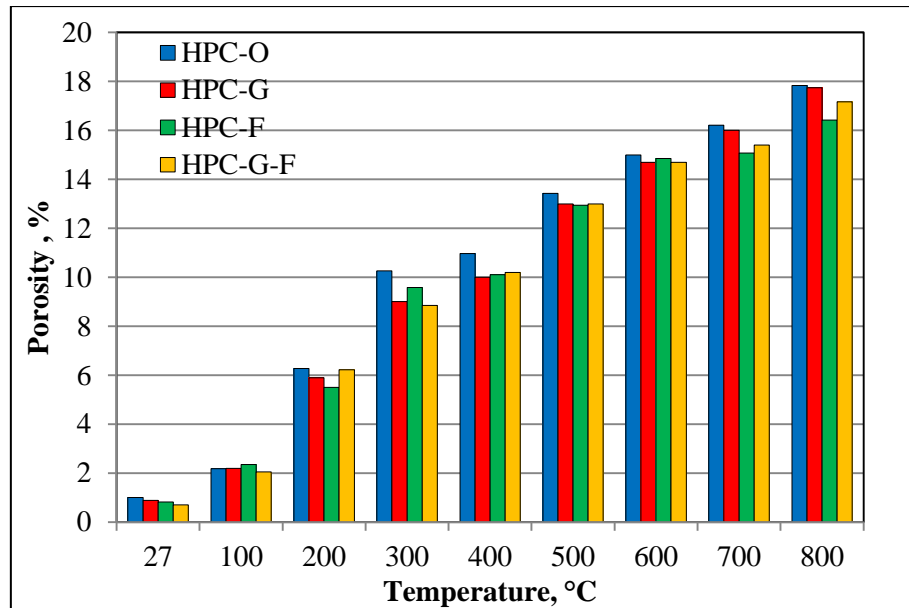
cracking generated by differential expansion between the paste and aggregates and the decomposition of C-S-H and C-H. These transformations create an additional void space in the heated concretes (Noumowe, et al., 1996, Ye, et al., 2007 and Fares, et al., 2009).



(a) 1 hour



(b) 2 hours

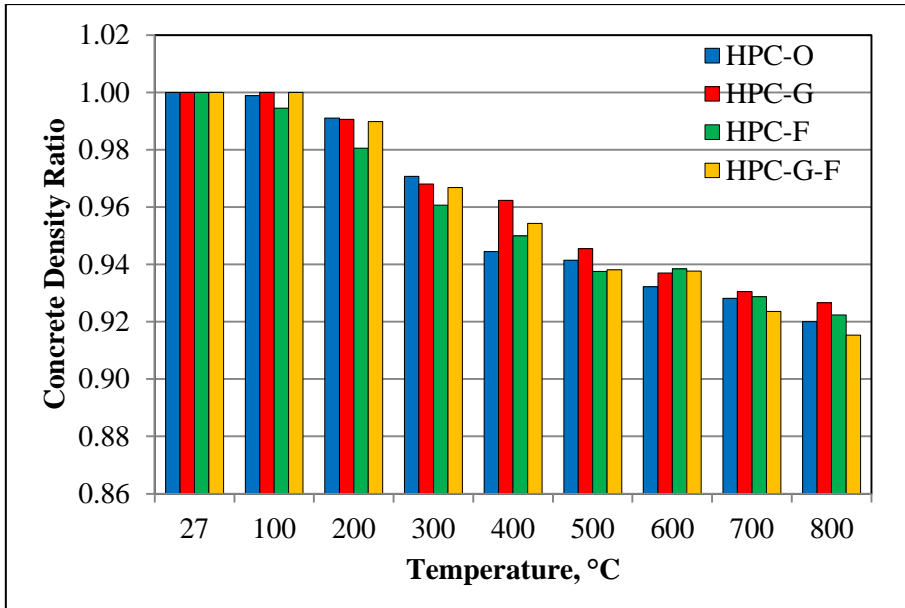


(c) 3 hours

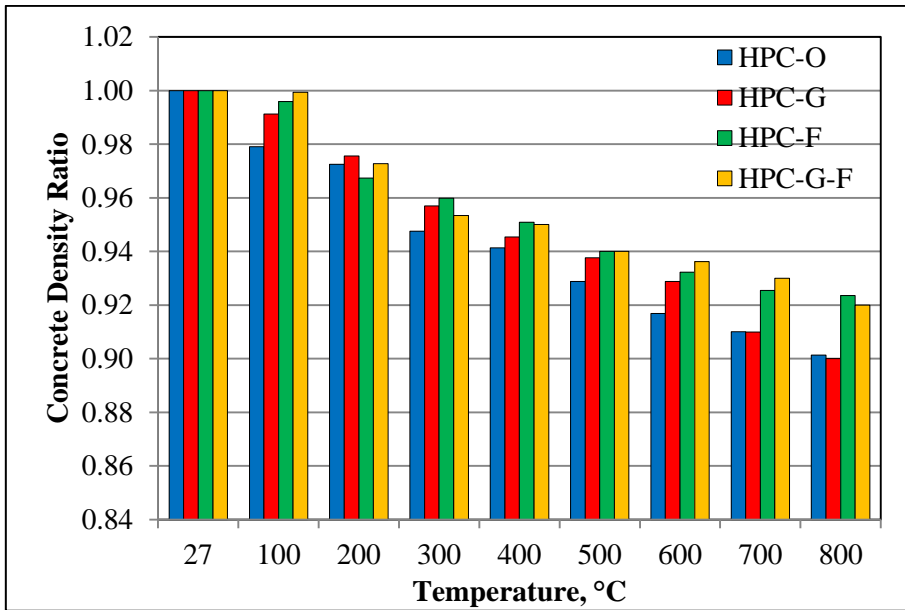
Fig. 4.4 (a)-(c): Variation in porosity with temperatures for different retention periods

4.5 EFFECT OF ELEVATED TEMPERATURE ON CONCRETE DENSITY

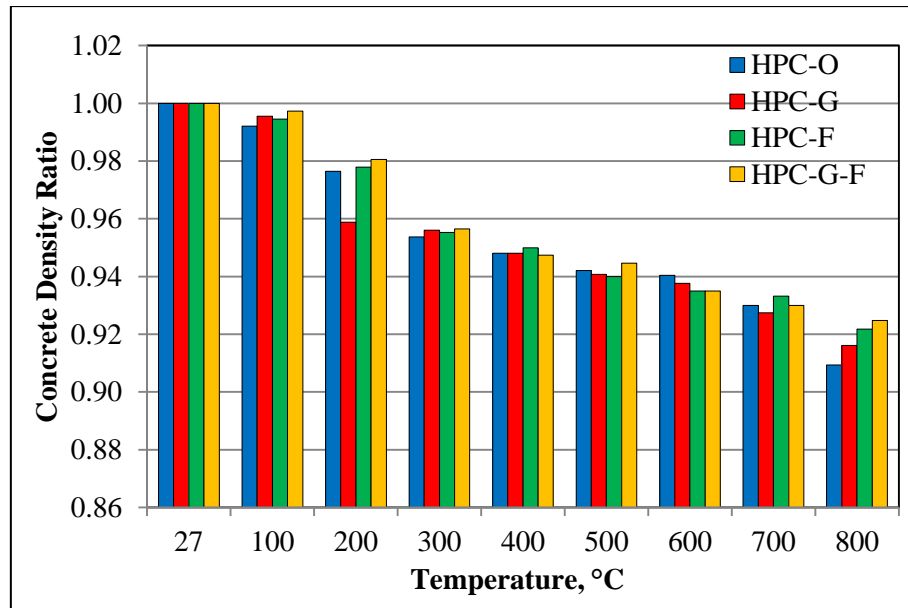
Density determinations have yielded a reduction of 4%, 6% and 8.5% at 300°C, 600°C and 800°C respectively. Bazant and Kaplan, (1996) have reported such density changes attributed to the departure of water during heating (dehydration of hydrates like the C-S-H and portlandite [C-H]) and associated with the thermal expansion of concrete.



(a) 1 hour



(b) 2 hours



(c) 3 hours

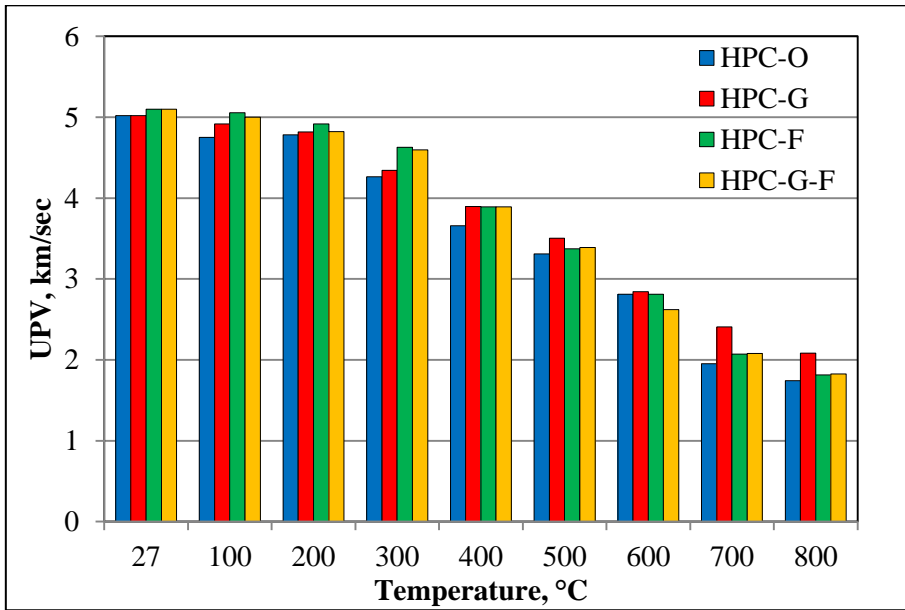
Fig. 4.5 (a)-(c): Variation in concrete density ratio with temperatures for different retention periods

4.6 UPV RECORDINGS IN EVALUATION OF CONCRETE EXPOSED TO ELEVATED TEMPERATURE

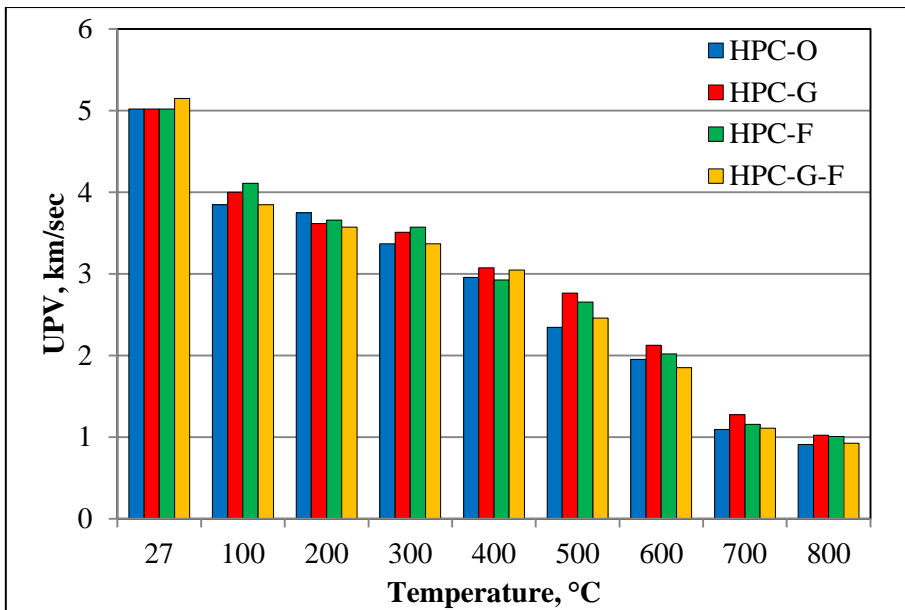
The UPV test is a well-established popular non-destructive test method that determines the velocity of longitudinal waves through concrete. UPV indirectly indicates the quality of concrete. UPV recordings obtained in the current investigation are shown in Fig. 4.6 (a) – (c). The test results of UPV are tabulated in Appendix II, B-13 to B-15.

All concrete mixes show reduction in UPV with an increase in exposure temperature and retention period. For ambient temperature level UPV is around 5 km/sec. Whereas, for 1 hour retention period at 300°C, 600°C and 800°C exposure levels, a reduced UPVs of 3.8, 2.35 and 2 km/sec have been recorded respectively.

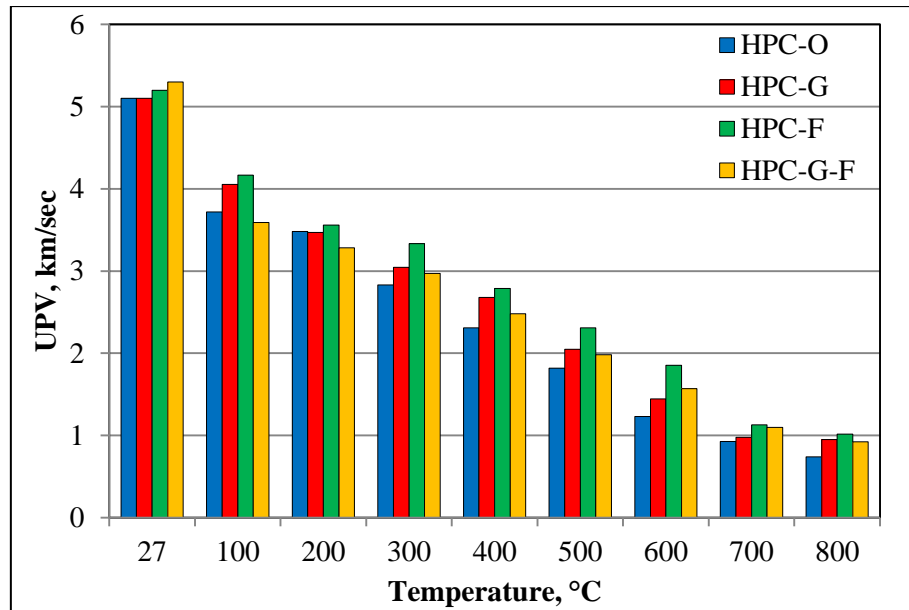
For retention period of 2 hours UPV ranges from 4 km/sec at 100°C to 1 km/sec at 800°C. And for 3 hours retention at 800°C UPV is 0.9 km/sec. Unblended concrete shows more reduction in UPV than blended.



(a) 1 hour



(b) 2 hours



(c) 3 hours

Fig. 4.6 (a)-(c): Variation in UPV with temperatures for different retention periods

Relative performances of blended and unblended concretes with reference to UPV recordings for various temperatures and retention periods are given in Fig. 4.7 (a) – (d). It is evident that, pulse velocity characteristics deteriorate in unblended concretes more than the blended counterparts. Transmission of pulse waves through the concrete mass is highly influenced by micro cracking. Disintegration of C-S-H gel at temperatures above 600°C increases the amount of air voids and decreases the transmission speed of sound waves. These observations are consistent to findings of Arioz, (2009) and Yang, et al., (2009).

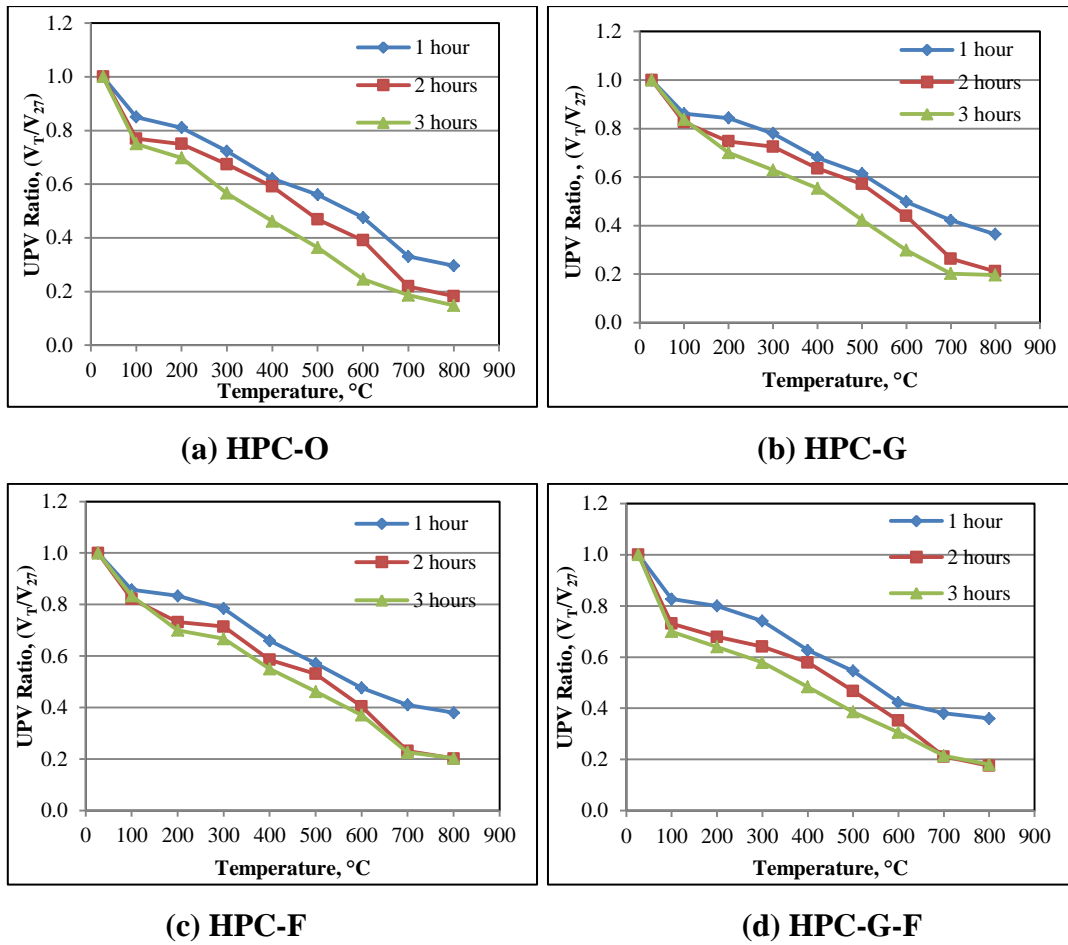
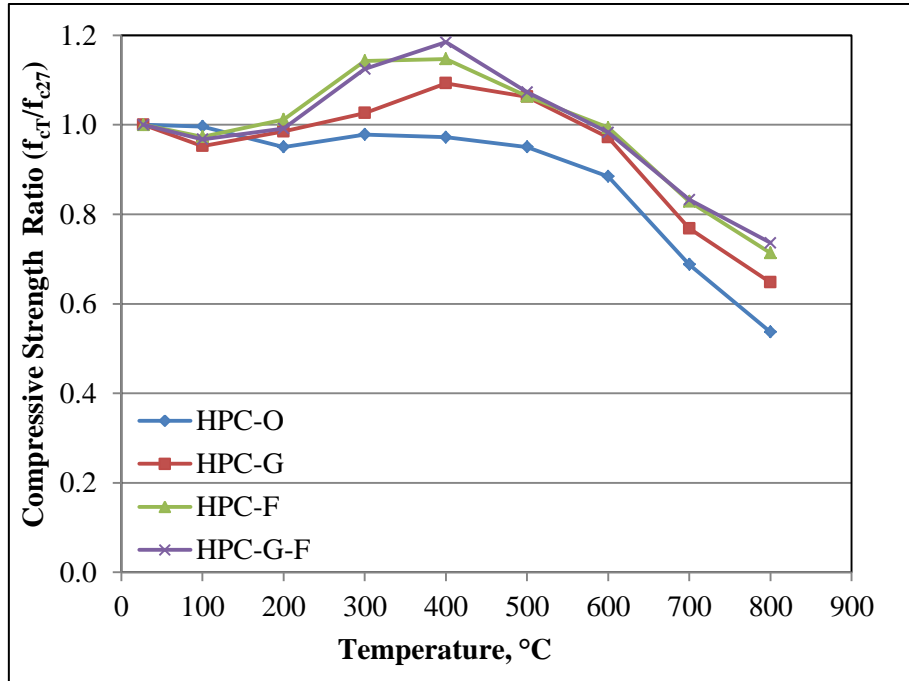


Fig. 4.7 (a)-(d): Variation in UPV ratio with temperature for different mixes

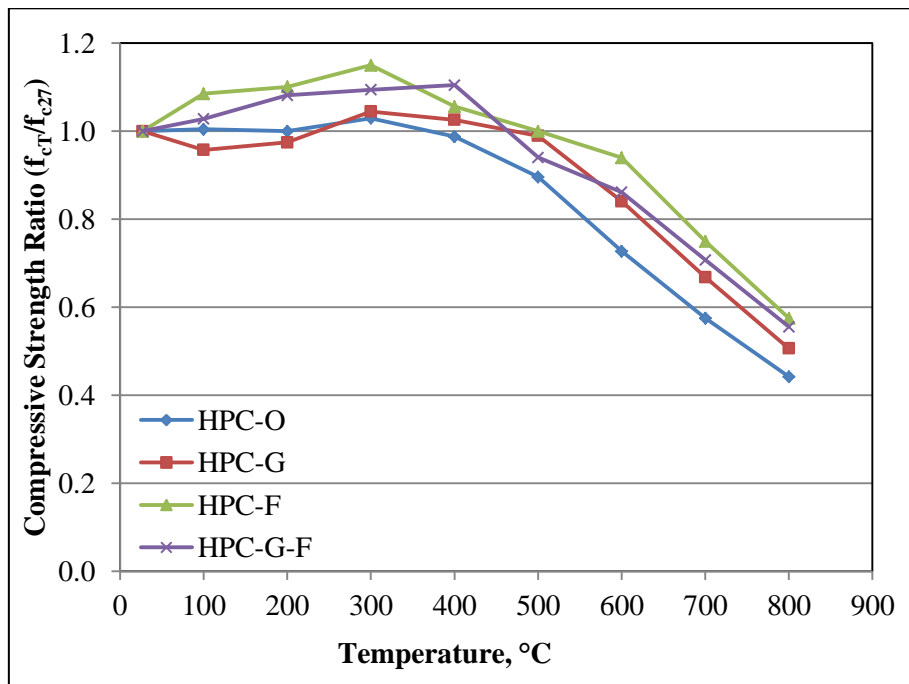
4.7 STRENGTH RETENTION CHARACTERISTICS OF CONCRETE BLENDS

Compressive strength of concrete has a significant influence on the performance of concrete members when exposed to elevated temperature. The test results of compressive strength are tabulated in Appendix II, B-16 to B-21. It is found that for 300 $^{\circ}\text{C}$ exposure temperature, unblended concrete shows 2% decrease in compressive strength, whereas blended shows an increase of 10%, as presented in Fig. 4.8(a), for 1 hour retention. For 600 $^{\circ}\text{C}$, unblended concrete reports 12% reduction in compressive strength whereas blended has retained its strength. 46% and 30% reduction in compressive strength are observed respectively for unblended and blended concretes for 800 $^{\circ}\text{C}$ exposure level.

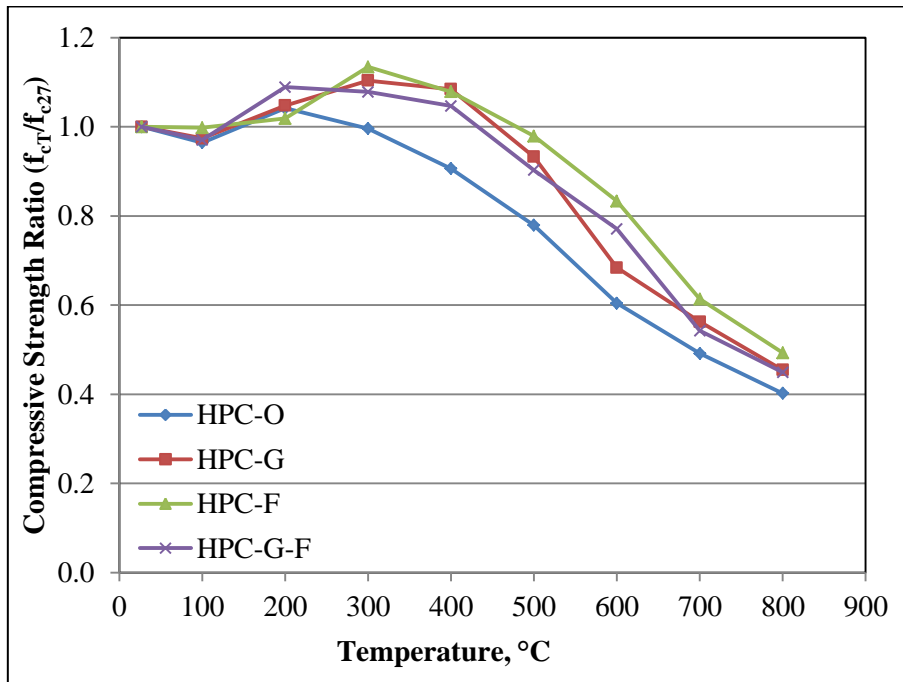
Trends for 2 hours and 3 hours retention periods are shown in Fig. 4.8 (b) and (c), and it is seen that strength reductions are more for higher durations of exposure.



(a) 1 hour



(b) 2 hours



(c) 3 hours

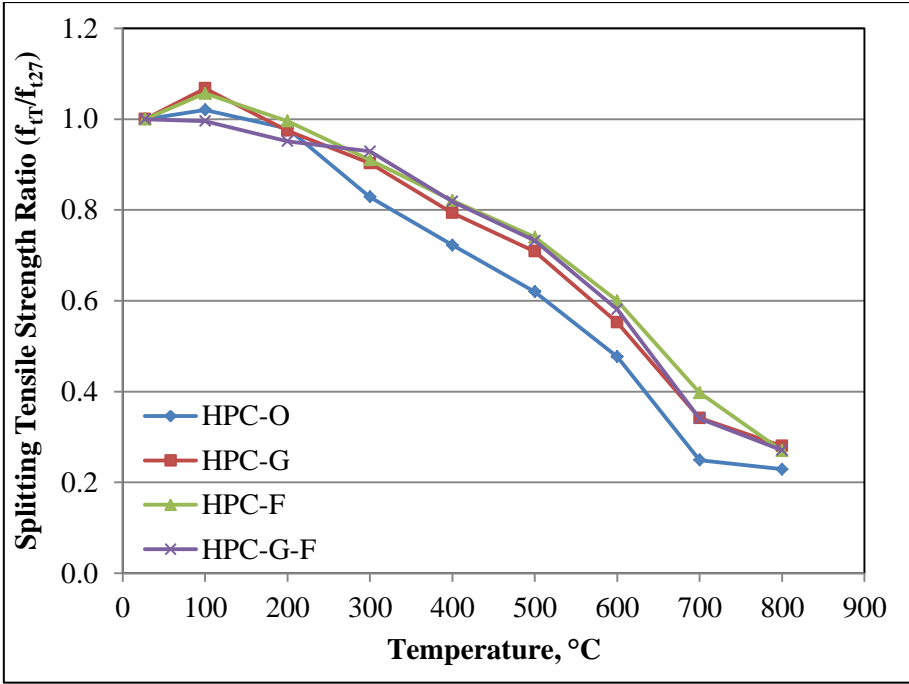
Fig. 4.8 (a)-(c): Variation in compressive strength ratio with temperatures for different retention periods

The observations made here are in agreement with the studies of (Khoury, 1992, Xu, et al. 2001, Poon, et al., 2001 and Savva, et al. 2005). The increase in compressive strength at levels up to 250°C is due to the increase in surface forces between the gel particles (Van der Waals forces) due to the removal of moisture content as reported by Khoury (1992). There is uniformity in opinion in the previous studies have shown that, rise in compressive strength which occurs after exposure to 250°C, is due to the hardening of cement paste caused by drying and further hydration of unhydrated cementitious materials which fills the pores result of pozzolanic reaction to form denser and closure structure (Xu, et al. 2001, Savva, et al., 2005, Husem, 2006).

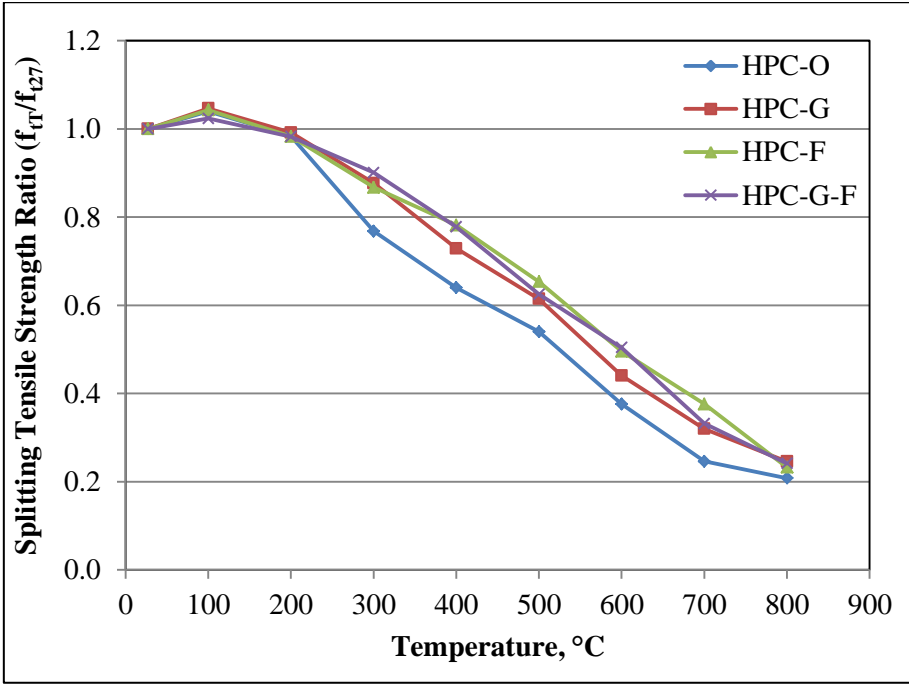
4.8 SPLITTING TENSILE STRENGTH OF CONCRETE

The test results of splitting tensile strength are tabulated in Appendix II, B-22 to B-27. Tensile strength of concrete becomes crucial at elevated temperatures to control cracking and spalling. Variation in splitting tensile strength ratio with temperature for different retention periods has been studied. It has been found that, with increase in temperature and retention periods, splitting tensile strength reduces and more so compared to compressive strength. This is due to the effect of crack coalescence which is more considerable in splitting tensile strength than the compressive strength. The initiation and growth of every new crack reduces the available load carrying area and this reduction causes an increase in the stresses at critical crack tip.

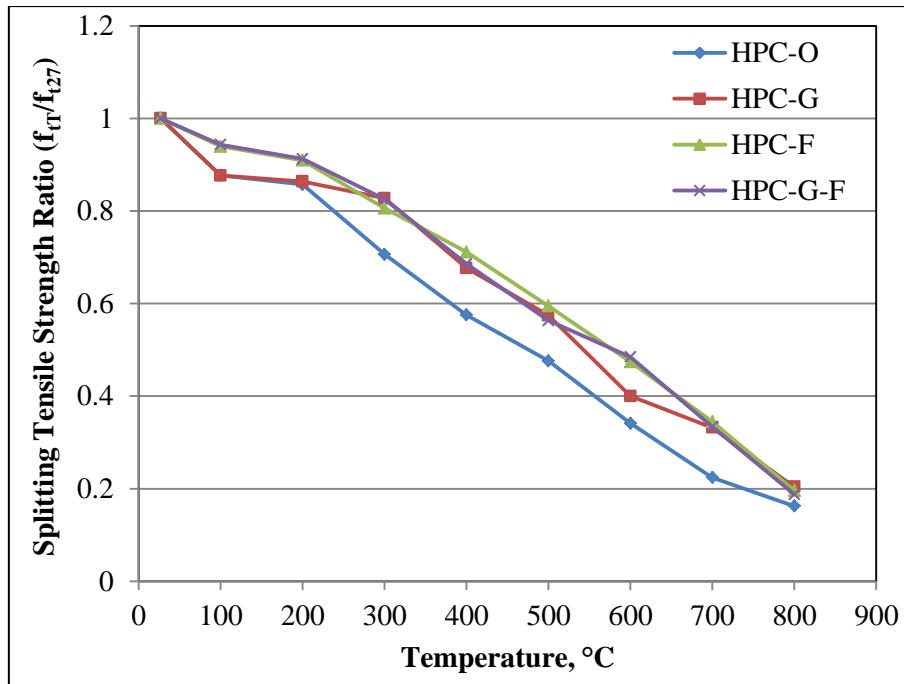
Figures 4.9 (a) – (c), depict variations in splitting tensile strength with temperature and exposure duration. Here again blended compositions have performed better than unblended concrete. Loss in splitting tensile strength is considerably sharp beyond 200°C as compared to that of compressive strength. Ghandehari et al. (2010) have attributed this reduction in split tensile strength to the decomposition of the hydration products and thermal incompatibility between aggregate and cement paste. The tensile strength is more sensitive to cracks, formed as a result of elevated temperature exposure, either on macro or on micro scale (Chan et al., 1999).



(a) 1 hour



(b) 2 hours



(c) 3 hours

Fig. 4.9 (a)-(c): Variation in splitting tensile strength ratio with temperatures for different retention periods

4.9 STATISTICAL ANALYSIS OF EXPERIMENTAL DATA

Analysis of variance (ANOVA) is a collection of statistical models that is used to analyse the differences between group means and their associated procedures (such as variation among and between the groups). In ANOVA setting, the observed variance in a particular variable is partitioned into components attributable to different sources of variation. In its simplest form, ANOVA provides a statistical test of whether or not the means of several groups are equal, and therefore generalizes t-test to more than two groups. Doing multiple two-sample t-tests would result in an increased chance of committing a type I error. For this reason, ANOVA are useful in comparing three or more variables for statistical significance.

Analysis of variance is an important statistical analysis and diagnostic tool, which helps to reduce the error variance and quantifies the dominance of control factor. To determine the influence of exposure temperature and retention period on strength characteristics, ANOVA has been performed and the details are presented as under.

Larger the value of compressive and splitting tensile strength characteristics gives better performance in HPC exposed to elevated temperature. Therefore, loss function “Larger is Better (LB)” was selected in this study to obtain the optimal conditions. This loss function was further transformed in to a signal to noise (S/N) ratio for determining the performance characteristics deviating from the desired value. Statistical analysis has been carried out using software Minitab version 15.

The results of ANOVA are presented in Tables 4.3 and 4.4. Exposure temperature has highest importance (88.64%, 89.39%, 87.85% and 85.93% for HPC-O, HPC-G, HPC-F and HPC-G-F respectively) on compressive strength and splitting tensile strengths (97.08%, 96.56%, 97.82% and 98.49% for HPC-O, HPC-G, HPC-F and HPC-G-F respectively) of HPC than the retention period.

The analysis indicated that experimental error is low. The larger F value indicates that, variation in control parameters makes lot of changes on the performance characteristics. From Table 4.3 and 4.4 it is observed that, P-level value is less than 0.05 which indicates both the exposure temperature and retention period are significant.

Table 4.3: Results of ANOVA for compressive strength of concrete

Control factor	Degree of freedom (DF)	Sum of square (SS)	Mean squares (MS)	F	Contribution (%)	P-level
HPC-O						
Temperature	8	6536.71	817.09	36.23	88.64	0.000
Retention period	2	476.77	238.38	10.57	6.46	0.001
Error	16	360.84	22.55		4.90	
Total	26	7374.32				
HPC-G						
Temperature	8	4999.62	624.95	22.78	89.39	0.000
Retention period	2	154.44	77.22	2.81	2.76	0.090
Error	16	438.96	27.24		7.85	
Total	26	5593.01				
HPC-F						
Temperature	8	4087.88	510.99	31.00	87.85	0.000
Retention period	2	301.81	150.90	9.15	6.49	0.002
Error	16	263.75	16.48		5.66	
Total	26	4653.44				
HPC-G-F						
Temperature	8	4926.71	615.84	19.37	85.93	0.000
Retention period	2	297.50	148.75	4.68	5.19	0.025
Error	16	508.81	31.80		8.88	
Total	26	5733.02				

Table 4.4: Results of ANOVA for splitting tensile strength of concrete

Control factor	Degree of freedom (DF)	Sum of square (SS)	Mean squares (MS)	F	Contribution (%)	P-level
HPC-O						
Temperature	8	65.78	8.22	221.96	97.08	0.000
Retention period	2	0.93	0.47	12.61	1.69	0.001
Error	16	0.59	0.04		1.23	
Total	26	67.31				
HPC-G						
Temperature	8	51.35	6.42	164.48	96.56	0.000
Retention period	2	1.21	0.60	15.44	2.28	0.000
Error	16	0.62	0.04		1.16	
Total	26	53.18				
HPC-F						
Temperature	8	47.57	5.95	329.45	97.82	0.000
Retention period	2	0.76	0.38	21.16	1.56	0.000
Error	16	0.29	0.018		0.62	
Total	26	48.63				
HPC-G-F						
Temperature	8	47.43	5.93	210.80	98.49	0.000
Retention period	2	0.57	0.29	10.20	0.01	0.001
Error	16	0.45	0.028		1.50	
Total	26	48.46				

S/N response graph of each level of the experimental parameters for compressive and splitting tensile strength of all mixes are shown in Figs. 4.10 and 4.11 respectively. Maximum compressive strength is found for HPC-O, HPC-G, HPC-F and HPC-G-F at 27°C and 300°C, 400°C, 300°C and 400°C respectively and at 1 hour retention period. The maximum splitting tensile strength is indicated for all mixes at 27°C respectively and at 1 hour retention period.

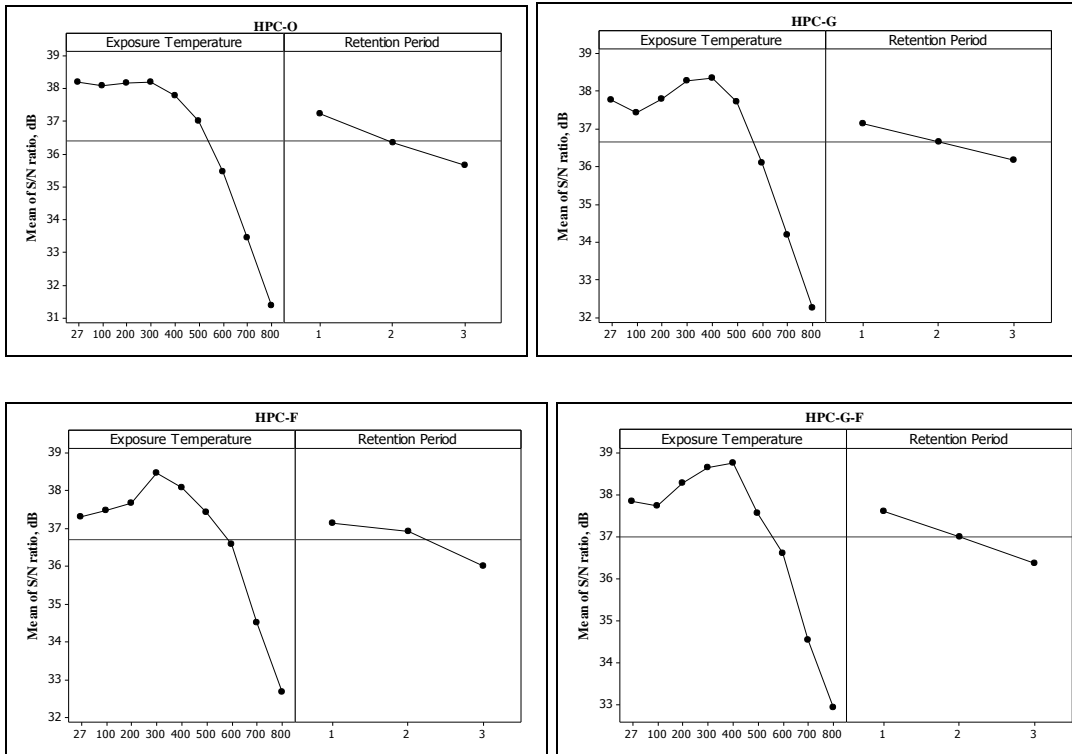


Fig. 4.10: S/N response graph for compressive strength

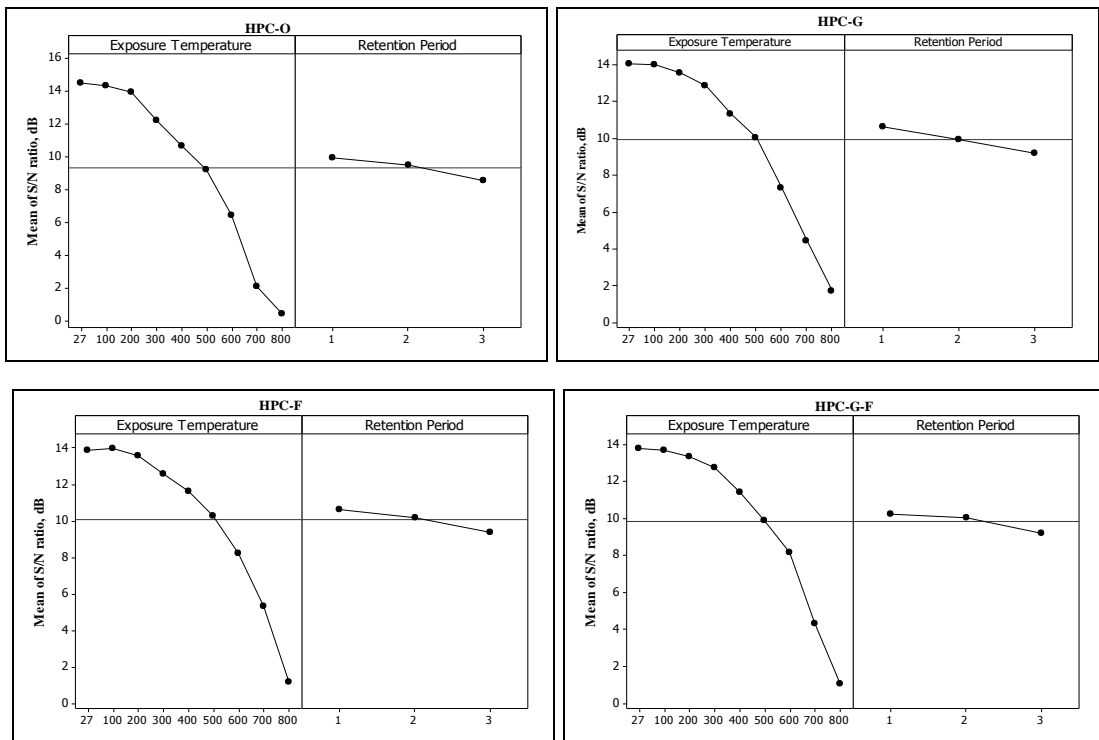


Fig. 4.11: S/N response graph for splitting tensile strength

Figure 4.12 and 4.13 shows, the S/N response graph of experimental parameters such as exposure temperature, retention period and type of mixes for the compressive and splitting tensile strength of concrete respectively. The type of concrete are represented as, H1 level for HPC-O mix, H2 level for HPC-G mix, H3 level for HPC-F mix and H4 level for HPC-G-F mix. As can be seen the degradation in compressive strength starts from 300°C, whereas for splitting tensile strength, degrades from ambient level. HPC-G-F mix shows better performance for compressive strength of concrete exposed to elevated temperature. Blended mixes have better strength retention characteristics, because the detrimental effects of Ca(OH)_2 can be eliminated using mineral admixtures such as FA and GGBFS.

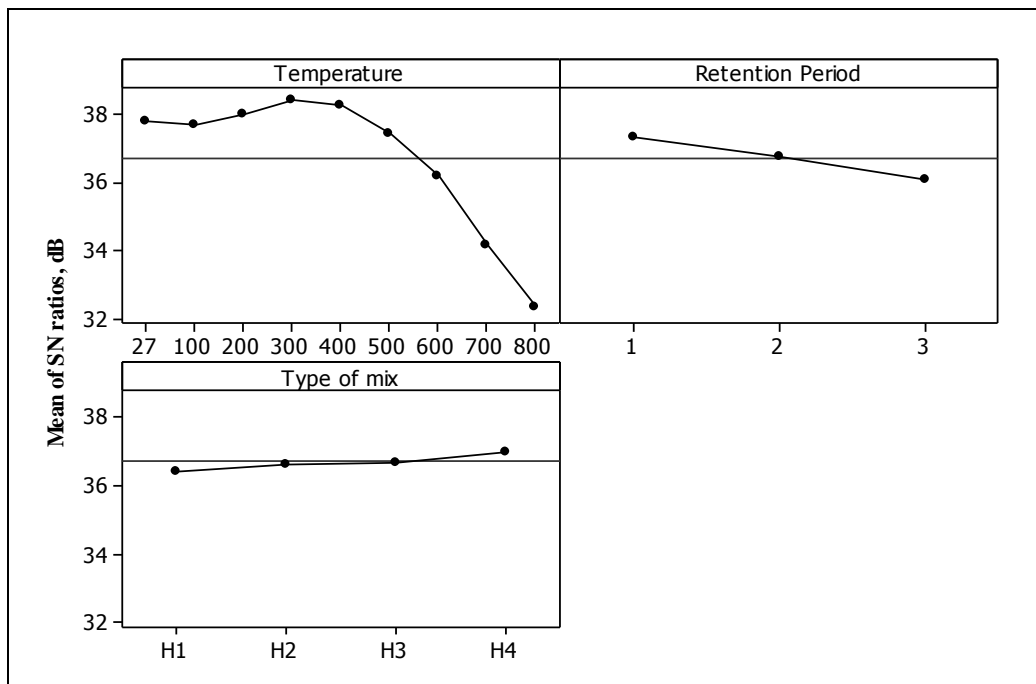


Fig. 4.12: S/N response graph of experimental parameters for compressive strength

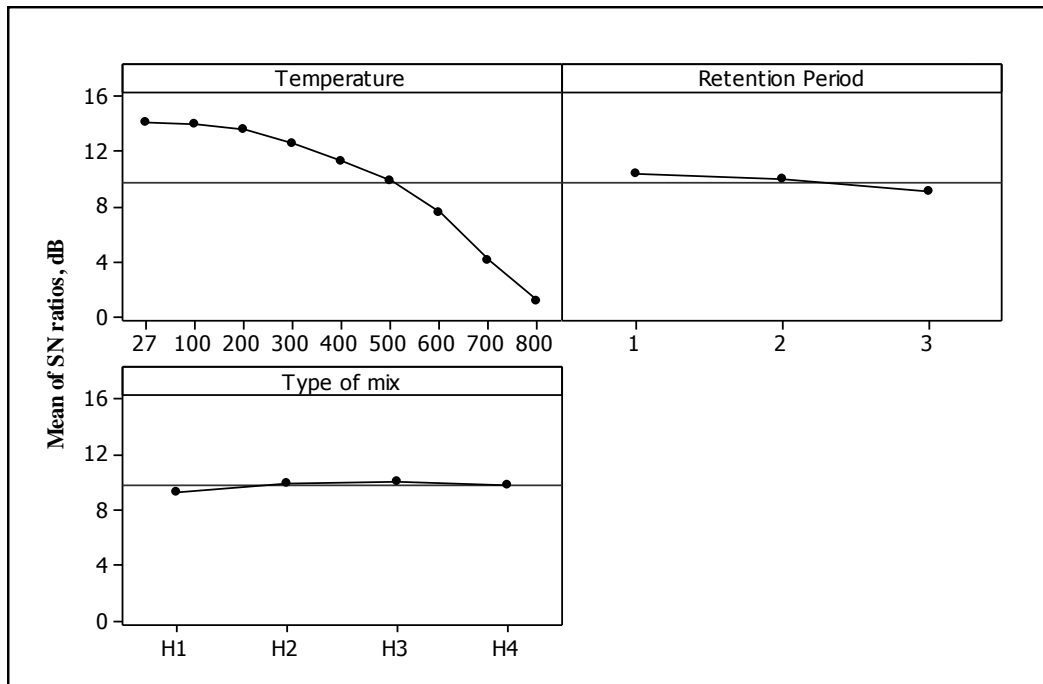


Fig. 4.13: S/N response graph of experimental parameters for splitting tensile strength

4.10 PREDICTION EQUATIONS FOR THE RESIDUAL STRENGTH ASSESSMENT OF CONCRETE EXPOSED TO ELEVATED TEMPERATURE

The experimental data have been employed to propose residual strength prediction equations for concrete exposed to elevated temperature. Multiple regression analysis was used for the development of models. For modelling and analysis Minitab version15 software was used. The proposed equations along with the range of exposure temperature are tabulated in Table 4.5. The additional compressive and splitting tensile strength prediction equations for different mixes based on exposure temperature, retention period, porosity and UPV are tabulated in Appendix II (B-28 and B-29).

Table 4.5: Residual compressive/splitting tensile strength prediction equations for different mixes based on exposure temperature and retention period

Type of Mix	Prediction Equations	Temperature Range	MRE
Compressive strength ratio from exposure temperature and retention period			
HPC-O	$f_{cr} = 1.05 - 0.000215 \times T - 0.0130 \times RP$	$100^{\circ}\text{C} < T \leq 450^{\circ}\text{C}$	3.0
	$f_{cr} = 1.66 - 0.00128 \times T - 0.0846 \times RP$	$450^{\circ}\text{C} < T \leq 800^{\circ}\text{C}$	4.7
Blended concretes	$f_{cr} = 1.03 + 0.000099 \times T - 0.0099 \times RP$	$100^{\circ}\text{C} < T \leq 450^{\circ}\text{C}$	4.2
	$f_{cr} = 1.83 - 0.00128 \times T - 0.0846 \times RP$	$450^{\circ}\text{C} < T \leq 800^{\circ}\text{C}$	4.9
Splitting tensile strength ratio from exposure temperature and retention period			
HPC-O	$f_{tr} = 1.14 - 0.00081 \times T - 0.0472 \times RP$	$100^{\circ}\text{C} < T \leq 250^{\circ}\text{C}$	4.7
	$f_{tr} = 1.27 - 0.00126 \times T - 0.0546 \times RP$	$250^{\circ}\text{C} < T \leq 800^{\circ}\text{C}$	8.9
Blended concretes	$f_{tr} = 1.10 - 0.00048 \times T - 0.0367 \times RP$	$100^{\circ}\text{C} < T \leq 250^{\circ}\text{C}$	9.0
	$f_{tr} = 1.33 - 0.00123 \times T - 0.0476 \times RP$	$250^{\circ}\text{C} < T \leq 800^{\circ}\text{C}$	5.1

Where,

f_{cr} = Compressive strength ratio, (f_{cT}/f_{c27})

f_{tr} = Splitting tensile strength ratio, (f_{tT}/f_{t27})

T = Exposure temperature in °C

RP = Retention period in hour

4.11 STRENGTH Vs TIME – TEMPERATURE

Area under the time temperature curve was taken as an indicator of heat energy available for bringing out changes in concrete strength characteristics and it was attempted to establish a relationship between strength and heat energy.

Figure 4.14 shows the typical time temperature curve for 800°C and 3 hours retention time, wherein the temperature build-up, constant temperature regime, and furnace cooling regime to ambient levels are shown as adopted in the present work. With

such plots for various temperature levels and exposures, area under the time temperature curve was determined and used as an parameter that changes strength characteristics. Table 4.6 gives the calculated area of time temperature curve for different temperatures and retention periods. From this time temperature area, time temperature factor was calculated. Time-temperature factor was defined as the ratio of area under the curve for designated temperature to the area of curve at 100°C exposure temperature for 1 hour retention period. Table 4.7 gives the time temperature factor and compressive strength ratio of unblended concrete for different temperatures and retention periods.

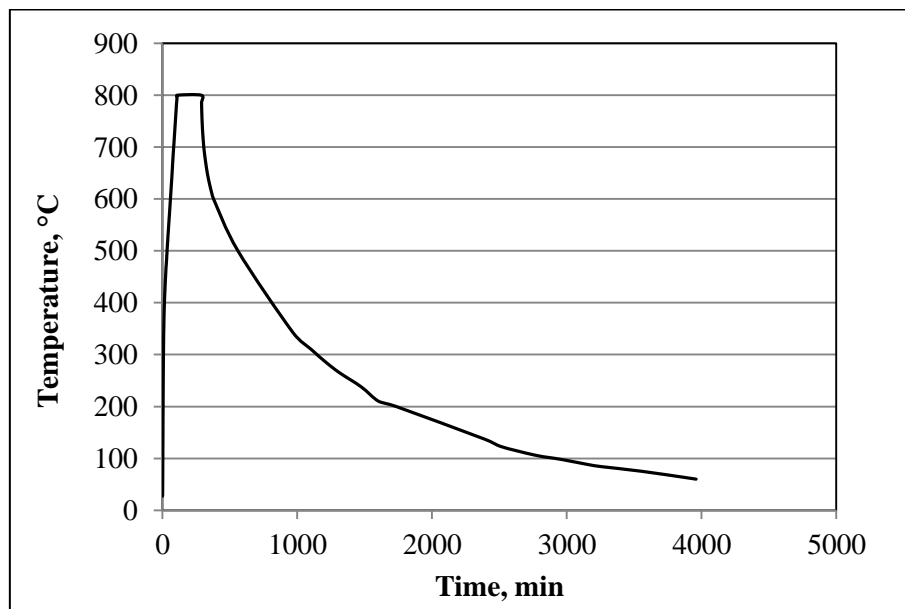


Fig 4.14: Typical time temperature curve for 800°C temperature and 3 hours retention period

Table 4.6: Area of the time temperature curve for different temperatures and retention period

Temperature, (°C)	Area under the curve, (°C. min)		
	1 hour	2 hours	3 hours
100	26341.5	32341.5	38341.5
200	133100.5	145100.5	157100.5
300	204862.0	222862.0	240862.0
400	221266.5	245266.5	269266.5
500	440244.5	470244.5	500244.5
600	597348.5	633348.5	669348.5
700	743739.5	785739.5	827739.5
800	894236.5	942236.5	990236.5

From Table 4.7 it can be seen for instance that, exposure for 1 hour at 600°C has same effect as exposure for 2 hours at 500°C and 3 hour retention at 400°C approximately, and hence equivalent heat effect can be obtained by riding along the diagonals of the time - temperature and strength ratio matrix depicted in the table.

Table 4.7: Results of Compressive strength ratio and Time temperature factor

Temperature, (°C)	Time Temperature factor			Compressive strength ratio		
	1 hour	2 hours	3 hours	1 hour	2 hours	3 hours
100	1.00	1.23	1.46	1.00	1.00	0.96
200	5.05	5.51	5.96	0.95	1.00	1.04
300	7.78	8.46	9.14	0.98	1.03	1.00
400	8.40	9.31	10.22	0.97	0.99	0.91
500	16.71	17.85	18.99	0.95	0.90	0.78
600	22.68	24.04	25.41	0.88	0.73	0.60
700	28.23	29.83	31.42	0.69	0.58	0.49
800	33.95	35.77	37.59	0.54	0.44	0.40

Plot between compressive strength ratio and time temperature factor, is shown in Fig. 4.15. With the available data, regression analysis has been carried out to propose Equation 4.1 for obtaining compressive strength ratio in terms of time-temperature factor.

$$f_{cr} = 1 \times 10^{-5} \times TTF^3 - 0.0012 \times TTF^2 + 0.0118 \times TTF + 0.9687 \quad (4.1)$$

Where,

f_{cr} = Compressive strength ratio

TTF = Time Temperature Factor

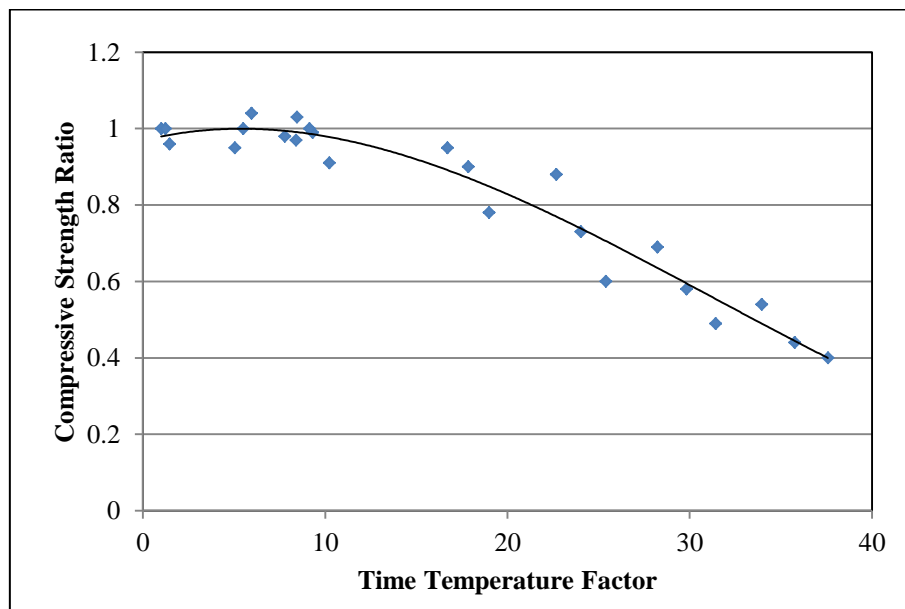


Fig 4.15: Plot between compressive strength ratio and time temperature factor

4.12 SUMMARY

Details of experimental and analytical investigations carried out to study the performance of blended HPC vis a vis unblended HPC at elevated temperatures has been elaborated. Colour change can be a potential indicator of temperature levels. Surface crack density patterns observed have shown that blended concretes do not allow formation and propagation of surface cracks as much as unblended does.

Porosity determination indicates thermal deterioration and hence reduction in densities and increase in porosity are on the increase with increase in temperature of exposure and retention period. Blended concretes report less weight loss, and more impermeability.

Table 4.8 Summary of test results highlighting strength performance of HPC subjected to elevated temperature

Type of Mix	Temperature Ranges	27°C - 300°C			300°C - 600°C			600°C - 800°C		
	Retention Period (hour)	1	2	3	1	2	3	1	2	3
HPC- O	Compressive	0.98	1.03	1.00	0.88	0.73	0.60	0.54	0.44	0.40
	Split tensile	0.83	0.77	0.71	0.48	0.38	0.34	0.23	0.21	0.16
HPC- G	Compressive	1.00	1.04	1.10	0.97	0.84	0.68	0.65	0.51	0.45
	Split tensile	0.90	0.88	0.83	0.55	0.44	0.40	0.28	0.25	0.20
HPC- F	Compressive	1.14	1.15	1.13	0.99	0.94	0.83	0.71	0.57	0.49
	Split tensile	0.91	0.87	0.81	0.60	0.50	0.47	0.27	0.23	0.20
HPC-G-F	Compressive	1.12	1.09	1.08	0.98	0.86	0.77	0.74	0.56	0.45
	Split tensile	0.93	0.90	0.83	0.58	0.50	0.48	0.27	0.24	0.19

Table 4.8 summarises the test results highlighting the residual compressive and split tensile strength ratio of concrete. It is evident from the table that, blended concrete shows better strength performance compared to HPC-O mix in each temperature range. HPC-F mix retains maximum compressive strength in the range of exposure

temperatures of 27°C- 300°C and 300°C- 600°C. While in the range of 600°C-800°C HPC-G-F retains maximum compressive strength.

The degradation in splitting tensile strength is different from the compressive strength and the decrease rate is more for split tensile strength with time-temperature. Here, again, blended concretes behave better at elevated temperature by retaining higher levels of strengths.

The reduction in strength is a function of exposure temperature and retention period and temperature being the dominant factor as shown by ANOVA. ANOVA results also endorse the better performance of blended concrete through S/N ratio plots.

The assessment of concrete exposed to elevated temperature by UPV test gives indirect information of quality of concrete and its usage potential for assessment has been demonstrated discussing results of tests conducted.

Prediction equations for compressive and split tensile strength in terms of temperature levels, and exposure periods have been proposed, which serve as an aid in the design office.

Assessment of residual strength can be made by using the strength factor prediction equation proposed based on time-temperature factor, where such data is available.

CHAPTER 5

DRILLING RESISTANCE – IN DAMAGE DIAGNOSIS

5.1 GENERAL

Extraction of concrete cores from structural elements is a standard practice in failure forensics for structural assessment and appraisal. It has been conceived to explore the potential usage of drilling resistance of concrete as an NDT tool. Also, possible application of A-weighted equivalent sound level during drilling resistance test and impact sound level as an indicator of strength characteristics has been attempted. Based on the experimental data, analysis has been carried out, to propose equations and nomograph for the residual strength assessment of concrete exposed to elevated temperature.

5.2 DRILLING RESISTANCE TEST ON CONVENTIONAL BUILDING MATERIALS

To study the potential of drilling resistance test in strength assessment, it was envisaged to conduct tests on a few building materials like wax, brick, wood, granite samples and cement mortar cubes. These materials have different density and strength characteristics. Penetration depth with drilling time for these materials has been presented in Fig. 5.1. For soft materials like wax, less drilling time is required to penetrate a designated depth. Whereas for granite which is harder, penetration time for the same depth is more than that for wax. Drilling time curve for cement mortar, that has intermediate hardness is in between the curves for hard and soft materials. It is recognized that denser the material, harder and stronger it is, and this fact has found place in concrete technology too. As can be seen from the curves, harder materials have more linear relationship between penetration depth Vs time, which makes usage potential of drilling resistance appealing.

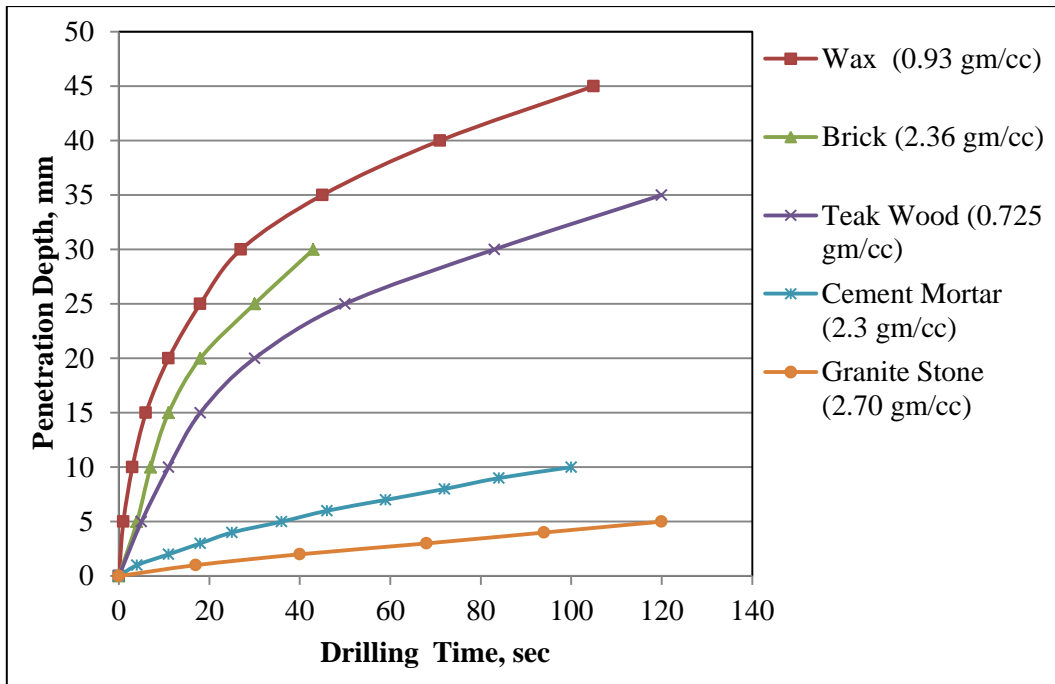


Fig. 5.1: Penetration depth with drilling time for building materials

5.3 DRILLING RESISTANCE TEST ON CONCRETE

Penetration depth with drilling time for concretes with varying strengths, are presented in Fig. 5.2. It was contemplated to perform the drilling test on a few samples of concrete with variations in mix proportions and water cement ratio, to generate as random a sample as possible and to check the veracity of linearity of drilling time with penetration depth. Figure shows that drilling time increases with strength. Within error bounds the curves are almost linear and indicate that drilling time for a designated depth or drilling depth for a specified time can be pointers to strength.

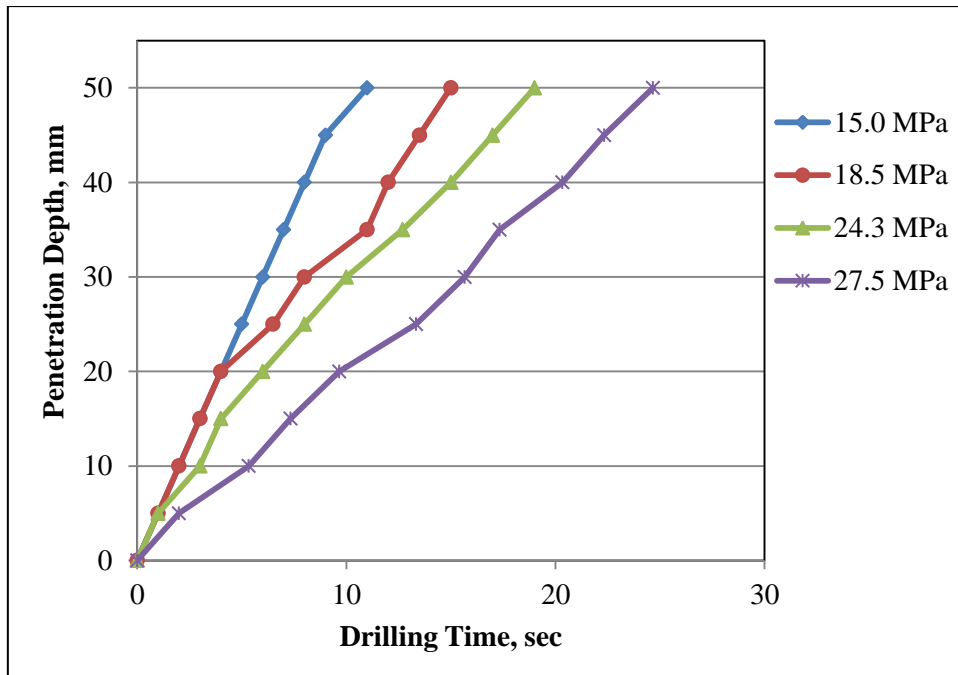


Fig. 5.2: Penetration depth with drilling time for concretes with varying strengths

5.4 DRILLING TIME TEST ON CONCRETE EXPOSED TO ELEVATED TEMPERATURE

In drilling test for concrete exposed to elevated temperature, drilling time has been measured for 50 mm depth of penetration at an interval of 5 mm. The test results are tabulated in Appendix II, B-30 to B-32. Figure 5.3 shows variation in drilling time for concrete specimen exposed to different temperatures.

Drilling time for designated depth increases with decrease in temperature exposure levels. The linearity between depth Vs time, again is apparent.

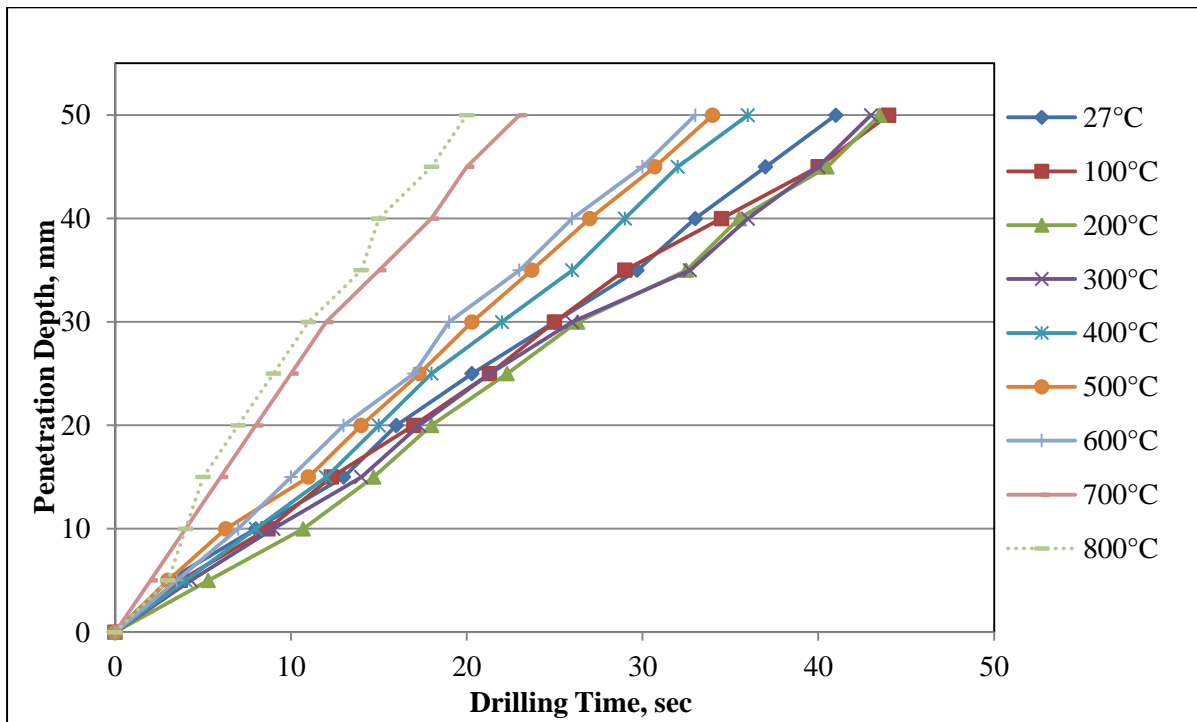


Fig. 5.3: Penetration depth with drilling time for concrete exposed to temperature

5.5 SOUND TEST ON CONCRETE EXPOSED TO ELEVATED TEMPERATURE

Sound levels measured during drilling test and steel ball impact test are detailed in the following sections.

5.5.1 Recordings of Sound Levels Associated with Drilling Test

Sound levels were recorded during the drilling resistance test, for analysis and interpretation and possible exploitation as an assessment tool. The A-weighted equivalent sound level while drilling resistance test was measured by dosimeter continuously from beginning of drilling to the 50 mm depth of penetration. Figure 5.4 shows the variation between normalised A-weighted equivalent sound level and

exposure temperatures. Normalised A-weighted equivalent sound level is that sound measured during drilling, free from the sound of drilling machine and hydraulic pump. Back ground noise was 75 dB. Suitable adjustments to recordings for back ground noise have been incorporated.

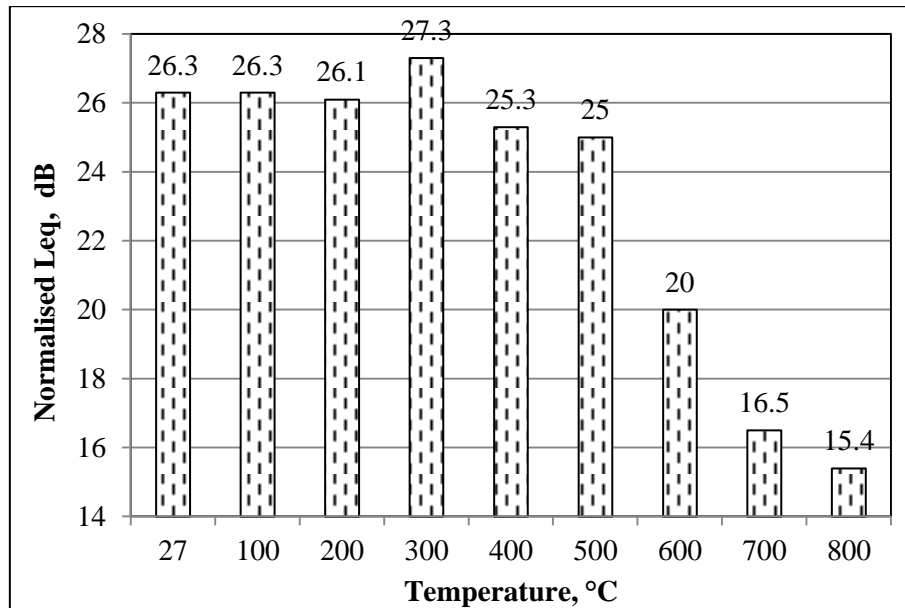


Fig. 5.4: Normalised A-weighted equivalent sound level with temperature

From Figure 5.4 it is observed that, concrete exposed up to 300°C, 400°C and 600°C produces 26 dB, 24 dB and 20 dB of normalised A-weighted equivalent sound respectively. For 700°C and 800°C, sound levels were 15 dB. It can be concluded that drilling sound levels vary with temperature exposure and hence can be employed in assessment of strength characteristics.

The process of drilling, in general, always produces sound as a by-product. This sound is generated from the rock-bit interface, regardless of the material the bit is drilling in. As exposure temperature increases, concrete gets deteriorated and becomes softer. The compositions of the surfaces influence the overall sound level by reflecting or absorbing the incident sound energy. The compressive strength of the

media being drilled affects the acoustic absorption properties. Harder media reflect more acoustic energy than softer media.

5.5.2 Impact Sound Test

Impact sound test is used to detect hollowness of concrete. Figure 5.5 shows the variation of normalised impact sound level with temperature.

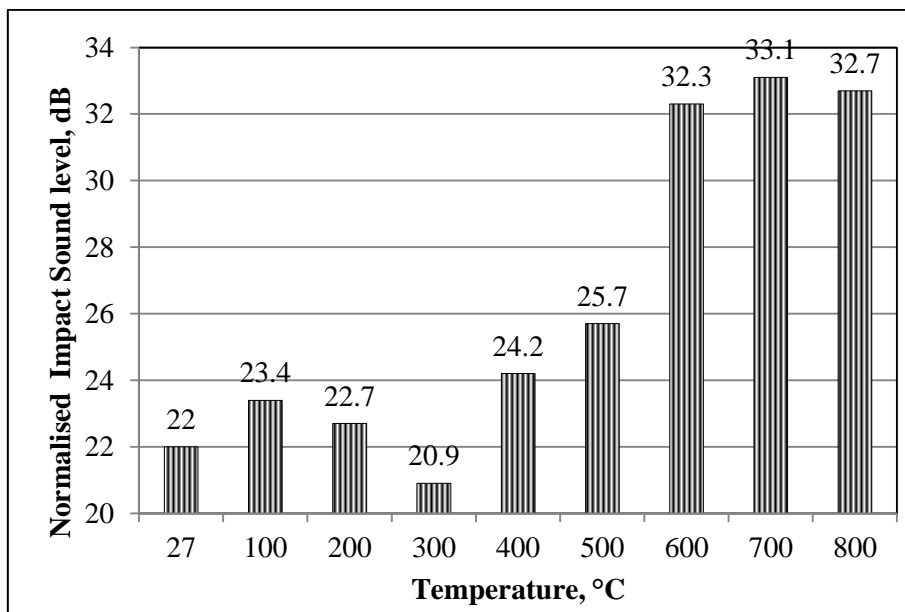


Fig. 5.5: Impact sound level with temperature

Figure 5.5 indicates that impact sound levels increase as temperature increases. This trend can be of help in preliminary assessment of concrete exposed to elevated temperatures, wherein impact sound levels can give an idea of exposure temperature levels.

5.6 NOMOGRAPH FOR COMPRESSIVE STRENGTH RATIO FROM DRILLING TIME RATIO AND TEMPERATURE

From the experimental results, and analysis, a parallel scale nomograph has been prepared and is presented in Fig. 5.6. Knowing two parameters from among the three related the third can be obtained.

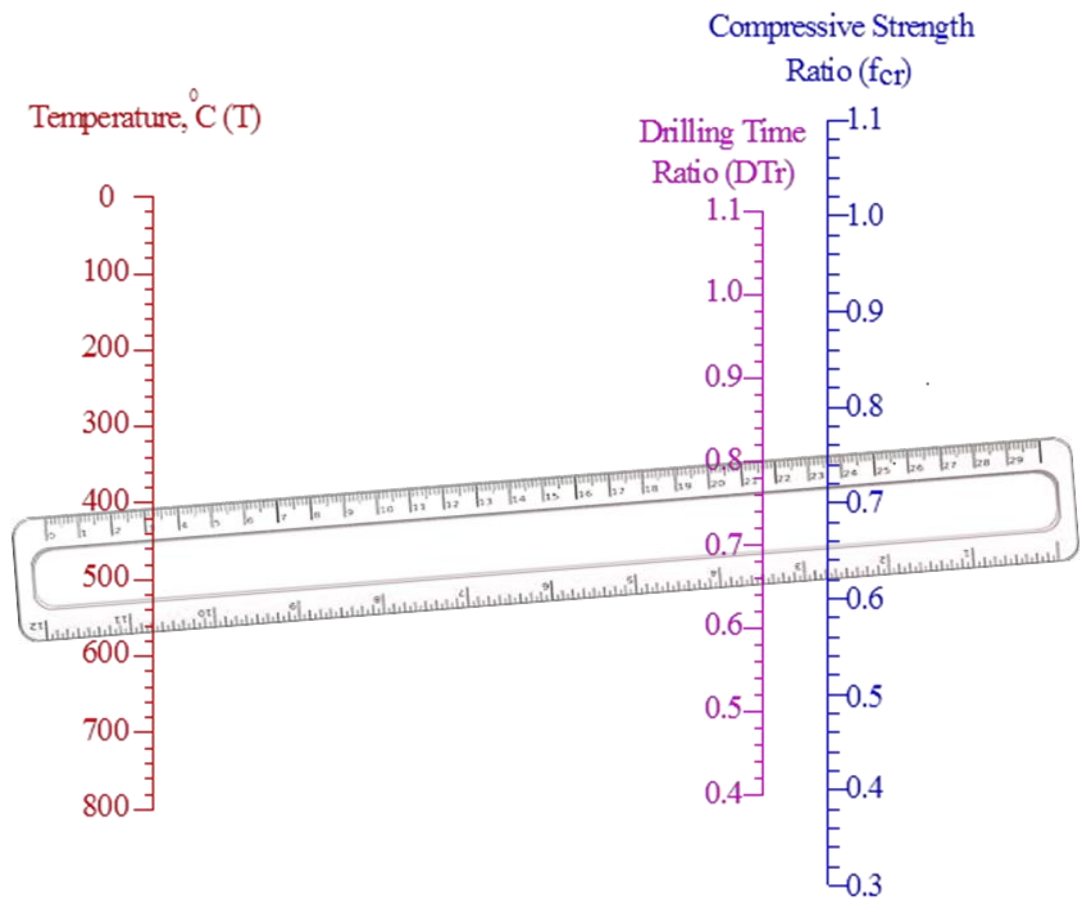


Fig 5.6: Parallel scale nomograph for compressive strength ratio

ILLUSTRATION:

If the concrete is exposed to 400°C and drilling time ratio 0.8 then, a straight edge held connecting 400°C temperature scale and 0.8 on drilling time ratio scale shall read 0.75 as the residual compressive ratio on strength scale.

5.7 SUMMARY

Possible application of drilling time, sound levels, and impact sound tests in assessment of concrete quality has been elaborated. The linearity of drilling depth with time is appealing and is amenable for exploitation as an NDT tool, as demonstrated. Nomograph of the kind presented here, are very handy in failure forensics.

CHAPTER 6

CORE RECOVERY - AS A MEANS OF NDT

6.1 GENERAL

It has been envisaged to investigate the difference in behaviour of unconfined and confined concrete by way of casting, curing, exposing to elevated temperature, cooling and later testing plain and reinforced concrete specimen. Physical observations and experimental results of porosity, density and compressive strength of cores extracted from plain cement concrete as well as from reinforced concrete beam elements exposed to elevated temperature have been presented. Based on experimental data, empirical relations have been proposed between standard cube compressive strength and core compressive strength of concrete exposed to elevated temperatures.

6.2 CORE RECOVERY TEST ON PLAIN CONCRETE EXPOSED TO ELEVATED TEMPERATURE

Core test is a more direct method of estimating the compressive strength of concrete by testing core samples extracted from the structure. The results of physical observations and compressive strength of concrete cores are presented in the following sections.

6.2.1 Physical Observations

Intact cores were recovered for all the exposure temperatures. No distress in the specimen were observed for exposure temperatures up to 500°C. Cores from concrete exposed to 600°C, 700°C and 800°C, were not as sound.

Figure 6.1 shows colour change in concrete cores. No colour change has been observed up to 200°C. For 300°C colour change pattern from normal to pink, and to brown-red at 400°C-600°C, and to buff at 700°C and 800°C are seen.

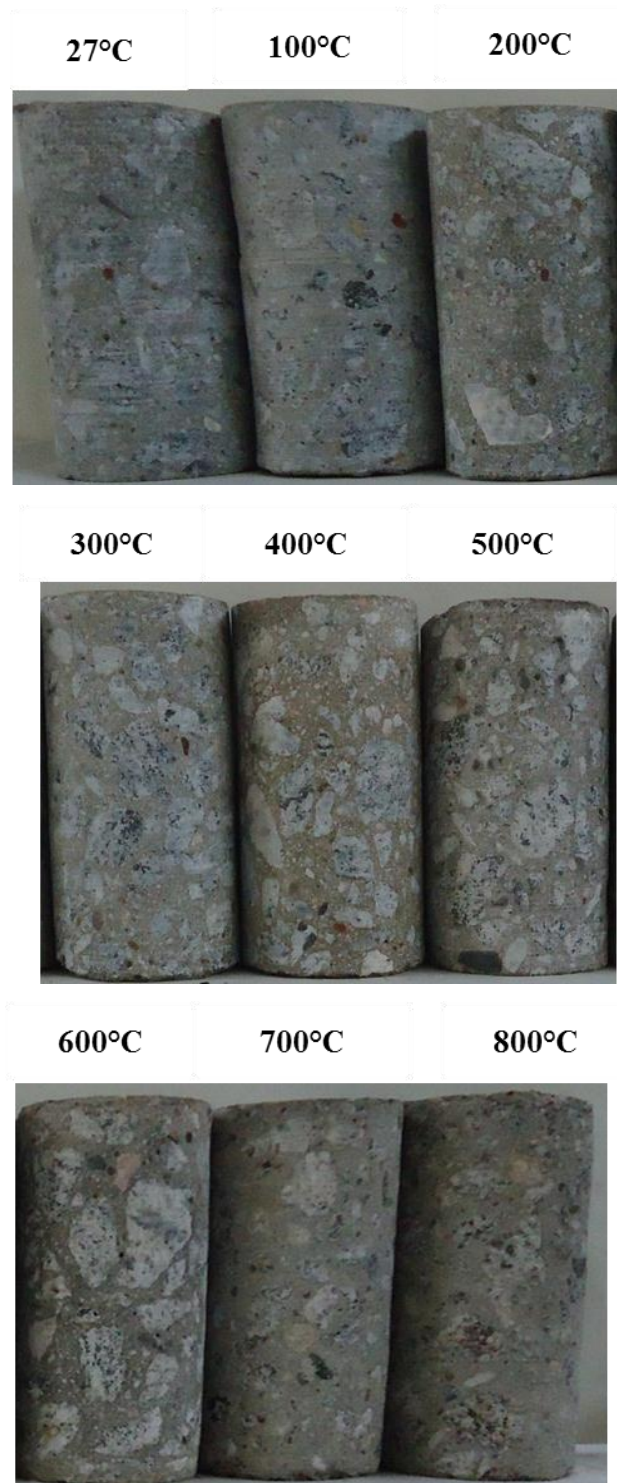


Fig. 6.1: Colour change in concrete cores

6.2.2 Compressive Strength

Compressive strength ratio of standard cube and core concrete with temperature are presented in Fig. 6.2. The test results are tabulated in Appendix II, B-33. Compressive strength ratio of core matches with that of standard cube within acceptable range of 6% error and strength deteriorates with elevation in temperature and hence it is prudent to accept that core results indicative to damage of concrete.

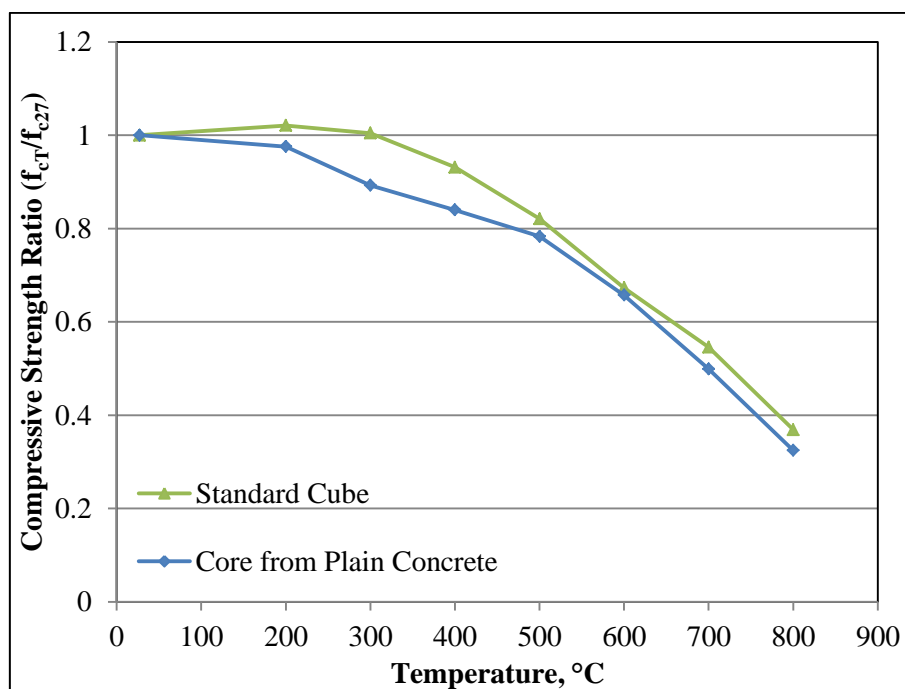


Fig. 6.2: Variation in compressive strength ratio of standard cube and core with temperature

6.2.3 Equation for Standard Cube Compressive Strength Prediction, from Core Compressive Strength for Plain Concrete

Equation 6.1 is proposed between standard cube compressive strength and core compressive strength of concrete exposed to elevated temperatures in plain concrete.

$$f_{cs} = 2.55 \times f_{co}^{0.90} \quad (6.1)$$

Where,

f_{cs} = Standard cube compressive strength in MPa

f_{co} = Core compressive strength in MPa

6.3 CORE RECOVERY TEST ON REINFORCED CONCRETE EXPOSED TO ELEVATED TEMPERATURES

In the previous section, the results of core recovery test carried out on plain concrete are reported. This section presents the results and discussion on physical observation of reinforced concrete elements, porosity, density and compressive strength of concrete cores extracted from reinforced concrete elements exposed to elevated temperatures. The test results are tabulated in Appendix II, B-34.

6.3.1 Physical Observations

The maximum crack width and depth of the crack on beam surface is tabulated in Table 6.1. For 400°C exposure no visible cracks were observed. Minor visible cracks were observed at the edge of beam specimen for 500°C exposure. These cracks penetrated deeper for temperatures of 600°C, 700°C and 800°C exposure. For 800°C exposure, maximum crack width of 0.7 mm has been observed.

Table 6.1: Maximum width on surface and depth of surface crack

Temperature, (°C)	Crack width, (mm)	Crack depth, (mm)
500	0.2	20
600	0.4	30
700	0.6	40
800	0.7	---

6.3.2 Porosity and Density

Figure 6.3 shows the variation between porosity and exposure temperature. Concrete porosity increases with increase in exposure temperature. The increase in porosity is around 2.5%, 4% and 6% over concrete at ambient temperature, for 300°C, 600°C and 800°C respectively.

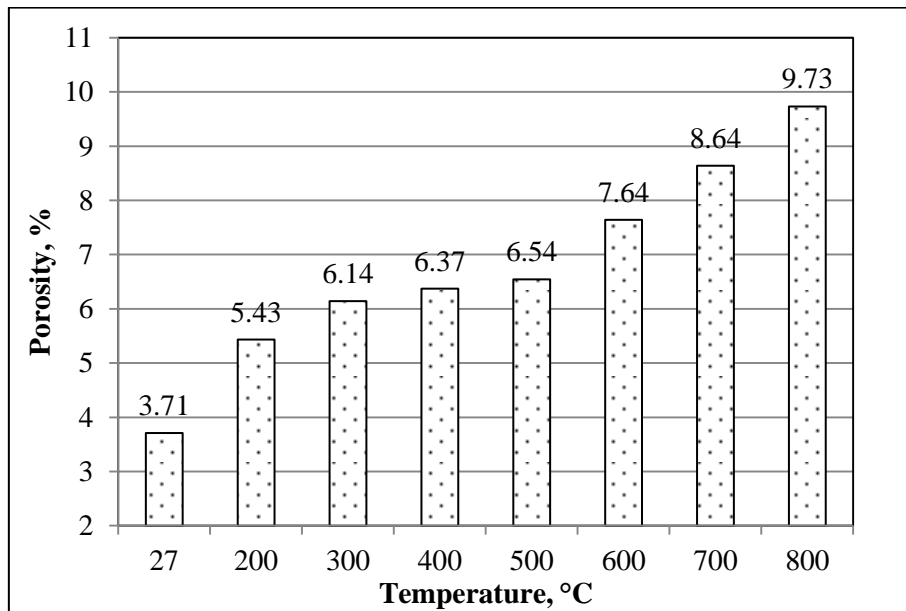


Fig. 6.3: Variation in porosity with temperature

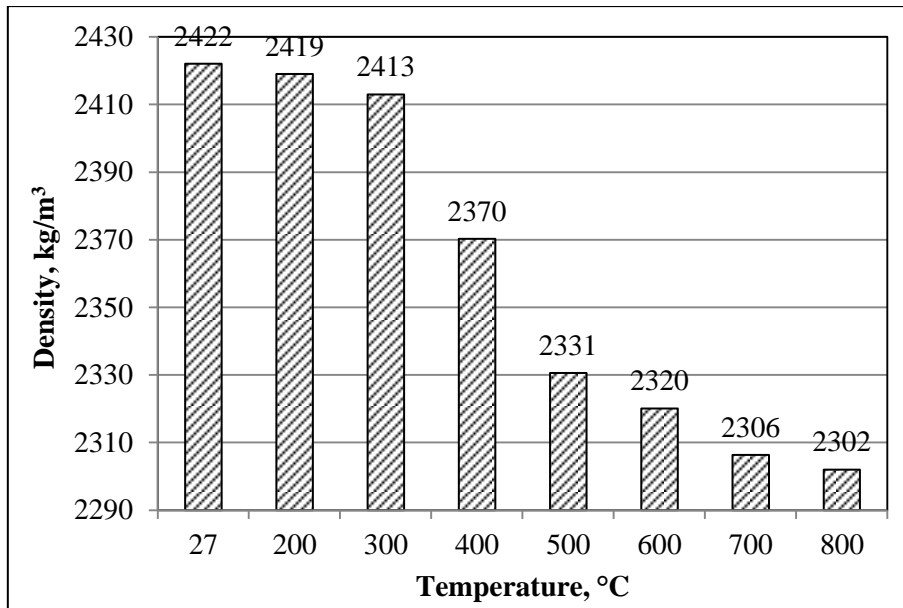


Fig. 6.4: Variation in density with temperature

Variation in density with temperature is presented in Fig. 6.4. For 300°C, there is no significant change in density. For exposure levels of 500°C and 600°C, around 4.5% decrease in density is observed whereas at 700°C and 800°C the decrease is around 6%.

6.3.3 UPV Test on Core Samples

For unexposed concrete core, UPV is found to be around 4.76 km/sec. For 200°C, 400°C, 600°C and 800°C the reduction in UPV's were about 14%, 27%, 55% and 71% respectively, details of which are presented in Fig. 6.5.

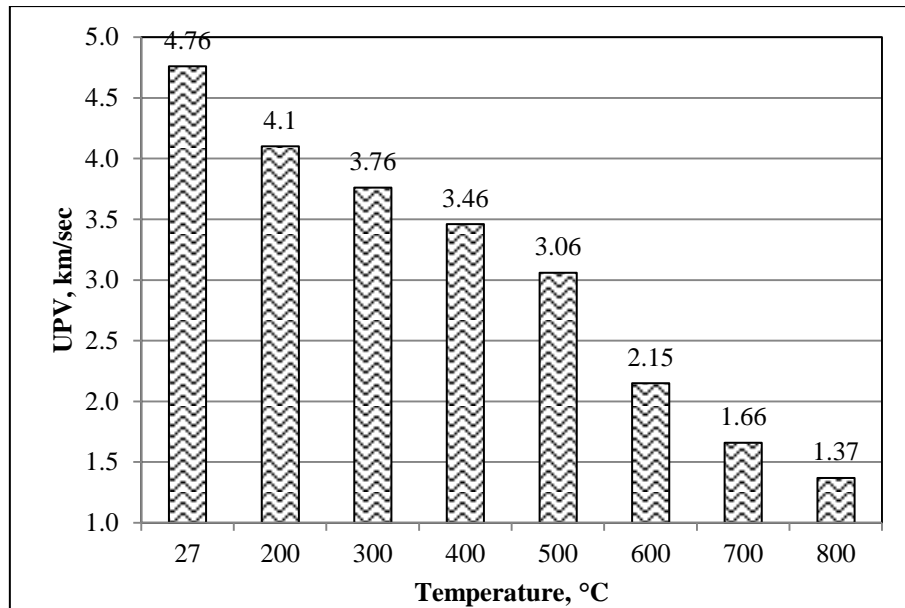


Fig. 6.5: Variation in UPV with temperature

6.3.4 Compressive Strength

Compressive strength test on core specimen has yielded, varying results as shown in Fig. 6.6. A comparison of compressive strength ratio of core extracted from plain and reinforced concrete beam cube is also available. Core compressive strength ratio of plain concrete is almost same as standard cube compressive strength ratio. Whereas, for cores extracted from reinforced concrete beams, compressive strength ratios deviate from the standard cube compressive ratio to the lower end. Similar findings by Khoury, (1992) attribute this difference in behaviour to uneven expansion and contraction between steel and concrete when subjected to elevated temperatures.

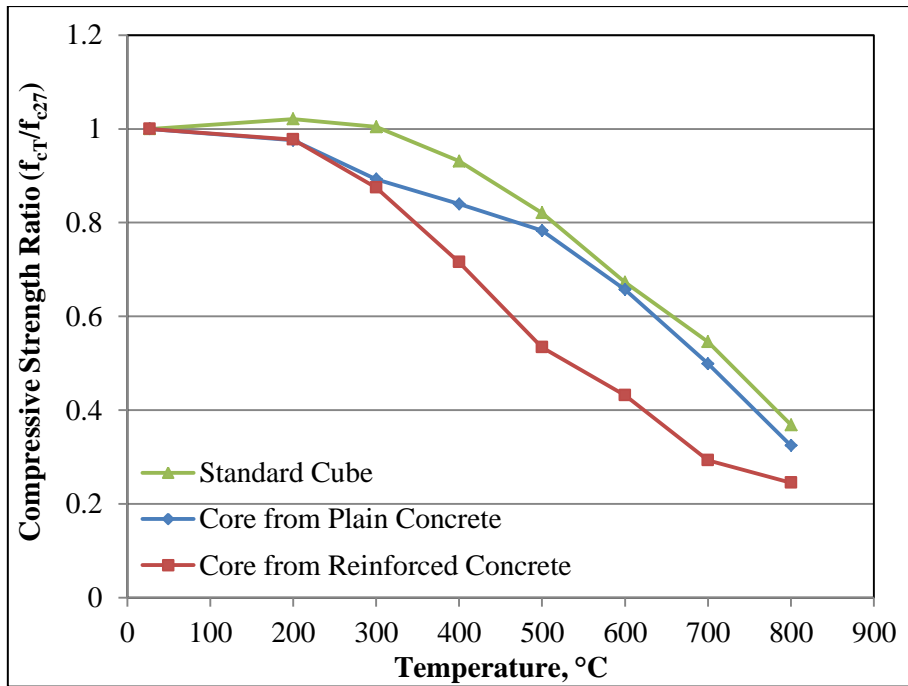


Fig. 6.6: Compressive strength ratio of standard cube and core extracted from plain concrete and reinforced concrete beam with temperature

6.3.5 Equation for Standard Cube Compressive Strength Prediction, from Core Compressive Strength for Reinforced Concrete

Equation 6.2 is proposed between standard cube compressive strength and core compressive strength of concrete exposed to elevated temperatures in reinforced concrete elements.

$$f_{cs} = 8.37 \times f_{co}^{0.62} \quad (6.2)$$

Where,

f_{cs} = Standard cube compressive strength in MPa

f_{co} = Core compressive strength in MPa

6.4 SUMMARY

Compressive strength of cores extracted from plain and reinforced concrete elements exposed to elevated temperatures give more relevant information on behavioural aspects. The behaviour of unconfined concrete is different from that of confined concrete. Contradicting the conventional belief that, confinement improves strength, counter intuitive results can be obtained from core tests as is evident from the current investigation. But such results are possible and need very careful interpretation. Hence extraction of cores for investigations in forensics needs to be carefully planned and locations do matter.

CHAPTER 7

CONCLUSIONS

A meaningful and successful attempt to study and appraise the effect of elevated temperature on HPC with pozzolanic blends has been made in this experimental and analytical investigation.

Analytical studies of experimental data have been made to identify key parameters that affect the behaviour.

Usage potential of drilling time's, drilling sound levels and impact sound levels, as effective NDT tools, have also been explored and techniques have been suggested.

Behavioural differences of plain and reinforced concrete have also been investigated, to make the study more exhaustive.

Major findings of this investigation are highlighted herein,

- Three distinct temperature regimes namely up to 300⁰C, between 300⁰C-600⁰C, and beyond 600⁰C for all retention periods, have been identified for change in concrete characteristics like weight loss, strength loss, and increase in porosity.
- Statistical analysis of experimental data indicates that between duration of exposure and temperature level, temperature dominates in bringing about changes in concrete characteristics.
- Elevated temperatures have more detrimental effect on splitting tensile strength than on compressive strength as suggested by data analysis.

- High performance concrete with pozzolanic blends has performed better at elevated temperatures vis a vis unblended concretes and hence it may be concluded that in addition to already recognized qualities it has better fire endurance characteristics too.
- Drilling resistance indirectly measured as penetration time and sound level recordings, during drilling can be a pointer of the extent of deterioration and a measure of residual strength as demonstrated by the present investigation.
- Residual strength assessment equations proposed with NDT results as input, are of immense use in damage assessment of concrete exposed to elevated temperatures and nomographs of the kind presented as a result of the investigation are valid decision making tools in failure forensics.
- Comparison of studies on PCC and RCC specimen have clearly brought out the need for careful interpretation of results from concrete core tests of fire damaged elements.

SCOPE FOR FUTURE WORK

Present investigation has focussed on performance of HPC at elevated temperatures and some quick and efficient techniques for assessment of residual strength.

A few of the possible research initiatives in this area in future that need consideration for refinement are as follows.

1. This study is limited to HPC of strength around 70 MPa, behaviour of still higher strength concrete is very much necessary, as the focus is on strength characteristics and fire endurance.
2. Investigation is limited to concrete as a material. Tests on structural elements under load exposed to elevated temperatures need to be investigated.

3. Drilling time, sound level test can be calibrated and validated over a wide and varied range of concrete, so as to make it acceptable as a recognized NDT technique.

APPENDIX I

Table A-1: Properties of fresh and hardened concrete

Type of mix	Slump, (mm)	Compressive strength, (MPa)
HPC-O	170	81.3
HPC-G	175	77.5
HPC-F	200	73.4
HPC-G-F	210	78.1

Table A-2: Test matrix for study of strength retention characteristics of concrete after elevated temperature exposure

Temperature, (°C)	Compressive strength test, UPV			Splitting tensile strength test, porosity and density		
	Retention periods			Retention periods, hours		
	1 hour	2 hours	3 hours	1 hour	2 hours	3 hours
27	3	3	3	3	3	3
100	3	3	3	3	3	3
200	3	3	3	3	3	3
300	3	3	3	3	3	3
400	3	3	3	3	3	3
500	3	3	3	3	3	3
600	3	3	3	3	3	3
700	3	3	3	3	3	3
800	3	3	3	3	3	3
Total No. of cubes	33 (2 sets extra) × 3 retention period × 4 mix = 396			33 (2 set extra) × 3 retention period × 4 mix = 396		

Table A-3: Test matrix of specimen for evaluation by different tests

Temperature, (°C)	Retention period (2 hours)		
	Drilling resistance test	Core recovery test	Compressive strength test
27	3	3	3
100	3	3	3
200	3	3	3
300	3	3	3
400	3	3	3
500	3	3	3
600	3	3	3
700	3	3	3
800	3	3	3
Total No. of cubes	33 (2 sets extra) × 1 mix (HPC-O) × 3 Tests = 99		

Table A-4: Test matrix of specimen for evaluation by core recovery test

Temperature, (°C)	Core recovery test
27	1
200	1
300	1
400	1
500	1
600	1
700	1
800	1
Total Number of HPC-O mix beams	8

Table A-5: Temperature build up and cooling time for muffle furnace

Temperature, (°C)	A	B		
		1 hour retention period	2 hours retention period	3 hours retention period
100	3	340	400	460
200	5	1540	1600	1660
300	8	1740	1800	1860
400	14	2140	2200	2260
500	34	2406	2466	2526
600	59	2881	2940	3001
700	83	3257	3317	3370
800	109	3732	3791	3851

Note:

A- Time required to reaching room to designated temperature in minutes

B- Time required to cooling designated to room temperature in minutes

APPENDIX II

Table B-1: Variation of loss in weight for HPC-O and HPC-G mix cubes after exposure to elevated temperature and retained for 1 hour

Temperature (°C)	HPC-O				HPC-G			
	Weight of cubes before exposure (kg)	Weight of cubes after exposure (kg)	Loss in weight (%)	Average loss in weight (%)	Weight of cubes before exposure (kg)	Weight of cubes after exposure (kg)	Loss in weight (%)	Average loss in weight (%)
100	2.630	2.622	0.304	0.36	2.571	2.563	0.311	0.30
	2.613	2.604	0.344		2.529	2.520	0.356	
	2.505	2.496	0.359		2.647	2.637	0.378	
	2.510	2.501	0.359		2.614	2.608	0.230	
	2.609	2.599	0.383		2.639	2.633	0.227	
	2.619	2.609	0.382		2.579	2.572	0.271	
200	2.629	2.597	1.217	1.33	2.599	2.563	1.385	1.13
	2.662	2.621	1.540		2.647	2.613	1.284	
	2.643	2.584	2.232		2.623	2.578	1.716	
	2.659	2.632	1.015		2.593	2.572	0.810	
	2.712	2.689	0.848		2.611	2.591	0.766	
	2.632	2.603	1.102		2.637	2.615	0.834	
300	2.562	2.491	2.771	3.17	2.621	2.553	2.594	2.91
	2.483	2.431	2.094		2.559	2.507	2.032	
	2.659	2.592	2.520		2.590	2.521	2.664	
	2.610	2.506	3.985		2.646	2.548	3.704	
	2.670	2.575	3.558		2.564	2.491	2.847	
	2.572	2.467	4.082		2.635	2.540	3.605	
400	2.616	2.517	3.784	4.47	2.613	2.509	3.980	4.17
	2.570	2.464	4.125		2.598	2.498	3.849	
	2.611	2.498	4.328		2.557	2.449	4.224	
	2.619	2.483	5.193		2.601	2.522	3.037	
	2.647	2.527	4.533		2.634	2.485	5.657	
	2.585	2.460	4.836		2.685	2.570	4.283	

500	2.574	2.423	5.866	5.09	2.565	2.406	6.199	5.06
	2.603	2.466	5.263		2.626	2.503	4.684	
	2.607	2.470	5.255		2.667	2.529	5.174	
	2.607	2.481	4.833		2.628	2.501	4.833	
	2.613	2.493	4.592		2.623	2.508	4.384	
	2.604	2.481	4.724		2.654	2.519	5.087	
600	2.663	2.514	5.595	5.63	2.660	2.500	6.015	5.53
	2.707	2.560	5.430		2.566	2.450	4.521	
	2.628	2.473	5.898		2.595	2.435	6.166	
	2.551	2.404	5.762		2.601	2.463	5.306	
	2.607	2.460	5.639		2.628	2.496	5.023	
	2.575	2.435	5.437		2.624	2.462	6.174	
700	2.642	2.468	6.586	5.96	2.621	2.470	5.761	5.91
	2.639	2.493	5.532		2.562	2.408	6.011	
	2.597	2.428	6.508		2.580	2.405	6.783	
	2.549	2.395	6.042		2.580	2.436	5.581	
	2.682	2.523	5.928		2.619	2.461	6.033	
	2.664	2.526	5.180		2.699	2.556	5.298	
800	2.566	2.385	7.054	6.44	2.649	2.476	5.532	6.15
	2.603	2.443	6.147		2.620	2.408	6.011	
	2.578	2.402	6.827		2.570	2.420	6.202	
	2.545	2.382	6.405		2.661	2.446	5.194	
	2.701	2.539	5.998		2.609	2.455	6.262	
	2.634	2.470	6.226		2.591	2.491	7.707	

Table B-2: Variation of loss in weight for HPC-F and HPC-G-F mix cubes after exposure to elevated temperature and retained for 1 hour

Temperature (°C)	HPC-F				HPC-G-F			
	Weight of cubes before exposure (kg)	Weight of cubes after exposure (kg)	Loss in weight (%)	Average loss in weight (%)	Weight of cubes before exposure (kg)	Weight of cubes after exposure (kg)	Loss in weight (%)	Average loss in weight (%)
100	2.510	2.502	0.319	0.30	2.618	2.608	0.382	0.32
	2.538	2.530	0.315		2.583	2.574	0.348	
	2.570	2.563	0.292		2.533	2.525	0.316	
	2.490	2.482	0.321		2.610	2.602	0.307	
	2.569	2.562	0.272		2.579	2.572	0.271	
	2.582	2.575	0.271		2.652	2.644	0.302	
200	2.560	2.525	1.367	1.26	2.640	2.590	1.894	1.30
	2.614	2.585	1.109		2.607	2.571	1.381	
	2.474	2.440	1.374		2.629	2.575	2.054	
	2.696	2.664	1.187		2.597	2.576	0.809	
	2.532	2.502	1.185		2.564	2.543	0.819	
	2.491	2.457	1.365		2.505	2.484	0.838	
300	2.563	2.485	3.043	2.78	2.578	2.487	3.530	3.03
	2.555	2.483	2.818		2.604	2.525	3.034	
	2.598	2.528	2.694		2.577	2.500	2.988	
	2.446	2.380	2.698		2.549	2.480	2.707	
	2.595	2.520	2.890		2.514	2.435	3.142	
	2.616	2.550	2.523		2.608	2.535	2.799	
400	2.617	2.500	4.471	4.26	2.513	2.399	4.536	4.40
	2.493	2.378	4.613		2.548	2.433	4.513	
	2.509	2.393	4.623		2.655	2.542	4.256	
	2.478	2.377	4.076		2.604	2.490	4.378	
	2.580	2.485	3.682		2.604	2.485	4.570	
	2.455	2.355	4.073		2.587	2.480	4.136	

500	2.495	2.371	4.970	4.75	2.600	2.478	4.692	4.87
	2.429	2.315	4.693		2.631	2.490	5.359	
	2.470	2.350	4.858		2.566	2.440	4.910	
	2.564	2.450	4.446		2.600	2.469	5.038	
	2.583	2.462	4.684		2.620	2.488	5.038	
	2.517	2.395	4.847		2.536	2.435	3.983	
600	2.522	2.399	4.877	4.95	2.602	2.470	5.073	5.07
	2.588	2.465	4.753		2.625	2.480	5.524	
	2.607	2.482	4.795		2.515	2.385	5.169	
	2.501	2.375	5.038		2.492	2.365	5.096	
	2.474	2.349	5.053		2.538	2.425	4.452	
	2.573	2.440	5.169		2.661	2.525	5.111	
700	2.589	2.462	4.905	5.10	2.597	2.442	5.968	5.36
	2.541	2.410	5.155		2.552	2.402	5.878	
	2.513	2.386	5.054		2.451	2.325	5.141	
	2.594	2.460	5.166		2.574	2.445	5.012	
	2.49	2.368	4.900		2.614	2.480	5.126	
	2.532	2.395	5.411		2.537	2.410	5.006	
800	2.486	2.450	5.369	5.25	2.536	2.445	5.853	5.66
	2.669	2.415	4.959		2.577	2.412	5.486	
	2.534	2.378	5.372		2.582	2.315	5.549	
	2.555	2.460	5.166		2.538	2.426	5.750	
	2.483	2.360	5.221		2.524	2.465	5.700	
	2.629	2.395	5.411		2.503	2.395	5.597	

Table B-3: Variation of loss in weight for HPC-O and HPC-G mix cubes after exposure to elevated temperature and retained for 2 hours

Temperature (°C)	HPC-O				HPC-G			
	Weight of cubes before exposure (kg)	Weight of cubes after exposure (kg)	Loss in weight (%)	Average loss in weight (%)	Weight of cubes before exposure (kg)	Weight of cubes after exposure (kg)	Loss in weight (%)	Average loss in weight (%)
100	2.560	2.546	0.547	0.46	2.655	2.644	0.414	0.39
	2.646	2.632	0.529		2.638	2.626	0.455	
	2.690	2.675	0.558		2.631	2.616	0.570	
	2.622	2.612	0.381		2.634	2.626	0.304	
	2.698	2.688	0.371		2.682	2.674	0.298	
	2.611	2.601	0.383		2.589	2.582	0.270	
200	2.632	2.588	1.672	2.18	2.585	2.535	1.934	2.05
	2.563	2.525	1.483		2.608	2.577	1.189	
	2.701	2.657	1.629		2.623	2.560	2.402	
	2.588	2.511	2.975		2.585	2.525	2.321	
	2.627	2.562	2.474		2.611	2.560	1.953	
	2.682	2.605	2.871		2.547	2.483	2.513	
300	2.586	2.477	4.215	4.05	2.628	2.525	3.919	3.91
	2.620	2.515	4.008		2.643	2.535	4.086	
	2.584	2.469	4.450		2.761	2.645	4.201	
	2.707	2.608	3.657		2.664	2.567	3.641	
	2.606	2.509	3.722		2.584	2.485	3.831	
	2.619	2.508	4.238		2.577	2.480	3.764	
400	2.660	2.521	5.226	4.60	2.639	2.515	4.699	4.46
	2.639	2.524	4.358		2.662	2.535	4.771	
	2.585	2.450	5.222		2.600	2.490	4.231	
	2.696	2.586	4.080		2.648	2.530	4.456	
	2.640	2.532	4.091		2.571	2.465	4.123	
	2.536	2.419	4.614		2.618	2.500	4.507	

500	2.635	2.490	5.503	5.37	2.630	2.497	5.076	5.24
	2.635	2.480	5.882		2.617	2.485	5.044	
	2.583	2.441	5.497		2.632	2.491	5.357	
	2.619	2.488	5.002		2.634	2.496	5.239	
	2.705	2.566	5.139		2.614	2.471	5.471	
	2.635	2.498	5.199		2.680	2.540	5.224	
600	2.629	2.473	5.934	5.72	2.590	2.445	5.598	5.60
	2.635	2.491	5.465		2.686	2.540	5.436	
	2.658	2.519	5.229		2.577	2.438	5.394	
	2.625	2.467	6.019		2.666	2.515	5.664	
	2.587	2.443	5.566		2.595	2.436	6.127	
	2.631	2.470	6.119		2.627	2.485	5.405	
700	2.583	2.427	6.039	6.13	2.593	2.440	5.901	6.05
	2.575	2.400	6.796		2.633	2.471	6.153	
	2.593	2.430	6.286		2.645	2.485	6.049	
	2.651	2.495	5.885		2.603	2.439	6.300	
	2.643	2.485	5.978		2.576	2.425	5.862	
	2.621	2.469	5.799		2.605	2.448	6.027	
800	2.700	2.544	5.778	6.36	2.618	2.450	6.417	6.21
	2.598	2.442	6.005		2.546	2.395	5.931	
	2.590	2.424	6.409		2.610	2.450	6.130	
	2.633	2.457	6.684		2.617	2.455	6.190	
	2.603	2.431	6.608		2.570	2.409	6.265	
	2.704	2.524	6.657		2.604	2.440	6.298	

Table B-4: Variation of loss in weight for HPC-F and HPC-G-F mix cubes after exposure to elevated temperature and retained for 2 hours

Temperature (°C)	HPC-F				HPC-G-F			
	Weight of cubes before exposure (kg)	Weight of cubes after exposure (kg)	Loss in weight (%)	Average loss in weight (%)	Weight of cubes before exposure (kg)	Weight of cubes after exposure (kg)	Loss in weight (%)	Average loss in weight (%)
100	2.562	2.550	0.468	0.40	2.536	2.522	0.552	0.40
	2.650	2.639	0.415		2.560	2.548	0.469	
	2.513	2.500	0.517		2.612	2.600	0.459	
	2.593	2.583	0.386		2.560	2.551	0.352	
	2.501	2.493	0.320		2.538	2.531	0.276	
	2.567	2.559	0.312		2.597	2.589	0.308	
200	2.535	2.496	1.538	1.78	2.606	2.561	1.727	1.82
	2.525	2.495	1.188		2.597	2.550	1.810	
	2.577	2.537	1.552		2.647	2.606	1.549	
	2.581	2.525	2.170		2.701	2.652	1.814	
	2.556	2.506	1.956		2.588	2.535	2.048	
	2.641	2.581	2.272		2.576	2.525	1.980	
300	2.515	2.420	3.777	3.67	2.532	2.445	3.436	3.74
	2.603	2.507	3.688		2.600	2.502	3.769	
	2.502	2.401	4.037		2.552	2.455	3.801	
	2.475	2.386	3.596		2.479	2.397	3.308	
	2.612	2.520	3.522		2.535	2.440	3.748	
	2.524	2.438	3.407		2.492	2.383	4.374	
400	2.608	2.497	4.256	4.31	2.602	2.481	4.650	4.36
	2.587	2.475	4.329		2.605	2.490	4.415	
	2.587	2.470	4.523		2.605	2.498	4.107	
	2.511	2.399	4.460		2.616	2.502	4.358	
	2.560	2.450	4.297		2.615	2.515	3.824	
	2.543	2.442	3.972		2.517	2.396	4.807	

500	2.593	2.472	4.666	4.65	2.581	2.441	5.424	5.03
	2.529	2.411	4.666		2.568	2.435	5.179	
	2.603	2.478	4.802		2.506	2.381	4.988	
	2.541	2.413	5.037		2.592	2.460	5.093	
	2.594	2.482	4.318		2.543	2.422	4.758	
	2.577	2.464	4.385		2.544	2.423	4.756	
600	2.617	2.494	4.700	5.04	2.578	2.442	5.275	5.19
	2.558	2.426	5.160		2.564	2.443	4.719	
	2.646	2.519	4.800		2.660	2.528	4.962	
	2.575	2.446	5.010		2.546	2.407	5.460	
	2.552	2.415	5.368		2.595	2.466	4.971	
	2.507	2.377	5.185		2.556	2.409	5.751	
700	2.511	2.384	5.058	5.13	2.533	2.391	5.606	5.44
	2.472	2.347	5.057		2.598	2.470	4.927	
	2.518	2.404	4.527		2.534	2.380	6.077	
	2.603	2.469	5.148		2.559	2.421	5.393	
	2.519	2.378	5.597		2.591	2.455	5.249	
	2.622	2.480	5.416		2.661	2.517	5.411	
800	2.557	2.404	5.984	5.56	2.621	2.466	5.914	5.97
	2.51	2.372	5.498		2.608	2.449	6.097	
	2.584	2.425	6.153		2.594	2.449	5.590	
	2.478	2.347	5.287		2.539	2.374	6.499	
	2.601	2.468	5.113		2.491	2.348	5.741	
	2.533	2.398	5.330		2.651	2.492	5.998	

Table B-5: Variation of loss in weight for HPC-O and HPC-G mix cubes after exposure to elevated temperature and retained for 3 hours

Temperature (°C)	HPC-O				HPC-G			
	Weight of cubes before exposure (kg)	Weight of cubes after exposure (kg)	Loss in weight (%)	Average loss in weight (%)	Weight of cubes before exposure (kg)	Weight of cubes after exposure (kg)	Loss in weight (%)	Average loss in weight (%)
100	2.668	2.650	0.675	0.65	2.680	2.662	0.672	0.61
	2.706	2.687	0.702		2.580	2.562	0.698	
	2.600	2.580	0.769		2.667	2.649	0.675	
	2.666	2.650	0.600		2.599	2.585	0.539	
	2.681	2.666	0.559		2.607	2.594	0.499	
	2.594	2.578	0.617		2.575	2.560	0.583	
200	2.592	2.520	2.778	2.68	2.665	2.594	2.664	2.39
	2.715	2.640	2.762		2.684	2.600	3.130	
	2.599	2.532	2.578		2.648	2.567	3.059	
	2.616	2.545	2.714		2.545	2.498	1.847	
	2.627	2.555	2.741		2.748	2.710	1.383	
	2.652	2.585	2.526		2.628	2.569	2.245	
300	2.669	2.557	4.196	4.20	2.642	2.522	4.542	4.14
	2.596	2.490	4.083		2.666	2.562	3.901	
	2.590	2.483	4.131		2.651	2.541	4.149	
	2.619	2.511	4.124		2.655	2.550	3.955	
	2.588	2.475	4.366		2.692	2.581	4.123	
	2.641	2.527	4.317		2.701	2.589	4.147	
400	2.605	2.475	4.990	4.94	2.671	2.541	4.867	4.88
	2.678	2.549	4.817		2.598	2.463	5.196	
	2.579	2.448	5.079		2.656	2.530	4.744	
	2.635	2.506	4.896		2.713	2.584	4.755	
	2.604	2.475	4.954		2.673	2.545	4.789	
	2.592	2.465	4.900		2.603	2.475	4.917	

500	2.605	2.460	5.566	5.52	2.653	2.501	5.729	5.43
	2.656	2.512	5.422		2.589	2.448	5.446	
	2.675	2.528	5.495		2.540	2.400	5.512	
	2.602	2.455	5.650		2.643	2.495	5.600	
	2.673	2.525	5.537		2.542	2.410	5.193	
	2.585	2.444	5.455		2.666	2.530	5.101	
600	2.650	2.492	5.962	5.86	2.609	2.457	5.826	5.75
	2.517	2.360	6.238		2.598	2.444	5.928	
	2.644	2.490	5.825		2.545	2.393	5.972	
	2.607	2.454	5.869		2.691	2.524	6.206	
	2.674	2.527	5.497		2.629	2.465	6.238	
	2.662	2.508	5.785		2.711	2.544	6.160	
700	2.582	2.423	6.158	6.21	2.574	2.410	6.371	6.10
	2.658	2.495	6.132		2.622	2.460	6.178	
	2.661	2.495	6.238		2.590	2.428	6.255	
	2.603	2.446	6.032		2.600	2.452	5.692	
	2.640	2.470	6.439		2.706	2.543	6.024	
	2.597	2.435	6.238		2.589	2.430	6.141	
800	2.622	2.445	6.751	6.71	2.642	2.485	5.942	6.40
	2.599	2.420	6.887		2.566	2.400	6.469	
	2.678	2.500	6.647		2.558	2.394	6.411	
	2.640	2.470	6.439		2.613	2.448	6.315	
	2.582	2.410	6.662		2.573	2.401	6.685	
	2.612	2.433	6.853		2.644	2.473	6.467	

Table B-6: Variation of loss in weight for HPC-F and HPC-G-F mix cubes after exposure to elevated temperature and retained for 3 hours

Temperature (°C)	HPC-F				HPC-G-F			
	Weight of cubes before exposure (kg)	Weight of cubes after exposure (kg)	Loss in weight (%)	Average loss in weight (%)	Weight of cubes before exposure (kg)	Weight of cubes after exposure (kg)	Loss in weight (%)	Average loss in weight (%)
100	2.531	2.518	0.514	0.53	2.587	2.574	0.503	0.62
	2.594	2.580	0.540		2.517	2.504	0.516	
	2.516	2.505	0.437		2.610	2.596	0.536	
	2.537	2.522	0.591		2.574	2.553	0.816	
	2.565	2.552	0.507		2.572	2.558	0.544	
	2.582	2.566	0.620		2.560	2.539	0.820	
200	2.521	2.465	2.221	2.40	2.581	2.490	3.526	2.87
	2.520	2.455	2.579		2.519	2.433	3.414	
	2.553	2.490	2.468		2.593	2.507	3.317	
	2.535	2.475	2.367		2.538	2.485	2.088	
	2.566	2.502	2.494		2.510	2.441	2.749	
	2.523	2.465	2.299		2.617	2.562	2.102	
300	2.471	2.370	4.087	4.11	2.673	2.572	3.779	4.05
	2.546	2.436	4.321		2.646	2.536	4.157	
	2.614	2.504	4.208		2.548	2.438	4.317	
	2.611	2.505	4.060		2.555	2.446	4.266	
	2.530	2.428	4.032		2.560	2.463	3.789	
	2.492	2.394	3.933		2.568	2.465	4.011	
400	2.603	2.469	5.148	4.64	2.544	2.413	5.149	4.74
	2.540	2.413	5.000		2.497	2.379	4.726	
	2.604	2.480	4.762		2.491	2.364	5.098	
	2.571	2.459	4.356		2.554	2.434	4.699	
	2.583	2.467	4.491		2.559	2.454	4.103	
	2.528	2.425	4.074		2.519	2.402	4.645	

500	2.463	2.345	4.807	4.94	2.635	2.496	5.275	4.91
	2.578	2.445	5.159		2.571	2.443	4.979	
	2.586	2.449	5.298		2.537	2.421	4.572	
	2.562	2.439	4.801		2.515	2.388	5.050	
	2.612	2.493	4.556		2.506	2.388	4.709	
	2.521	2.394	5.038		2.555	2.431	4.853	
600	2.589	2.450	5.369	5.16	2.515	2.394	4.811	4.96
	2.572	2.444	4.977		2.611	2.485	4.826	
	2.563	2.433	5.072		2.621	2.490	4.998	
	2.560	2.426	5.234		2.569	2.438	5.099	
	2.575	2.447	4.971		2.612	2.481	5.015	
	2.574	2.437	5.322		2.526	2.400	4.988	
700	2.495	2.355	5.611	5.44	2.586	2.452	5.182	5.29
	2.524	2.391	5.269		2.561	2.423	5.389	
	2.559	2.416	5.588		2.596	2.449	5.663	
	2.590	2.450	5.405		2.583	2.452	5.072	
	2.566	2.437	5.027		2.618	2.489	4.927	
	2.537	2.392	5.715		2.568	2.426	5.530	
800	2.657	2.501	5.871	5.90	2.591	2.445	5.635	6.03
	2.507	2.349	6.302		2.547	2.394	6.007	
	2.585	2.425	6.190		2.512	2.355	6.250	
	2.557	2.412	5.671		2.57	2.415	6.031	
	2.591	2.445	5.635		2.572	2.42	5.910	
	2.589	2.440	5.755		2.589	2.425	6.334	

Table B-7: Change in porosity for HPC-O and HPC-G mix cubes after exposure to elevated temperature and retained for 1 hour

Temperature (°C)	HPC-O					HPC-G				
	Dry weight of cubes (kg)	Saturated weight of cubes in water (kg)	Saturated weight of cubes in air (kg)	Porosity (%)	Average porosity (%)	Dry weight of cubes (kg)	Saturated weight of cubes in water (kg)	Saturated weight of cubes in air (kg)	Porosity (%)	Average porosity (%)
27	2.511	1.490	2.525	1.4	0.97	2.562	1.534	2.572	1.0	0.83
	2.527	1.525	2.535	0.8		2.564	1.611	2.572	0.8	
	2.594	1.550	2.602	0.8		2.605	1.612	2.612	0.7	
100	2.622	1.564	2.645	2.1	2.04	2.563	1.537	2.576	1.3	1.60
	2.604	1.558	2.630	2.4		2.52	1.517	2.538	1.8	
	2.496	1.493	2.512	1.6		2.637	1.591	2.656	1.8	
200	2.597	1.570	2.632	3.3	4.36	2.563	1.553	2.600	3.5	3.53
	2.621	1.583	2.665	4.1		2.613	1.593	2.650	3.5	
	2.584	1.577	2.645	5.7		2.578	1.570	2.615	3.5	
300	2.506	1.540	2.597	8.6	8.33	2.548	1.571	2.636	8.3	7.80
	2.575	1.585	2.649	7.0		2.491	1.522	2.570	7.5	
	2.467	1.515	2.566	9.4		2.540	1.566	2.620	7.6	
400	2.483	1.519	2.598	10.7	10.22	2.522	1.571	2.625	9.8	10.01
	2.527	1.558	2.633	9.9		2.485	1.540	2.590	10.0	
	2.460	1.511	2.567	10.1		2.570	1.609	2.680	10.3	
500	2.423	1.498	2.560	12.9	12.41	2.406	1.503	2.535	12.5	12.33
	2.466	1.532	2.587	11.5		2.503	1.566	2.628	11.8	
	2.456	1.527	2.593	12.9		2.529	1.589	2.666	12.7	
600	2.514	1.592	2.672	14.6	14.64	2.500	1.585	2.660	14.9	15.14
	2.560	1.620	2.710	13.8		2.404	1.521	2.560	15.0	
	2.473	1.564	2.640	15.5		2.473	1.564	2.640	15.5	
700	2.468	1.555	2.649	16.5	15.67	2.470	1.560	2.627	14.7	15.20
	2.493	1.566	2.646	14.2		2.408	1.517	2.565	15.0	
	2.428	1.529	2.603	16.3		2.405	1.517	2.573	15.9	
800	2.385	1.530	2.565	17.4	17.04	2.496	1.589	2.635	13.3	16.34
	2.443	1.552	2.621	16.7		2.468	1.615	2.668	19.0	
	2.402	1.538	2.580	17.1		2.412	1.556	2.584	16.7	

Table B-8: Change in porosity for HPC-F and HPC-G-F mix cubes after exposure to elevated temperature and retained for 1 hour

Temperature (°C)	HPC-F					HPC-G-F				
	Dry weight of cubes (kg)	Saturated weight of cubes in water (kg)	Saturated weight of cubes in air (kg)	Porosity (%)	Average porosity (%)	Dry weight of cubes (kg)	Saturated weight of cubes in water (kg)	Saturated weight of cubes in air (kg)	Porosity (%)	Average porosity (%)
27	2.539	1.511	2.545	0.6	0.98	2.559	1.508	2.567	0.8	0.70
	2.541	1.494	2.553	1.1		2.572	1.526	2.580	0.8	
	2.497	1.447	2.510	1.2		2.548	1.506	2.554	0.6	
100	2.496	1.456	2.510	1.3	1.53	2.608	1.554	2.623	1.4	1.39
	2.522	1.508	2.540	1.7		2.574	1.530	2.587	1.2	
	2.554	1.514	2.570	1.5		2.522	1.495	2.538	1.5	
200	2.494	1.499	2.540	4.4	4.13	2.590	1.558	2.636	4.3	4.20
	2.572	1.525	2.617	4.1		2.571	1.546	2.608	3.5	
	2.412	1.461	2.450	3.8		2.575	1.552	2.627	4.8	
300	2.347	1.426	2.420	7.3	7.59	2.443	1.469	2.508	6.3	5.78
	2.490	1.500	2.570	7.5		2.416	1.446	2.475	5.7	
	2.499	1.505	2.585	8.0		2.500	1.494	2.557	5.4	
400	2.377	1.457	2.485	10.5	9.94	2.478	1.530	2.583	10.0	10.04
	2.457	1.500	2.565	10.1		2.485	1.521	2.589	9.7	
	2.333	1.421	2.425	9.2		2.460	1.514	2.570	10.4	
500	2.371	1.476	2.495	12.2	12.31	2.478	1.542	2.610	12.4	12.05
	2.293	1.416	2.415	12.2		2.490	1.546	2.615	11.7	
	2.327	1.434	2.455	12.5		2.419	1.503	2.545	12.1	
600	2.378	1.487	2.530	14.6	14.19	2.449	1.533	2.600	14.2	14.20
	2.449	1.520	2.600	14.0		2.480	1.560	2.632	14.2	
	2.470	1.549	2.620	14.0		2.377	1.487	2.525	14.3	
700	2.442	1.509	2.600	14.5	15.02	2.442	1.531	2.605	15.2	15.02
	2.408	1.488	2.575	15.4		2.402	1.496	2.560	14.8	
	2.369	1.470	2.530	15.2		2.298	1.438	2.450	15.0	
800	2.329	1.484	2.485	15.6	16.12	2.381	1.525	2.550	16.5	16.41
	2.533	1.618	2.715	16.6		2.412	1.542	2.585	16.6	
	2.378	1.514	2.545	16.2		2.417	1.546	2.585	16.2	

Table B-9: Change in porosity for HPC-O and HPC-G mix cubes after exposure to elevated temperature and retained for 2 hours

Temperature (°C)	HPC-O					HPC-G				
	Dry weight of cubes (kg)	Saturated weight of cubes in water (kg)	Saturated weight of cubes in air (kg)	Porosity (%)	Average porosity (%)	Dry weight of cubes (kg)	Saturated weight of cubes in water (kg)	Saturated weight of cubes in air (kg)	Porosity (%)	Average porosity (%)
27	2.690	1.608	2.700	0.9	1.01	2.648	1.579	2.660	1.1	0.84
	2.634	1.579	2.645	1.0		2.657	1.590	2.664	0.7	
	2.619	1.608	2.63	1.1		2.560	1.528	2.568	0.8	
100	2.546	1.526	2.571	2.4	2.19	2.644	1.574	2.663	1.7	2.01
	2.632	1.580	2.655	2.1		2.626	1.574	2.648	2.0	
	2.675	1.616	2.697	2.0		2.616	1.571	2.640	2.2	
200	2.511	1.544	2.589	7.5	6.09	2.525	1.532	2.587	5.9	5.46
	2.562	1.573	2.630	6.4		2.560	1.550	2.612	4.9	
	2.605	1.602	2.651	4.4		2.483	1.521	2.540	5.6	
300	2.477	1.541	2.580	9.9	10.02	2.504	1.547	2.600	9.1	9.05
	2.515	1.566	2.618	9.8		2.529	1.573	2.625	9.1	
	2.469	1.526	2.578	10.4		2.645	1.632	2.744	8.9	
400	2.521	1.566	2.644	11.4	10.79	2.495	1.548	2.600	10.0	10.05
	2.524	1.572	2.626	9.7		2.522	1.558	2.630	10.1	
	2.450	1.522	2.568	11.3		2.462	1.546	2.565	10.1	
500	2.490	1.564	2.631	13.2	13.31	2.473	1.555	2.605	12.6	12.74
	2.480	1.552	2.626	13.6		2.460	1.542	2.595	12.8	
	2.441	1.534	2.578	13.1		2.479	1.554	2.615	12.8	
600	2.467	1.553	2.631	15.2	14.59	2.497	1.570	2.650	14.2	13.94
	2.443	1.529	2.585	13.4		2.436	1.527	2.580	13.7	
	2.470	1.554	2.633	15.1		2.461	1.545	2.610	14.0	
700	2.495	1.578	2.661	15.3	16.07	2.428	1.534	2.585	14.9	15.18
	2.485	1.560	2.652	15.3		2.404	1.512	2.565	15.3	
	2.469	1.569	2.661	17.6		2.429	1.511	2.595	15.3	
800	2.457	1.559	2.651	17.8	17.70	2.450	1.554	2.632	16.9	17.20
	2.431	1.546	2.619	17.5		2.368	1.506	2.545	17.0	
	2.524	1.606	2.723	17.8		2.428	1.539	2.619	17.7	

Table B-10: Change in porosity for HPC-F and HPC-G-F mix cubes after exposure to elevated temperature and retained for 2 hours

Temperature (°C)	HPC-F					HPC-G-F				
	Dry weight of cubes (kg)	Saturated weight of cubes in water (kg)	Saturated weight of cubes in air (kg)	Porosity (%)	Average porosity (%)	Dry weight of cubes (kg)	Saturated weight of cubes in water (kg)	Saturated weight of cubes in air (kg)	Porosity (%)	Average porosity (%)
27	2.517	1.483	2.525	0.8	0.88	2.550	1.506	2.557	0.7	0.70
	2.507	1.470	2.517	1.0		2.492	1.475	2.497	0.5	
	2.612	1.535	2.622	0.9		2.552	1.504	2.562	0.9	
100	2.55	1.515	2.576	2.5	2.40	2.522	1.495	2.546	2.3	2.08
	2.639	1.570	2.663	2.2		2.548	1.523	2.571	2.2	
	2.500	1.470	2.527	2.6		2.600	1.549	2.619	1.8	
200	2.501	1.513	2.555	5.2	5.05	2.617	1.575	2.677	5.4	5.45
	2.483	1.490	2.532	4.7		2.505	1.491	2.562	5.3	
	2.554	1.546	2.610	5.3		2.492	1.510	2.550	5.6	
300	2.420	1.474	2.521	9.6	9.30	2.424	1.440	2.495	6.7	8.05
	2.507	1.522	2.601	8.7		2.496	1.505	2.580	7.8	
	2.401	1.452	2.501	9.5		2.455	1.466	2.560	9.6	
400	2.497	1.533	2.600	9.7	10.25	2.481	1.540	2.585	10.0	10.11
	2.465	1.502	2.581	10.8		2.479	1.534	2.585	10.1	
	2.464	1.502	2.575	10.3		2.481	1.532	2.590	10.3	
500	2.472	1.530	2.606	12.5	12.63	2.441	1.525	2.572	12.5	12.72
	2.411	1.489	2.543	12.5		2.435	1.517	2.570	12.8	
	2.478	1.534	2.618	12.9		2.381	1.484	2.513	12.8	
600	2.469	1.531	2.614	13.4	14.71	2.421	1.520	2.565	13.8	14.04
	2.378	1.473	2.541	15.3		2.455	1.531	2.605	14.0	
	2.480	1.535	2.653	15.5		2.517	1.576	2.675	14.4	
700	2.450	1.526	2.615	15.2	15.07	2.452	1.534	2.617	15.2	15.15
	2.437	1.518	2.592	14.4		2.489	1.521	2.592	9.6	
	2.392	1.490	2.559	15.6		2.426	1.559	2.651	20.6	
800	2.404	1.498	2.586	16.7	16.37	2.466	1.552	2.649	16.7	16.13
	2.372	1.477	2.537	15.6		2.449	1.536	2.631	16.6	
	2.425	1.514	2.609	16.8		2.449	1.535	2.627	16.3	

Table B-11: Change in porosity for HPC-O and HPC-G mix cubes after exposure to elevated temperature and retained for 3 hours

Temperature (°C)	HPC-O					HPC-G				
	Dry weight of cubes (kg)	Saturated weight of cubes in water (kg)	Saturated weight of cubes in air (kg)	Porosity (%)	Average porosity (%)	Dry weight of cubes (kg)	Saturated weight of cubes in water (kg)	Saturated weight of cubes in air (kg)	Porosity (%)	Average porosity (%)
27	2.688	1.620	2.698	0.9	0.99	2.553	1.535	2.563	1.0	0.89
	2.665	1.602	2.675	0.9		2.578	1.545	2.587	0.9	
	2.660	1.589	2.672	1.1		2.668	1.602	2.677	0.8	
100	2.652	1.595	2.675	2.1	2.18	2.585	1.552	2.607	2.1	2.19
	2.666	1.605	2.690	2.2		2.594	1.565	2.616	2.1	
	2.578	1.552	2.601	2.2		2.560	1.542	2.585	2.4	
200	2.563	1.554	2.630	6.2	6.27	2.498	1.508	2.555	5.4	5.90
	2.579	1.567	2.645	6.1		2.710	1.565	2.790	6.5	
	2.595	1.580	2.665	6.5		2.569	1.563	2.630	5.7	
300	2.511	1.555	2.618	10.1	10.26	2.550	1.585	2.645	9.0	9.04
	2.486	1.541	2.597	10.5		2.581	1.610	2.678	9.1	
	2.527	1.569	2.636	10.2		2.578	1.606	2.675	9.1	
400	2.484	1.542	2.600	11.0	10.96	2.541	1.585	2.650	10.2	10.00
	2.549	1.582	2.668	11.0		2.463	1.535	2.565	9.9	
	2.456	1.531	2.570	11.0		2.521	1.570	2.625	9.9	
500	2.455	1.530	2.600	13.6	13.42	2.495	1.565	2.635	13.1	13.04
	2.538	1.653	2.680	13.8		2.397	1.506	2.530	13.0	
	2.444	1.525	2.580	12.9		2.516	1.576	2.657	13.0	
600	2.454	1.548	2.606	14.4	15.00	2.524	1.596	2.681	14.5	14.68
	2.527	1.597	2.690	14.9		2.465	1.554	2.620	14.5	
	2.508	1.586	2.680	15.7		2.544	1.606	2.710	15.0	
700	2.423	1.583	2.592	16.7	16.21	2.452	1.553	2.620	15.7	15.99
	2.500	1.586	2.678	16.3		2.543	1.605	2.730	16.6	
	2.504	1.588	2.673	15.6		2.430	1.538	2.595	15.6	
800	2.435	1.549	2.631	18.1	17.83	2.455	1.560	2.643	17.4	17.74
	2.417	1.536	2.607	17.7		2.388	1.519	2.573	17.6	
	2.496	1.590	2.690	17.6		2.394	1.520	2.590	18.3	

Table B-12: Change in porosity for HPC-F and HPC-G-F mix cubes after exposure to elevated temperature and retained for 3 hours

Temperature (°C)	HPC-F					HPC-G-F				
	Dry weight of cubes (kg)	Saturated weight of cubes in water (kg)	Saturated weight of cubes in air (kg)	Porosity (%)	Average porosity (%)	Dry weight of cubes (kg)	Saturated weight of cubes in water (kg)	Saturated weight of cubes in air (kg)	Porosity (%)	Average porosity (%)
27	2.578	1.525	2.588	0.9	0.82	2.592	1.544	2.603	1.0	0.70
	2.579	1.521	2.590	1.0		2.529	1.493	2.535	0.6	
	2.537	1.497	2.542	0.5		2.528	1.491	2.533	0.5	
100	2.522	1.490	2.544	2.1	2.35	2.574	1.533	2.597	2.2	2.05
	2.552	1.517	2.580	2.6		2.504	1.485	2.525	2.0	
	2.566	1.519	2.591	2.3		2.596	1.543	2.617	2.0	
200	2.432	1.468	2.490	5.7	5.57	2.497	1.494	2.565	6.3	6.23
	2.431	1.462	2.490	5.7		2.441	1.458	2.510	6.6	
	2.475	1.490	2.530	5.3		2.562	1.533	2.625	5.8	
300	2.505	1.510	2.610	9.5	9.56	2.446	1.476	2.539	8.7	8.85
	2.428	1.470	2.524	9.1		2.463	1.478	2.560	9.0	
	2.394	1.448	2.500	10.1		2.465	1.497	2.559	8.9	
400	2.459	1.518	2.578	11.2	11.25	2.413	1.493	2.520	10.4	10.19
	2.467	1.515	2.588	11.3		2.379	1.475	2.480	10.0	
	2.425	1.479	2.545	11.3		2.364	1.465	2.465	10.1	
500	2.439	1.500	2.571	12.3	12.95	2.388	1.483	2.521	12.8	13.07
	2.493	1.538	2.645	13.7		2.388	1.492	2.520	12.8	
	2.394	1.473	2.529	12.8		2.431	1.513	2.575	13.6	
600	2.426	1.506	2.600	15.9	14.86	2.438	1.524	2.590	14.3	14.69
	2.447	1.513	2.610	14.9		2.481	1.543	2.645	14.9	
	2.437	1.513	2.585	13.8		2.387	1.486	2.545	14.9	
700	2.450	1.526	2.615	15.2	15.07	2.452	1.534	2.617	15.2	15.40
	2.437	1.518	2.592	14.4		2.489	1.521	2.650	14.3	
	2.392	1.490	2.559	15.6		2.426	1.559	2.600	16.7	
800	2.501	1.562	2.681	16.1	16.43	2.455	1.538	2.650	17.5	17.16
	2.349	1.460	2.525	16.5		2.394	1.503	2.572	16.7	
	2.425	1.520	2.606	16.7		2.355	1.480	2.538	17.3	

Table B-13: Variation in UPV for all mix cubes after exposure to elevated temperature and retained for 1 hour

Temperature (°C)	HPC-O		HPC-G		HPC-F		HPC-G-F	
	UPV (km/sec)	Average UPV (km/sec)	UPV (km/sec)	Average UPV (km/sec)	UPV (km/sec)	Average UPV (km/sec)	UPV (km/sec)	Average UPV (km/sec)
27	5.0	5.0	5.1	5.0	5.1	5.1	5.3	5.1
	5.3		4.9		5.1		5.0	
	4.8		4.8		5.1		5.0	
100	4.7	4.7	5.0	4.9	5.3	5.1	5.0	5.0
	4.8		5.0		5.0		5.0	
	4.8		4.8		5.0		5.0	
200	4.8	4.8	5.0	4.8	5.0	4.9	4.8	4.8
	4.9		4.5		5.0		4.5	
	4.8		5.0		4.8		5.0	
300	4.3	4.3	4.5	4.3	4.5	4.6	4.8	4.5
	4.3		4.2		4.5		4.5	
	4.3		4.3		4.8		4.3	
400	3.6	3.7	3.8	3.9	4.0	3.9	4.0	3.9
	3.7		4.0		3.8		3.7	
	3.7		3.8		4.0		4.0	
500	3.3	3.3	3.4	3.5	3.3	3.4	3.4	3.4
	3.2		3.5		3.6		3.3	
	3.4		3.6		3.3		3.4	
600	2.7	2.8	2.7	2.8	2.8	2.8	2.5	2.6
	2.9		2.8		2.8		2.5	
	2.8		2.9		2.9		2.6	
700	1.9	2.0	2.4	2.1	2.0	2.1	2.2	2.1
	2.0		2.4		2.2		2.0	
	2.0		2.4		2.2		2.2	
800	1.8	1.7	2.0	1.8	1.8	1.8	1.8	1.8
	1.7		2.1		1.8		1.8	
	1.7		2.2		1.7		1.7	

Table B-14: Variation in UPV for all mix cubes after exposure to elevated temperature and retained for 2 hours

Temperature (°C)	HPC-O		HPC-G		HPC-F		HPC-G-F	
	UPV (km/sec)	Average UPV (km/sec)	UPV (km/sec)	Average UPV (km/sec)	UPV (km/sec)	Average UPV (km/sec)	UPV (km/sec)	Average UPV (km/sec)
27	5.0	5.0	4.9	5.0	4.9	5.0	5.6	5.2
	5.3		5.0		4.9		5.0	
	4.8		5.1		5.2		5.0	
100	3.7	3.8	4.2	4.0	4.2	4.1	3.7	3.8
	4.0		3.8		4.2		4.0	
	3.8		4.0		4.0		3.8	
200	3.8	3.8	3.6	3.6	3.6	3.7	3.7	3.6
	3.7		3.6		3.8		3.4	
	3.7		3.6		3.6		3.6	
300	3.2	3.4	3.4	3.5	3.7	3.6	3.3	3.4
	3.6		3.6		3.6		3.4	
	3.3		3.6		3.4		3.3	
400	3.1	3.0	2.9	3.1	2.9	2.9	3.0	3.0
	2.9		3.2		3.0		3.0	
	2.9		3.1		2.9		3.2	
500	2.4	2.3	2.7	2.8	2.6	2.7	2.4	2.5
	2.3		2.8		2.7		2.4	
	2.4		2.8		2.7		2.6	
600	2.0	2.0	2.0	2.1	1.9	2.0	1.8	1.9
	1.8		2.2		2.2		2.0	
	2.1		2.2		2.0		1.8	
700	1.1	1.1	1.3	1.3	1.2	1.2	1.1	1.1
	1.1		1.2		1.2		1.1	
	1.1		1.3		1.1		1.1	
800	0.9	0.9	1.1	1.0	1.1	1.0	0.9	0.9
	1.0		1.1		1.0		0.9	
	0.9		1.0		1.0		1.0	

Table B-15: Variation in UPV for all mix cubes after exposure to elevated temperature and retained for 3 hours

Temperature (°C)	HPC-O		HPC-G		HPC-F		HPC-G-F	
	UPV (km/sec)	Average UPV (km/sec)	UPV (km/sec)	Average UPV (km/sec)	UPV (km/sec)	Average UPV (km/sec)	UPV (km/sec)	Average UPV (km/sec)
27	5.3	5.2	5.3	5.1	5.1	5.2	5.3	5.3
	5.2		5.0		5.3		5.3	
	5.1		5.0		5.2		5.3	
100	3.6	3.7	4.2	4.1	4.0	4.2	3.6	3.6
	4.0		3.8		4.2		3.6	
	3.6		4.2		4.3		3.7	
200	3.4	3.5	3.4	3.5	3.7	3.6	3.2	3.3
	3.7		3.6		3.6		3.4	
	3.3		3.4		3.4		3.3	
300	3.0	2.8	3.1	3.0	3.3	3.3	3.0	3.0
	2.9		3.1		3.2		3.0	
	2.6		2.9		3.4		3.0	
400	2.2	2.3	2.5	2.7	2.6	2.8	2.5	2.5
	2.5		2.6		2.9		2.5	
	2.2		2.9		2.8		2.5	
500	1.8	1.8	2.1	2.0	2.3	2.3	2.0	2.0
	1.8		2.0		2.3		2.0	
	1.9		2.1		2.4		2.0	
600	1.2	1.2	1.6	1.4	1.9	1.9	1.5	1.5
	1.3		1.4		1.9		1.5	
	1.2		1.4		1.9		1.7	
700	0.9	0.9	0.9	1.0	1.1	1.1	1.0	1.1
	1.0		1.0		1.1		1.1	
	0.9		1.0		1.1		1.1	
800	0.8	0.7	0.9	0.9	1.0	1.0	1.0	0.9
	0.8		0.9		1.0		0.9	
	0.7		1.0		1.0		1.0	

Table B-16: Variation in Compressive strength for HPC-O and HPC-G mix cubes after exposure to elevated temperature and retained for 1 hour

Temperature (°C)	HPC-O			HPC-G		
	Compressive strength (MPa)	Average Compressive strength (MPa)	Compressive strength ratio	Compressive strength (MPa)	Average Compressive strength (MPa)	Compressive strength ratio
27	85.0	83.8	1.00	83.0	77.2	1.00
	82.5			76.0		
	84.0			72.5		
100	86.0	83.5	0.99	75.0	73.5	0.95
	84.5			73.0		
	80.0			72.5		
200	80.0	79.7	0.95	77.5	76.0	0.98
	80.0			77.5		
	79.0			73.0		
300	80.0	82.0	0.98	80.0	77.3	1.00
	86.0			77.0		
	80.0			75.0		
400	78.0	81.5	0.97	85.0	84.3	1.09
	81.5			88.0		
	85.0			80.0		
500	80.0	79.7	0.95	80.0	82.0	1.06
	89.0			86.0		
	70.0			80.0		
600	77.5	74.2	0.88	70.0	75.0	0.97
	73.0			70.0		
	72.0			85.0		
700	56.5	57.7	0.69	59.0	56.5	0.73
	60.0			55.0		
	56.5			55.5		
800	45.0	45.0	0.54	50.0	50.0	0.65
	45.0			50.0		
	45.0			50.0		

Table B-17: Variation in Compressive strength for HPC-F and HPC-G-F mix cubes after exposure to elevated temperature and retained for 1 hour

Temperature (°C)	HPC-F			HPC-G-F		
	Compressive strength (MPa)	Average Compressive strength (MPa)	Compressive strength ratio	Compressive strength (MPa)	Average Compressive strength (MPa)	Compressive strength ratio
27	74.3	73.8	1.00	75.0	77.7	1.00
	72.9			78.0		
	74.3			80.0		
100	70.0	71.8	0.97	77.0	75.2	0.97
	67.5			74.0		
	78.0			74.5		
200	70.0	74.7	1.01	81.0	77.0	0.99
	75.5			72.0		
	78.5			78.0		
300	77.5	84.3	1.14	91.0	87.3	1.12
	84.5			82.0		
	91.0			89.0		
400	78.5	84.7	1.15	94.0	92.0	1.18
	85.5			92.0		
	90.0			90.0		
500	79.0	78.5	1.06	87.0	83.3	1.07
	82.0			78.0		
	74.5			85.0		
600	81.0	73.3	0.99	81.0	76.3	0.98
	67.5			78.0		
	71.5			70.0		
700	56.5	61.2	0.83	67.5	64.7	0.83
	62.0			65.0		
	65.0			61.5		
800	55.0	52.7	0.71	58.0	57.2	0.74
	53.0			59.5		
	50.0			54.0		

Table B-18: Variation in Compressive strength for HPC-O and HPC-G mix cubes after exposure to elevated temperature and retained for 2 hours

Temperature (°C)	HPC-O			HPC-G		
	Compressive strength (MPa)	Average Compressive strength (MPa)	Compressive strength ratio	Compressive strength (MPa)	Average Compressive strength (MPa)	Compressive strength ratio
27	75.0	80.0	1.00	80.0	78.3	1.00
	80.0			75.0		
	85.0			80.0		
100	78.0	80.3	1.00	80.0	75.0	0.96
	83.0			75.0		
	80.0			70.0		
200	80.0	80.0	1.00	82.0	76.3	0.97
	80.0			77.0		
	80.0			70.0		
300	80.0	82.3	1.03	75.0	81.8	1.04
	82.0			88.0		
	85.0			82.5		
400	77.0	79.0	0.99	80.0	80.3	1.03
	80.0			81.0		
	80.0			80.0		
500	70.0	71.7	0.90	77.5	77.5	0.99
	70.0			80.0		
	75.0			75.0		
600	62.0	58.2	0.73	65.5	65.8	0.84
	60.0			64.0		
	52.5			68.0		
700	45.0	46.0	0.58	58.0	52.3	0.67
	48.0			51.0		
	45.0			48.0		
800	35.0	35.3	0.44	41.0	39.7	0.51
	35.0			40.0		
	36.0			38.0		

Table B-19: Variation in Compressive strength for HPC-F and HPC-G-F mix cubes after exposure to elevated temperature and retained for 2 hours

Temperature (°C)	HPC-F			HPC-G-F		
	Compressive strength (MPa)	Average Compressive strength (MPa)	Compressive strength ratio	Compressive strength (MPa)	Average Compressive strength (MPa)	Compressive strength ratio
27	75.0	74.5	1.00	78.0	78.0	1.00
	74.3			78.0		
	74.3			78.0		
100	80.0	80.8	1.09	76.0	80.2	1.03
	82.5			84.5		
	80.0			80.0		
200	85.0	82.0	1.10	90.0	84.3	1.08
	83.0			78.0		
	78.0			85.0		
300	80.0	85.7	1.15	85.0	85.3	1.09
	87.0			80.0		
	90.0			91.0		
400	85.0	78.7	1.06	90.0	86.2	1.10
	77.0			80.0		
	74.0			88.5		
500	78.5	74.5	1.00	75.0	73.3	0.94
	75.0			70.0		
	70.0			75.0		
600	70.0	70.0	0.94	65.0	67.2	0.86
	70.0			71.5		
	70.0			65.0		
700	53.5	55.8	0.75	50.0	55.2	0.71
	54.0			57.0		
	60.0			58.5		
800	43.0	42.8	0.57	42.0	43.3	0.56
	45.0			40.5		
	40.5			47.5		

Table B-20: Variation in Compressive strength for HPC-O and HPC-G mix cubes after exposure to elevated temperature and retained for 3 hours

Temperature (°C)	HPC-O			HPC-G		
	Compressive strength (MPa)	Average Compressive strength (MPa)	Compressive strength ratio	Compressive strength (MPa)	Average Compressive strength (MPa)	Compressive strength ratio
27	75.0	80.0	1.00	79.0	77.0	1.00
	80.0			72.0		
	85.0			80.0		
100	76.0	77.2	0.96	80.0	75.0	0.97
	80.0			75.0		
	75.5			70.0		
200	80.0	83.3	1.04	80.0	80.7	1.05
	80.0			80.0		
	90.0			82.0		
300	81.0	79.7	1.00	83.0	85.0	1.10
	80.0			82.0		
	78.0			90.0		
400	69.5	72.5	0.91	88.0	83.5	1.08
	78.0			85.5		
	70.0			77.0		
500	68.0	62.3	0.78	75.0	71.8	0.93
	59.0			65.0		
	60.0			75.5		
600	52.5	48.3	0.60	61.0	52.7	0.68
	47.5			50.0		
	45.0			47.0		
700	41.0	39.3	0.49	45.0	43.3	0.56
	38.5			45.0		
	38.5			40.0		
800	32.0	32.2	0.40	35.0	35.0	0.45
	34.5			35.0		
	30.0			35.0		

Table B-21: Variation in Compressive strength for HPC-F and HPC-G-F mix cubes after exposure to elevated temperature and retained for 3 hours

Temperature (°C)	HPC-F			HPC-G-F		
	Compressive strength (MPa)	Average Compressive strength (MPa)	Compressive strength ratio	Compressive strength (MPa)	Average Compressive strength (MPa)	Compressive strength ratio
27	67.5	72.0	1.00	81.0	78.7	1.00
	74.3			75.0		
	74.3			80.0		
100	76.0	71.8	1.00	75.0	76.3	0.97
	72.0			82.0		
	67.5			72.0		
200	65.0	73.3	1.02	80.0	85.7	1.09
	77.5			85.0		
	77.5			92.0		
300	85.0	81.7	1.13	89.5	84.8	1.08
	80.0			80.0		
	80.0			85.0		
400	75.0	77.7	1.08	85.0	82.3	1.05
	80.0			80.0		
	78.0			82.0		
500	69.0	70.5	0.98	75.0	71.0	0.90
	72.0			70.0		
	70.5			68.0		
600	65.0	60.0	0.83	63.5	60.7	0.77
	60.0			57.5		
	55.0			61.0		
700	45.0	44.2	0.61	43.0	42.7	0.54
	42.5			45.0		
	45.0			40.0		
800	33.5	35.5	0.49	32.0	35.3	0.45
	38.0			38.0		
	35.0			36.0		

Table B-22: Variation in Split tensile strength for HPC-O and HPC-G mix cubes after exposure to elevated temperature and retained for 1 hour

Temperature (°C)	HPC-O			HPC-G		
	Split tensile strength (MPa)	Average Split tensile strength (MPa)	Split tensile strength ratio	Split tensile strength (MPa)	Average Split tensile strength (MPa)	Split tensile strength ratio
27	5.26	5.24	1.00	4.30	5.07	1.00
	5.26			5.01		
	5.20			5.91		
100	5.78	5.35	1.02	5.39	5.40	1.07
	5.14			5.46		
	5.14			5.39		
200	4.94	5.14	0.98	4.49	49.4	0.97
	5.33			5.39		
	5.14			4.94		
300	4.17	4.34	0.83	3.98	4.58	0.90
	4.49			4.94		
	4.37			4.82		
400	3.66	3.79	0.72	3.85	4.02	0.79
	4.37			3.72		
	3.34			4.49		
500	3.02	3.25	0.62	3.40	3.60	0.71
	3.53			3.85		
	3.21			3.53		
600	2.44	2.50	0.48	3.08	2.80	0.55
	2.50			2.57		
	2.57			2.76		
700	1.25	1.31	0.25	1.41	1.73	0.34
	1.38			1.67		
	1.28			2.12		
800	1.03	1.20	0.23	1.35	1.41	0.28
	1.22			1.41		
	1.35			1.48		

Table B-23: Variation in Split tensile strength for HPC-F and HPC-G-F mix cubes after exposure to elevated temperature and retained for 1 hour

Temperature (°C)	HPC-F			HPC-G-F		
	Split tensile strength (MPa)	Average Split tensile strength (MPa)	Split tensile strength ratio	Split tensile strength (MPa)	Average Split tensile strength (MPa)	Split tensile strength ratio
27	4.72	4.90	1.00	5.01	4.84	1.00
	4.98			4.72		
	5.01			4.78		
100	4.88	5.18	1.06	4.82	4.82	1.00
	5.20			5.01		
	5.46			4.62		
200	4.69	4.88	1.00	4.49	4.60	0.95
	4.82			4.49		
	5.14			4.82		
300	4.62	4.46	0.91	4.37	4.49	0.93
	3.92			4.62		
	4.85			4.49		
400	4.04	4.02	0.82	4.37	3.96	0.82
	3.85			3.72		
	4.17			3.79		
500	3.60	3.63	0.74	3.53	3.54	0.73
	3.76			3.76		
	3.53			3.34		
600	3.15	2.95	0.60	3.02	2.82	0.58
	2.89			2.70		
	2.82			2.76		
700	2.12	1.95	0.40	1.80	1.65	0.34
	1.80			1.35		
	1.93			1.80		
800	1.28	1.34	0.27	1.28	1.31	0.27
	1.25			1.22		
	1.48			1.41		

Table B-24: Variation in Split tensile strength for HPC-O and HPC-G mix cubes after exposure to elevated temperature and retained for 2 hours

Temperature (°C)	HPC-O			HPC-G		
	Split tensile strength (MPa)	Average Split tensile strength (MPa)	Split tensile strength ratio	Split tensile strength (MPa)	Average Split tensile strength (MPa)	Split tensile strength ratio
27	5.14	5.35	1.00	5.20	5.05	1.00
	5.14			5.14		
	5.78			4.82		
100	5.78	5.36	1.04	5.59	5.29	1.05
	5.46			5.14		
	5.46			5.14		
200	4.82	5.26	0.98	4.82	5.01	0.99
	5.39			4.94		
	5.59			5.26		
300	3.66	4.11	0.77	4.37	4.43	0.88
	4.49			4.17		
	4.17			4.75		
400	3.85	3.42	0.64	3.21	3.68	0.73
	3.53			3.85		
	2.89			3.98		
500	3.21	2.89	0.54	2.57	3.10	0.61
	2.57			3.53		
	2.89			3.21		
600	1.86	2.01	0.38	2.38	2.23	0.44
	2.25			2.18		
	1.93			2.12		
700	1.35	1.32	0.25	1.38	1.62	0.32
	1.38			1.93		
	1.22			1.54		
800	1.09	1.11	0.21	1.09	1.24	0.25
	1.09			1.28		
	1.16			1.35		

Table B-25: Variation in Split tensile strength for HPC-F and HPC-G-F mix cubes after exposure to elevated temperature and retained for 2 hours

Temperature (°C)	HPC-F			HPC-G-F		
	Split tensile strength (MPa)	Average Split tensile strength (MPa)	Split tensile strength ratio	Split tensile strength (MPa)	Average Split tensile strength (MPa)	Split tensile strength ratio
27	4.62	5.01	1.00	4.82	4.96	1.00
	5.26			5.01		
	5.14			5.07		
100	5.39	5.22	1.04	5.14	5.08	1.02
	5.14			5.42		
	5.14			4.69		
200	5.14	4.92	0.98	5.07	4.88	0.98
	5.14			4.43		
	4.49			5.14		
300	4.11	4.34	0.87	4.62	4.47	0.90
	4.82			4.17		
	4.11			4.62		
400	4.17	3.92	0.78	3.88	3.86	0.78
	3.72			3.53		
	3.85			4.17		
500	3.08	3.27	0.65	3.02	3.10	0.63
	3.53			3.21		
	3.21			3.08		
600	2.82	2.48	0.50	2.63	2.50	0.50
	2.25			2.50		
	2.38			2.38		
700	1.93	1.88	0.38	1.48	1.65	0.33
	1.80			1.54		
	1.93			1.93		
800	1.28	1.17	0.23	1.09	1.20	0.24
	1.06			1.41		
	1.16			1.09		

Table B-26: Variation in Split tensile strength for HPC-O and HPC-G mix cubes after exposure to elevated temperature and retained for 3 hours

Temperature (°C)	HPC-O			HPC-G		
	Split tensile strength (MPa)	Average Split tensile strength (MPa)	Split tensile strength ratio	Split tensile strength (MPa)	Average Split tensile strength (MPa)	Split tensile strength ratio
27	5.14	5.39	1.00	5.01	5.03	1.00
	5.33			5.14		
	5.71			4.94		
100	4.62	4.70	0.88	4.69	4.40	0.88
	5.01			4.37		
	4.56			4.17		
200	4.37	4.62	0.86	4.82	4.34	0.86
	4.49			4.04		
	5.01			4.17		
300	4.04	3.81	0.71	3.72	4.16	0.83
	3.85			4.17		
	3.53			4.59		
400	2.89	3.10	0.58	3.21	3.40	0.68
	2.89			3.53		
	3.53			3.47		
500	2.89	2.57	0.48	3.02	2.89	0.57
	2.57			2.63		
	2.25			3.02		
600	1.73	1.84	0.34	2.18	2.01	0.40
	1.93			1.80		
	1.86			2.05		
700	1.28	1.21	0.22	1.80	1.67	0.33
	1.09			1.41		
	1.25			1.80		
800	0.90	0.88	0.16	1.16	1.03	0.20
	0.90			0.96		
	0.83			0.96		

Table B-27: Variation in Split tensile strength for HPC-F and HPC-G-F mix cubes after exposure to elevated temperature and retained for 3 hours

Temperature (°C)	HPC-F			HPC-G-F		
	Split tensile strength (MPa)	Average Split tensile strength (MPa)	Split tensile strength ratio	Split tensile strength (MPa)	Average Split tensile strength (MPa)	Split tensile strength ratio
27	5.07	4.96	1.00	4.49	4.90	1.00
	5.01			5.01		
	4.82			5.20		
100	4.49	4.70	0.94	4.69	4.60	0.94
	4.69			4.82		
	4.82			4.37		
200	4.37	4.52	0.91	4.82	4.47	0.91
	5.01			4.11		
	4.17			4.49		
300	3.60	4.00	0.81	4.30	4.04	0.83
	4.37			4.04		
	4.04			3.79		
400	3.47	3.53	0.71	3.34	3.36	0.69
	3.72			3.21		
	3.40			3.53		
500	3.08	2.95	0.59	2.89	2.76	0.56
	2.57			3.08		
	3.21			2.31		
600	2.25	2.35	0.47	2.44	2.38	0.48
	2.57			2.44		
	2.25			2.25		
700	1.48	1.71	0.31	1.54	1.64	0.33
	1.73			2.02		
	1.93			1.35		
800	0.87	0.97	0.20	0.83	0.92	0.19
	1.00			0.90		
	1.06			1.03		

Table B- 28: Compressive/Splitting tensile strength prediction equations for different mixes based on exposure temperature, retention period and porosity

Type of Mix	Prediction Equations	Temperature Range	MRE
Compressive strength from exposure temperature, retention period and porosity			
HPC-O	$f_c = 91.8 - 0.085 \times T - 4.24 \times RP + 2.48 \times P$	$100^\circ\text{C} < T \leq 450^\circ\text{C}$	2.0
	$f_c = 143 - 0.125 \times T - 9.45 \times RP + 0.71 \times P$	$450^\circ\text{C} < T \leq 800^\circ\text{C}$	3.7
Blended concretes	$f_c = 81.1 - 0.0446 \times T - 2.0 \times RP + 1.88 \times P$	$100^\circ\text{C} < T \leq 450^\circ\text{C}$	4.3
	$f_c = 146 - 0.114 \times T - 8.04 \times RP + 0.27 \times P$	$450^\circ\text{C} < T \leq 800^\circ\text{C}$	3.7
Splitting tensile strength from exposure temperature, retention period and porosity			
HPC-O	$f_t = 5.66 - 0.00124 \times T - 0.093 \times RP - 0.170 \times P$	$100^\circ\text{C} < T \leq 250^\circ\text{C}$	7.5
	$f_t = 6.41 - 0.00678 \times T - 0.257 \times RP + 0.023 \times P$	$250^\circ\text{C} < T \leq 800^\circ\text{C}$	7.9
Blended concretes	$f_t = 5.46 - 0.0023 \times T - 0.167 \times RP - 0.003 \times P$	$100^\circ\text{C} < T \leq 250^\circ\text{C}$	3.6
	$f_t = 6.70 - 0.00685 \times T - 0.248 \times RP + 0.0257 \times P$	$250^\circ\text{C} < T \leq 800^\circ\text{C}$	4.7

Where,

f_c = Compressive strength

f_t = Splitting tensile strength

T = Exposure temperature in °C

RP = Retention period in hour

P = Porosity in %

Table B -29: Compressive/Splitting tensile strength prediction equations for different mixes based on exposure temperature, retention period and UPV

Type of Mix	Prediction Equations	Temperature Range	MRE
Compressive strength from exposure temperature, retention period and UPV			
HPC-O	$f_c = 77.7 - 0.0068 \times T - 2.3 \times RP + 2.1 \times V$	$100^\circ\text{C} < T \leq 450^\circ\text{C}$	2.7
	$f_c = 95.0 - 0.0712 \times T - 4.97 \times RP + 9.51 \times V$	$450^\circ\text{C} < T \leq 800^\circ\text{C}$	2.8
Blended concretes	$f_c = 74.3 + 0.0115 \times T - 0.71 \times RP + 0.85 \times V$	$100^\circ\text{C} < T \leq 450^\circ\text{C}$	4.5
	$f_c = 138.0 - 0.103 \times T - 7.20 \times RP + 1.79 \times V$	$450^\circ\text{C} < T \leq 800^\circ\text{C}$	3.7
Splitting tensile strength from exposure temperature, retention period and UPV			
HPC-O	$f_t = 7.15 - 0.00564 \times T - 0.231 \times RP - 0.222 \times V$	$100^\circ\text{C} < T \leq 250^\circ\text{C}$	3.8
	$f_t = 2.2 - 0.00278 \times T + 0.103 \times RP + 0.761 \times V$	$250^\circ\text{C} < T \leq 800^\circ\text{C}$	5.2
Blended concretes	$f_t = 6.87 - 0.00376 \times T - 0.222 \times RP - 0.265 \times V$	$100^\circ\text{C} < T \leq 250^\circ\text{C}$	3.5
	$f_t = 6.82 - 0.00647 \times T - 0.236 \times RP - 0.004 \times V$	$250^\circ\text{C} < T \leq 800^\circ\text{C}$	4.6

Where,

f_c = Compressive strength

f_t = Splitting tensile strength

T = Exposure temperature in °C

RP = Retention period in hour

V = Ultrasonic Pulse Velocity in km/sec

Table B-30: Variation in drilling time with different penetration depth after exposure to elevated temperature

Drilling Depth (mm)	Drilling Time (sec)											
	27°C				100°C				200°C			
	1	2	3	Average	1	2	3	Average	1	2	3	Average
0	0	0	0	0.0	0	0	0	0.0	0	0	0	0.0
5	3	2	4	3.0	5	3	3	3.7	5	6	5	5.3
10	8	7	10	8.3	10	7	9	8.7	11	10	11	10.7
15	12	13	14	13.0	14	11	12	12.3	15	14	13	14.0
20	17	16	15	16.0	18	16	17	17.0	19	18	17	18.0
25	21	21	19	20.3	22	20	22	21.3	23	24	20	22.3
30	26	26	23	25.0	26	25	24	25.0	27	28	24	26.3
35	32	30	27	29.7	32	27	28	29.0	34	33	31	32.7
40	36	33	30	33.0	36	34	34	34.7	36	36	35	35.7
45	38	35	35	36.0	40	38	42	40.0	40	42	40	40.7
50	41	40	42	41.0	44	42	46	44.0	43	45	43	43.7

Table B-31: Variation in drilling time with different penetration depth after exposure to elevated temperature

Drilling Depth (mm)	Drilling Time (sec)											
	300°C				400°C				500°C			
	1	2	3	Average	1	2	3	Average	1	2	3	Average
0	0	0	0	0.0	0	0	0	0.0	0	0	0	0.0
5	4	4	5	4.3	4	4	4	4.0	3	4	2	3.0
10	9	8	10	9.0	7	8	9	8.0	6	7	6	6.3
15	14	14	14	14.0	11	12	13	12.0	11	11	11	11.0
20	18	17	17	17.3	15	13	17	15.0	14	15	13	14.0
25	22	21	21	21.3	18	17	19	18.0	17	19	17	17.7
30	28	25	27	26.7	21	22	23	22.0	20	22	19	20.3
35	33	32	33	32.7	24	26	28	26.0	23	24	24	23.7
40	37	35	36	36.0	27	29	31	29.0	26	29	26	27.0
45	40	40	40	40.0	30	32	30	30.7	31	30	31	30.7
50	42	43	44	43.0	35	37	36	36.0	34	34	34	34.0

Table B-32: Variation in drilling time with different penetration depth after exposure to elevated temperature

Drilling Depth (mm)	Drilling Time (sec)											
	600°C				700°C				800°C			
	1	2	3	Average	1	2	3	Average	1	2	3	Average
0	0	0	0	0.0	0	0	0	0.0	0	0	0	0.0
5	4	4	3	3.7	2	2	2	2.0	4	3	2	3.0
10	8	7	6	7.0	4	4	4	4.0	5	4	3	4.0
15	11	10	9	10.0	6	7	5	6.0	6	5	4	5.0
20	14	12	13	13.0	8	8	8	8.0	8	7	6	7.0
25	18	17	16	17.0	10	10	10	10.0	10	10	10	10.0
30	20	18	19	19.0	12	12	12	12.0	13	12	12	12.3
35	23	21	24	22.7	15	15	15	15.0	14	14	14	14.0
40	26	25	27	26.0	18	18	18	18.0	15	15	15	15.0
45	30	28	32	30.0	20	20	20	20.0	19	18	17	18.0
50	33	32	34	33.0	25	23	21	23.0	21	19	20	20.0

Table B-33: Variation in compressive strength for standard cube and core from plain cube and reinforced concrete beam specimen

Temperature (°C)	Standard cube specimen			Core specimen from plain concrete cube			Core specimen from Reinforced Concrete beam		
	Compressive strength (MPa)	Average Compressive strength (MPa)	Compressive strength ratio	Compressive strength (MPa)	Average Compressive strength (MPa)	Compressive strength ratio	Compressive strength (MPa)	Average Compressive strength (MPa)	Compressive strength ratio
27	75.0	80.0	1.00	76.4	78.5	1.00	70.8	71.6	1.00
	80.0			81.2			78.2		
	85.0			77.9			65.9		
200	80.0	82.3	1.03	71.7	76.6	0.98	73.3	70.0	0.98
	82.0			81.7			65.9		
	84.0			76.4			70.8		
300	80.0	80.0	1.00	74.5	70.1	0.89	58.6	62.7	0.88
	80.0			78.8			65.9		
	80.0			76.4			63.5		
400	75.0	74.5	0.93	71.7	65.9	0.84	48.9	51.3	0.72
	76.0			64.0			58.6		
	72.5			74.5			46.4		
500	65.0	65.6	0.82	66.9	61.5	0.78	34.2	38.3	0.53
	67.0			64.0			41.5		
	65.0			66.9			39.1		
600	53.5	53.8	0.67	62.1	51.9	0.66	26.9	30.9	0.43
	53.0			57.3			29.3		
	55.0			65.0			36.6		
700	45.0	42.7	0.55	52.5	39.2	0.50	24.4	21.0	0.29
	45.0			47.8			20.5		
	47.0			54.5			18.1		
800	28.5	29.5	0.37	41.1	25.5	0.32	19.5	17.6	0.25
	28.0			38.2			16.1		
	32.0			38.2			17.1		

Table B-34: Variation in porosity and UPV for core from reinforced concrete beam specimen

Temperature (°C)	Porosity					UPV	
	Dry weight of cubes (gm)	Saturated weight of cubes in water (gm)	Saturated weight of cubes in air (gm)	Porosity (%)	Average porosity (%)	UPV (km/sec)	Average UPV in (km/sec)
27	1413	852	1434	3.61	3.71	4.41	4.4
	1079	647	1098	4.21		4.28	
	1399	846	1418	3.32		4.55	
200	1270	765	1301	5.78	5.43	4.18	4.1
	1383	833	1412	5.01		4.11	
	1376	827	1408	5.51		4.00	
300	1416	865	1452	6.13	6.14	3.89	3.8
	1378	840	1412	5.94		3.70	
	1407	862	1444	6.36		3.70	
400	1400	847	1435	5.95	6.37	3.44	3.5
	1408	852	1449	6.87		3.45	
	1392	842	1429	6.30		3.49	
500	1361	824	1398	6.45	6.54	2.95	3.1
	1375	829	1413	6.51		2.99	
	1412	865	1451	6.66		3.23	
600	1345	810	1390	7.76	7.64	2.23	2.2
	1341	807	1385	7.61		2.13	
	1351	813	1395	7.56		2.10	
700	1263	770	1310	8.70	8.64	1.63	1.7
	1277	776	1325	8.74		1.79	
	1355	825	1404	8.46		1.56	
800	1332	809	1392	10.29	9.73	1.34	1.4
	1416	881	1472	9.48		1.36	
	1108	676	1153	9.43		1.40	

REFERENCES

Books/ Journals Articles/ Reports:

- Aitcin, P. C. (1998). "High Performance Concrete." *E and FN SPON, New York*.
- Arioz, O. (2007), "Effects of elevated temperatures on properties of concrete." *Fire Safety Journal*, 42 (8), 516-522.
- Arioz, O. (2009), "Retained properties of concrete exposed to high temperatures: Size effect." *Fire and Materials*, 33(5), 211–222.
- Bazant, Z. P. and Kaplan, M. F. (1996). "Concrete at high temperatures: material properties and mathematical models." *Pearson Education Ltd. UK*.
- Bungey, J. H. and Soutsos, M. N. (2001). "Reliability of partially-destructive tests to assess the strength of concrete on site." *Construction and Building Materials*, 15(2-3), 81-92.
- Bungey, J. H., Millard, S. G. and Grantham, M. G. (2006). "Testing of concrete in structures." *Taylor and Francis, London and New York*.
- Chan, Y.N., Peng, G. F. and Sun, W. (1999). "Residual strength and pore structure of high-strength concrete and normal strength concrete after exposure to high temperatures." *Cement and Concrete Composite*, 21(1), 23-27.
- Chan, S.Y.N., Luo, X. and Sun, W. (2000). "Compressive strength and pore structure of high performance concrete after exposure to high temperature up to 800°C." *Cement and Concrete Research*, 30(2), 247-251.
- Chan, S.Y.N., Luo, X. and Sun, W. (2000). "Effect of high temperature and cooling regimes on the compressive strength and pore properties of high performance concrete." *Construction and Building Materials*, 14(5), 261-266.
- Chang, W. T., Wang, C. T. and Huang, C. W. (1994). "Concrete at temperatures above 1000°C." *Fire Safety Journal*, 23(3), 223-243.

- Chen, B., and Liu, J. (2004). "Residual strength of hybrid-fiber-reinforced high-strength concrete after exposure to high temperatures." *Cement and concrete research*, 34(6), 1065–1069.
- Demirel, B. and Kelestemur, O. (2010). "Effect of elevated temperature on the mechanical properties of concrete produced with finely ground pumice and silica fume." *Fire Safety Journal*, 45 (6-8), 385-391.
- Dong, X., Ding, Y. and Wang, T. (2008). "Spalling and mechanical properties of fiber reinforced High-Performance Concrete subjected to fire." *Journal of Wuhan University of Tech.*, 23(5), 743-749.
- Douglas, M. (2004). "Design and analysis of experiments." 7th edition, *John Wiley and Sons, New York*.
- Ersoy, A. and Waller, M. D. (1997). "Drilling detritus and the operating parameters of thermally stable PDC core bits." *International Journal of Rock Mechanics Mining Science*, 34(7), 763-766.
- Fares, H., Noumowe, A. and Remond, S. (2009). "Self-consolidating concrete subjected to high temperature mechanical and physicochemical properties." *Cement and Concrete Research*, 39(12), 1230-1238.
- Forster, S. W. (1994). "High Performance Concrete stretching the paradigm." *Concrete International*, 16 (10), 33-34.
- Fu, Y. and Li, L. (2011). "Study on mechanism of thermal spalling in concrete exposed to elevated temperatures." *Materials and Structures*, 44(1), 361-376.
- Ghandehari, M., Behnood, A. and Khanzadi, M. (2010). "Residual mechanical properties of high-strength concretes after exposure to elevated temperatures." *Journal of Materials in Civil Engineering*, 22(1), 59-64.
- Gonzalez, R. C. and Woods, R. F. (1992). "Digital image processing." *Addison-Wesley, Reading, Mass.*
- Handoo, S. K., Agarwal, S. and Agarwal, S. K. (2002). "Physicochemical, mineralogical, and morphological characteristics of concrete exposed to elevated temperatures." *Cement and Concrete Research*, 32(7), 1009–1018.

- Hoff, G., Bilodeau, A., and Malhotra, M. (2000). "Elevated temperature effects on HSC residual strength." *Concrete International*, 22 (4), 41–47.
- Hosam, EL. D.H.S., Alaa M. R. and Elsokary, T. (2011). "Effect of elevated temperature on physico-mechanical properties of blended cement concrete." *Construction and Building Materials*, 25(2), 1009-1017.
- Husem, M. (2006). "The effects of high temperature on compressive and flexural strengths of ordinary and high performance concrete." *Fire Safety Journal*, 41(2), 155-163.
- Khoury, G. A. (1992). "Compressive strength of concrete at high temperature: a reassessment." *Magazine of Concrete Research*, 44(161), 291–309.
- Khoury, G. A. (2000). "Effect of fire on concrete and concrete structures." *Prog.Struct.Engng Mater*, 2, 429-447.
- Kodur V. K. R. and Sultan M A (2003). "Effect of temperature on thermal properties of High Strength Concrete." *Journal of Materials in Civil Engineering*, 15(2) 101-107.
- Lau, A. and Anson, M. (2006). "Effect of high temperatures on high performance steel fibre reinforced concrete." *Cement and Concrete Research*, 36(9), 1698-1707.
- Li, M., Qian, C. X. and Sun, W. (2004). "Mechanical properties of high strength concrete after fire." *Cement and Concrete Research*, 34(6), 1001–1005.
- Lie, T.T. (1992). "Structural fire protection: Manual of Practice." *ASCE Manuals and Reports on Engineering Practice No. 78, American Society of Civil Engineers, New York, NY*.
- Lin, D. F., Wang, H. Y. and Luo H. L. (2004). "Assessment of fire-damaged mortar using digital image process." *Journal of Materials in Civil Engineering*, 16(4), 383-386.
- Ling, T. C., Poon, C. S. and Kou, S.C. (2012). "Influence of recycled glass content and curing conditions on the properties of self-compacting concrete after exposure to elevated temperatures." *Cement and Concrete Composite*, 34(2),265-272.

- Liu, C. T. and Huang, J. S. (2009), "Fire performance of highly flowable reactive powder concrete." *Construction and Building Materials*, 23 (5), 2072–2079.
- Luo, X., Sun, W. and Chan, Y. N. (2000). "Residual compressive strength and microstructure of high performance concrete after exposure to high temperature." *Materials and Structure*, 33(5), 294-298.
- Mehta, P. K. and Aitcn, P. C. (1990). "Principles underlying the production of high performance concrete." *Cement, Concrete, and Aggregate*, 12 (2), 70-80.
- Miklusova, V., Usalova, L., Ivanicova, L. and Krepelka, F. (2006). "Acoustic signal-new feature in monitoring of rock disintegration process." *Contrib geophys geodesy SAS 36(SI 6SGK)*, 125–133.
- Nadeem, A., Memon, S. A. and Lo, T. Y. (2013). "Qualitative and quantitative analysis and identification of flaws in the microstructure of fly ash and metakaolin blended high performance concrete after exposure to elevated temperatures." *Construction and Building Materials*, 38(January), 731–741.
- Neville, A. M. (2005). "Properties of concrete." *Pearson Education, South Asia*.
- Noumowe, A. N., Clastres, P., Debick, G. and Costaz, J. L. (1996). "Transient heating effect on high strength concrete." *Nuclear Engineering and Design*, 166 (1), 99-108.
- Peng, G. F., Bian, S. H., Guo, Z. Q., Zhao, J., Peng, X. L. and Jiang, Y. C. (2008). "Effect of thermal shock due to rapid cooling on residual mechanical properties of fiber concrete exposed to high temperatures." *Construction and Building Materials*, 22(5), 948–955.
- Poon, C. S., Azhar, S., Anson, M. and Wong, Y. L. (2001). "Comparison of the strength and durability performance of normal and high strength pozzolanic concretes at elevated temperatures." *Cement and Concrete Research*, 31(9), 1291–1300.
- Rahim, A., Sharma, U. K., Murugesan, K., Sharma, A. and Arora, P. (2013). "Multi-response optimization of post-fire residual compressive strength of high performance concrete." *Construction and Building Materials*, 38, 265-273.
- Sanjayan, G. and Stocks, L.J. (1993). "Spalling of high strength silica fume concrete in fire." *ACI Material Journal*, 90(2), 170-173.

- Savva, A., Manita, P. and Sideris, K. K.(2005). “Influence of elevated temperatures on the mechanical properties of blended cement concretes prepared with limestone and siliceous aggregates.” *Cement and Concrete Composites*, 27(2), 239–248.
- Sarshar R and Khoury G A (1993). “Material and Environmental Factors Influencing the Compressive Strength of Unsealed Cement Paste and Concrete at High Temperatures.” *Magazine of Concrete Research*, 45(162), 51–61.
- Short, N. R., Purkiss, J. A. and Guise, S. E. (2001). “Assessment of fire damaged concrete using colour image analysis.” *Construction and Building Materials*, 15(1), 9-15.
- Sideris, K. K., Manita, P. and Chaniotakis, E. (2009). “Performance of thermally damaged fibre reinforced concretes.” *Construction and Building Materials*, 23(3), 1232–1239.
- Steve K. (1997). “Concrete Technology Today.” *Portland Cement Association report*, 18(2), 1-7.
- Teng, W. C. and Lo, T. Y. (2009). “Mechanical and fracture properties of normal and high –strength concretes with fly ash after exposure to high temperatures.” *Magazine of Concrete Research*, 61(5), 323-330.
- Uysal, M., Yilmaz, K. and Ipek, M. (2012). “Properties and behavior of self-compacting concrete produced with GBFS and FA additives subjected to high temperatures.” *Construction and Building Materials*, 28(1), 321–326.
- Vardhan, H., Adhikari, G. R., Govindaraj, M. (2009). “Estimating rock properties using sound level during drilling.” *International Journal of Rock Mechanics and Mining Sciences*, 46(3), 604–612.
- Wang, H. Y. (2008). “The effect of elevated temperature on cement paste containing GGBFS.” *Cement and Concrete Composites*, 30(10), 992-999.
- Xiao, J., Xie, M. and Zhang, Ch. (2006). “Residual compressive behaviour of pre-heated high-performance concrete with blast–furnace–slag.” *Fire Safety Journal*, 41(2), 91-98.

Xu, Y., Wong, Y. L., Poon, C. S. and Anson, M. (2001). "Impact of high temperature on PFA concrete." *Cement and Concrete Research*, 31(7), 1065-1073.

Yang, H., Lin, Y., Hsiao, C. and Liu, J. Y. (2009). "Evaluating residual compressive strength of concrete at elevated temperatures using ultrasonic pulse velocity." *Fire Safety Journal*, 44(1), 121-130.

Ye, G., Liu, X., De Schutter, G., Taerwe, L. and Vandeveld, P. (2007). "Phase distribution and microstructural changes of SCC at elevated temperatures." *Cement and Concrete Research*, 37(6), 978–987.

Zborovjan, M., Lesso, I. and Dorcak, L. (2003). "Acoustic identification of rocks during drilling process." *Journal of Acta Montanistica Slovaca*, 8(4), 91-93.

Codes/ Standards/ Specifications

ASTM designation C192-90a, (1994), Standard practice for making and curing concrete test specimen in the laboratory.

BS 6699:1992, Specification for ground granulated blast furnace slag for use with portland cement, *British Standards Institution*.

IS 383:1970, Specifications for coarse and fine aggregates from natural sources for concrete, Bureau of Indian Standards (BIS), New Delhi.

IS 456:2000, Plain and reinforced concrete- code of practice, BIS, New Delhi.

IS 516:1959, Methods of tests for strength of concrete, BIS, New Delhi.

IS 650: 1966, Standard specification for testing cement specification, BIS, New Delhi.

IS 1641:2002, Fire Safety of Buildings (General): General Principles of Fire Grading and Classification, BIS, New Delhi.

IS 2386:1975, Methods of test for aggregates for concrete, BIS, New Delhi.

IS 3812(Part 1):2003, Pulverized fuel ash: specification, BIS, New Delhi.

IS 4031:1988, Method of physical test for hydraulic cement, BIS, New Delhi.

IS 4032:1985, Method of chemical analysis of hydraulic cement, BIS, New Delhi.

IS 5816:1999, Splitting tensile strength of concrete- method of Test, BIS, New Delhi.

IS 8112:1989, Specifications for 43 grade ordinary portland cement, BIS, New Delhi.

IS13311 (Part 1):1999, Non- destructive testing of concrete methods of tests, BIS, New Delhi.

The concrete Society, Technical Report No. 68, "Assessment, design and repair of fire damaged concrete structure."A *Cement and Concrete Industry Publication*, December, 2008.

LIST OF PUBLICATIONS

International/National Journals

1. Yaragal, S. C., Babu Narayan, K. S., Venkataramana, K., Kulkarni, K. S., Gowda, H. C., Reddy, G. R. and Sharma, A. (2010). “Studies on Normal Strength Concrete cubes subjected to elevated temperatures.” *Journal of Structural Fire Engineering*, 1(4), 248-262.
2. Kulkarni, K. S., Yaragal, S. C. and Babu Narayan, K. S. (2011). “Effect of elevated temperatures on mechanical properties of microcement based high performance concrete.” *International Journal of Applied Engineering and Technology*, 1(1), 24-31.
3. Kulkarni, K. S., Yaragal, S. C. and Babu Narayan, K. S. (2011). “An overview of High Performance Concrete at elevated temperatures.” *International Journal of Applied Engineering and Technology*, 1(1), 48-60.
4. Kulkarni, K. S., Babu Narayan, K. S. and Yaragal, S. C. (2012). “Correlation between residual compressive strength and splitting tensile strength of thermally deteriorated HPC.” *International Journal of Civil Engineering Research*, 3(3), 137-147.
5. Kulkarni, K. S., Yaragal, S. C. and Babu Narayan, K. S. (2012). “Performance of High Strength Concrete subjected to elevated temperatures.” *International Journal of Earth science and Engineering*, 5(4), 593-598.
6. Kulkarni, K. S., Yaragal, S. C. and Babu Narayan, K. S. (2013). “Forensic engineering of fire damaged structures- state of art.” *International Journal of Forensic Engineering*, 1(3/4), 342 – 354.
7. Kulkarni, K. S., Babu Narayan, K. S. and Yaragal, S. C. (2013). “Effect of elevated temperatures on physical and residual strength properties of HPC.” *International Journal of Scientific & Engineering Research*, 4(5), 71-74.

International/National Conferences

8. Kulkarni, K. S., Yaragal, S. C. and Babu Narayan, K. S. (2010). “Statistical analysis for mechanical properties on normal strength concrete subjected to elevated temperatures.” *Proc. International Conference on Earth Sciences and Engineering (ICEE 2010), 21 August 2010, at Hyderabad, India,*
9. Kulkarni, K. S., Babu Narayan, K. S. and Yaragal, S. C. (2010). “Assessment of fire damaged reinforced concrete structures.” *Proc. International conference on Innovative World of Structural Engineering (ICIWSE-2010), 25 -27 December 2010, Aurangabad, India, 597-604.*
10. Kulkarni, K. S., Yaragal, S. C. and Babu Narayan, K. S. (2012). “Performance of High Strength Concrete subjected to elevated temperatures.” *Proc. 2ndInternational Engineering Symposium (IES-2012), 5-7 March 2012, at Kumamoto University, Japan, C1-1-1-C1-1-6.*
11. Kulkarni, K. S., Yaragal, S. C. and Babu Narayan, K. S. (2012). “Colorimetry as a simple tool for assessment of fire damaged concrete.” *Proc. National Conference on Contemporary Civil Engineering & Practice (CCERP 2012), 20-21 April 2012, at MIT Manipal, India, 974-981.*
12. Kulkarni, K. S., Babu Narayan, K. S. and Yaragal, S. C., (2012). “Effect of elevated temperatures on normal and high strength blended cement concrete.” *Proc. International Conference on Emerging trends in Engineering (ICETE-12), 15-16 May 2012, at NMAM Institute of Technology, Nitte, India, 473-476.*
13. Kulkarni, K. S., Babu Narayan, K. S. and Yaragal, S. C., “Effect of elevated temperature on the compressive strength and surface porosity of HPC.” *Proc. UKIERI concrete congress on Innovations in Concrete Construction, 5 - 8 March 2013, at Dr. B. R. Ambedkar NIT, Jalandhar, India., 2075- 2081.*

14. Kulkarni, K. S., Babu Narayan, K S. and Yaragal, S. C., “Effect of elevated temperatures on physical and residual strength properties of HPC.” *Proc. International Conference on Innovations in Civil Engineering (ICICE-2013)* at SCMS, Karukutty, Kerala, India, 71-74.

A technical paper titled “Statistical analysis for mechanical properties on normal strength concrete subjected to elevated temperatures”, presented by Kulkarni, K. S., Yaragal, S. C. and Babu Narayan, K S, in International Conference on Earth Sciences and Engineering (ICEE 2010), has been adjudged as best paper.

CURRICULUM VITAE

Name : KULKARNI KISHOR SITARAM

Contact No. : +91-9663530674

E-Mail : kishorsk1@gmail.com, kishorsk1@rediffmail.com.

Date of Birth : 27-06-1984

Educational Qualifications

Degree	University	Year of Passing	Division
B. E. (Civil)	Shivaji University, Kolhapur, Maharashtra, India.	2005	I st class with distinction
M. E. (Structures)		2007	I st class with distinction

Teaching Experience

Name of Institute	Post held	Period
K.E. Society's, Rajarambapu Institute of Technology, Sakarale, Sangli, Maharashtra, India	Lecturer	Sept 2006 to Dec 2008

Industrial Experience / Interaction

Organization	Nature of work	Period
University of Dundee, Scotland, U.K.	Research Interaction	15 th March 2011 to 15 th April 2011

Research Publications

	International	National
Journal Papers	7	--
Conference Publications	14	3

Awards, Membership and Recognition

- ❖ Nominated from NITK, Surathkal for 'IIST Research Scholar Day' function held at Indian Institute of Space Science and Technology, Trivandrum.
- ❖ Affiliate Member of ASCE.